# Characterization of PCSK9-mediated LDLR Degradation in Hepatic and Fibroblast Cells

**MY-ANH NGUYEN**

Thesis submitted to the Faculty of Graduate and Postdoctoral Studies

In partial fulfillment of the requirements

For the degree of

**MASTER of SCIENCE**

Department of Biochemistry, Microbiology and Immunology

University of Ottawa

Ottawa, Ontario, Canada

**Abstract**

The discovery that proprotein convertase subtilisin/kexin type 9 (PCSK9) mediates degradation of low-density lipoprotein receptors (LDLR) indicates a critical role in LDL metabolism. PCSK9 is a secreted protein that binds to the epidermal growth factor-like (EGF)-A domain of LDLR and directs the receptor for degradation in lysosomes by an unknown mechanism. A gain-of-function mutation, D374Y, increases binding to LDLR EGF-A >10-fold and is associated with a severe form of hypercholesterolemia in humans. Similar to previous studies, data obtained in my project has established that PCSK9 was capable of promoting robust LDLR degradation in liver-derived cell lines; however, minimal effects on LDLR levels were detected in several lines of fibroblast cells despite normal LDLR-dependent cellular uptake of PCSK9. Importantly, a PCSK9 degradation assay showed that $^{125}$I-labeled wild-type PCSK9 was internalized and degraded equally in both hepatic and fibroblast cells, indicating dissociation of wild-type PCSK9 from recycling LDLRs in fibroblasts. Moreover, PCSK9 recycling assays confirmed that no recycling of wild-type PCSK9 to the cell surface could be detected in fibroblast cells. In contrast, more than 60% of internalized PCSK9-D374Y recycled to the cell surface in these cells, and thus had reduced ability to direct the LDLR for lysosomal degradation despite persistent binding. Co-localization studies indicated that PCSK9-D374Y trafficked to both lysosomes and recycling compartments in fibroblast cells, whereas wild-type PCSK9 exclusively trafficked to lysosomes. We conclude that two factors diminish PCSK9 activity in fibroblast cells: i) an increased dissociation from the LDLR in early endosomal compartments, and ii) a decreased ability of bound PCSK9 to direct the LDLR to lysosomes for degradation. Finally, an LDLR variant that binds to PCSK9 in a $Ca^{2+}$-independent manner could partially restore wild-type PCSK9 activity, but not PCSK9-D374Y activity, in fibroblast cells.

**Acknowledgments**

"Đi một ngày đàng, học một sàng khôn" is a famous expression in my mother-tongue language, Vietnamese. It means the more you go, the more you learn. At least, it's absolutely right in my case. Coming to Canada and becoming a graduate student at University of Ottawa Heart Institute have really been the biggest turning point in my life. I have grown a lot, both on a personal and professional level. Two years are not long time but also not short time, especially if you have to live far away from your loved ones, if you have to leave all you've known and restart your life from the beginning. Luckily, I have many special people around who give me constant strength, motivation, and encouragement to keep going the way I have chosen. First of all, I know that I always can count on my family. I don't dedicate this achievement for anyone of my family because for me, each of them is meaningful on their own. When everything gets me down, just some simple things such as my grandmother's voice, unlimited chatting with my sisters, funny stories of my brother, or sweet hugs from my aunt are enough to make my day. I can be sure that sometimes nobody in my family can understand what I am doing or what I am talking about, but they are always there for me whenever I need. My life is never complete without them.

Importantly, I want to express my special thanks to Dr. Thomas Lagace. Tom is a perfect supervisor who not only knows how to firmly push you forward but also knows how to gently help you realize your valuable abilities and develop them. I can honestly say that I have learnt a lot from him. From the bottom of my heart, I am really grateful to him for his endless patience and guidance. He was always willing to listen to me, even many of my crazy opinions or silly questions, to clear my mind when I was confused, and to bring me back the right way when I got lost. He never gave up on me no matter how many times I made him disappointed.

Besides, I am very grateful to a number of PIs especially for their assistance and guidance that I needed most during this program. I would like to thank Dr. Xiaohui Zha and Pasan Fernando, who were my TAC member over the years, for giving me critical discussions as well as valuable advices about my project. I also want to thank Dr. Ross Milne who always supported me in a special way. His constant encouragement usually made me stronger to overcome many difficulties throughout, more hopeful to complete my project, and more determined to pursue my further goals in science.

There will be a mistake if I don't say thanks to many people who I am lucky enough to work with. First of all are my wonderful labmates: Geoff Leblond and Tanja Kosenko who trained me at the very beginning and always devoted their time as well as effort to assist me whenever I needed; Mia Golder who was always there to teach me anything I did not know, to explain anything I did not understand, and to show me anything I needed to improve. I cannot remember how many times they helped me get out of my problems, even minor or major. All of them are my best teachers. Also, thanks to Maroun Khalil who showed me how to go through countless headaches related to confocal microscope (for sure, he is one of whole-hearted and patient mentors who I have ever got), to Suzanne Crowe who helped me with flow cytometry experiments, to every people at the fourth floor of the Heart Institute who was always available for help with chemical, equipment or anything and everything. Thanks all of you for making my graduate student experiences at the Heart Institute more memorable.

To my dearest friends who always stayed beside me and supported me during this period of my life, I love all of you so much and thank for always being my true friends no matter how freaky I am sometimes.

Finally, thanks to you, my special one, although you always say that there's no need to say thanks between us and I never can express enough thanks to you.

**Contents**

**List of Abbreviations**

| | |
|---|---|
| ABCA1 | ATP-binding cassette transporter |
| ADH | Autosomal dominant hypercholesterolemia |
| AE | Adverse effect |
| Apo | Apolipoprotein |
| ApoER2 | Apolipoprotein E receptor 2 |
| AP-2 | Adaptor protein 2 |
| ARH | Autosomal recessive hypercholesterolemia |
| bHLH-Zip | Basic helix-loop-helix leucine zipper |
| BAPTA | 1,2-bis(o-aminophenoxy)ethane-N,N,N',N'-tetraacetic acid |
| BCA | Bicinchoninic acid |
| BSA | Bovine albumin serum |
| CHD | Coronary heart disease |
| COPII | Coat protein complex II |
| EGF | Epidermal growth factor |
| ER | Endoplasmic reticulum |
| ESCRT | Endosomal sorting complex required for trafficking |
| FBS | Fetal bovine serum |
| FH | Familial hypercholesterolemia |
| HDL | High-density lipoprotein |
| HMGCR | 3-hydroxyl-3-methylglutaryl coenzyme reductase |
| HRS | Hepatocyte growth factor-regulated Tyr-kinase substrate |
| INSIG-1 | Insulin-induced gene 1 |
| LA | LDLR type-A |
| LDL | Low-density lipoprotein |
| LDL-C | Low-density lipoprotein cholesterol |
| LDLR | Low-density lipoprotein receptor |
| LRP8 | Low-density lipoprotein receptor-related protein 8 |
| LXR | Liver X receptor |
| NARC-1 | Neural apoptosis regulated convertase 1 |
| NCLPDS | Newborn calf lipoprotein-deficient serum |

| | |
|---|---|
| PCSK9 | Proprotein convertase subtilisin/kexin type 9 |
| Rab4 | RAS-related GTP-binding protein 4 |
| RAP | Receptor-associated protein |
| S1P | Site-1 protease |
| S2P | Site-2 protease |
| SCAP | SREBP cleavage-activating protein |
| SIRT1 | Sirtuin 1 |
| SRE | Sterol response element |
| SREBP | Sterol regulatory element binding protein |
| TCA | Trichloroacetic acid |
| TCEP | Tris(2-carboxyethyl)phosphine hydrochloride |
| TfR | Transferrin receptor |
| TSG101 | Tumor susceptibility gene 101 |
| VLDL | Very low-density lipoprotein |
| VLDLR | Very low-density lipoprotein receptor |

**List of Figures**

## 1. Introduction

Coronary heart disease (CHD), which leads to one of every five deaths each year, remains a persistent health burden in westernized countries (1). The link between CHD and lipids has been firmly established; in which elevated levels of plasma cholesterol is considered as the leading risk factor for CHD. Lowering cholesterol levels, particularly circulating low-density lipoprotein cholesterol (LDL-C) has been the focus of the prevention of CHD and its sequels for almost 35 years (2). While 3-hydroxyl-3-methylglutaryl coenzyme reductase (HMGCR) inhibitors (statins) are the most effective drugs to treat cardiovascular diseases in many groups, their potential adverse effects (AE), such as muscle AEs (myositis as well as rhabdomyolysis) and other nonmuscle AEs (pancreatic and hepatic dysfunction), should be considered (3).

The discovery that proprotein convertase subtilisin/kexin type 9 (PCSK9) functions as a strong negative regulator of hepatic low-density lipoprotein receptor (LDLR) levels suggested a critical role in low-density lipoprotein (LDL) metabolism (4-7). Importantly, gain-of-function mutations in *PCSK9* lead to hypercholesterolemia and premature atherosclerosis, while loss-of-function mutations result in lowered plasma LDL-C levels and significant protection from CHD without apparent AEs on other aspects of human physiology (8). Thus, PCSK9 is a validated therapeutic target for cholesterol lowering. Blocking antibodies raised against PCSK9 that prevent the LDLR interaction are actively being developed by pharmaceutical companies, and some are now entering Phase III clinical trials to lower plasma cholesterol levels in patients (9, 10). However, less invasive and cost effective alternatives are still sought, therefore it is important to determine the mechanisms of PCSK9-mediated LDLR degradation in the endolysosomal system.

## 1.1 Regulation of cholesterol metabolism

### 1.1.1 Cholesterol, the central lipid of mammalian cells

Cholesterol has been extensively studied since the French chemist, M. E. Chevreul, discovered it in 1815. For over 100 years, cholesterol's structure, biosynthetic pathways as well as feedback mechanisms regulating cholesterol metabolism have been revealed and characterized (11).

Mammalian cells acquire cholesterol endogenously as well as exogenously. Whereas extrahepatic tissues obtain most of their cholesterol from *de novo* biosynthesis, in hepatocytes, most cellular cholesterol is derived from the circulation in the form of apolipoprotein (Apo) B-containing lipoproteins such as LDL (12). Cholesterol is synthesized in the endoplasmic reticulum (ER) and cytoplasm from the two-carbon building block, acetyl-CoA, through the mevalonate pathway (13). The cholesterol biosynthetic pathway has been considered as a complex pathway related to more than 40 cytosolic and membrane-bound enzymes. At least 14 enzymes in this biosynthetic pathway are subjected to feedback regulation by cellular cholesterol levels, of which the rate-limiting enzyme is HMGCR that catalyzes the conversion of HMG-CoA to mevalonate and is the common target for cholesterol lowering drugs such as statins as mentioned above (14, 15). After the first committed step in cholesterol synthesis that converts squalene to the first sterol (lanosterol), cholesterol is synthesized by a series of oxidation, reduction and demethylation reactions (16, 17). There are evidences for two alternative pathways in the last steps of cholesterol synthesis that differ in the point at which Δ24 double bond is reduced. Both 7-dehydrocholestrol and desmosterol have been demonstrated to be the immediate precursors of cholesterol (18, 19).

In addition to *de novo* synthesis, cells can obtain cholesterol via the LDLR-mediated

uptake of plasma lipoproteins (20). Enterocytes of the small intestine play a key role in absorbing and packaging dietary cholesterol, along with triglycerides, into chylomicrons. When chylomicrons reach the circulation via the lymph, lipoprotein lipase hydrolyzes some of the triglycerides, and the chylomicron remnants will be taken up by hepatocytes. Hepatocytes also secrete lipids in the form of very low-density lipoprotein (VLDL) particles that are processed in the circulation into LDL, the main lipoprotein that delivers cholesterol to the peripheral cells (21). LDL along with other ApoE/ApoB-containing lipoproteins is subsequently taken up through LDLR-mediated endocytosis (22).

Among many lipids in mammalian cells, cholesterol has an undeniable importance. Based on its biophysical properties, cholesterol serves as a vital constituent of mammalian cell membranes. Particularly, cholesterol condenses and rigidifies bilayers of phospholipids with unsaturated fatty acyl chains. On the other hand, it helps to modulate membrane fluidity and permeability of bilayers containing saturated phospholipids and sphingolipids (23). Cholesterol also plays an important role in the production of all steroid hormones, bile acids, and vitamin D as well as in cellular functions such as transmembrane signaling processes, membrane trafficking and cell proliferation (24, 25). Nevertheless, insufficient or excessive levels of cellular cholesterol can result in abnormal cellular processes, and subsequently, lead to serious diseases such as atherosclerosis and type II diabetes (26). It is no wonder that cholesterol homeostasis is among the most intensely regulated processes in cell biology.

### 1.1.2 SREBPs: main regulators of cholesterol homeostasis

Cells have developed a tightly controlled manner to regulate cholesterol homeostasis via membrane-bound transcription factors called sterol regulatory element binding proteins (SREBPs). SREBPs are members of the basic helix-loop-helix leucine zipper (bHLH-Zip) family of transcription factors that regulate genes encoding proteins required for cholesterol,

fatty acid, and phospholipid synthesis (28, 29, 30). SREBPs consist of three isoforms: SREBP-1a, SREBP-1c and SREBP-2. SREBP-1a and SREBP-1c are products of the same gene *Srebp-1*, but differ in their first exons by the alternative transcriptional start site. SREBP-2 is the product of a separate gene, *Srebp-2*. SREBP-1c mainly regulates fatty acid synthesis and insulin-mediated glucose metabolism, whereas SREBP-2 is involved in cholesterol synthesis. In contrast, SREBP-1a seems to activate genes in both biosynthetic pathways (28, 30, 31).

SREBPs are synthesized as inactive precursors that attach to the ER membrane in a hairpin fashion (32, 33). To exert their transcriptional activity, SREBPs must translocate from the ER to the Golgi for the proteolytic processing that converts precursor membrane-bound SREBPs into their soluble active forms. Following translation, SREBPs bind to SREBP cleavage-activating protein (SCAP) that plays a major role in trafficking of SREBPs by acting as an escort protein and sterol sensor (34). However, during sterol-rich conditions, SREBPs are retained in the ER by the binding of SCAP to the insulin-induced gene 1 (INSIG-1). This ER anchor protein binds to the sterol-sensing domain of SCAP and prevents the SCAP/SREBP complex from entering the coat protein complex II (COPII)-dependent ER-Golgi trafficking (35, 36). When intracellular cholesterol levels are low, SCAP undergoes a conformational change, allowing its dissociation from INSIG-1; subsequently, resulting in the interaction with the COPII trafficking complex and the proper transport of SREBPs to the Golgi. Here, SREBPs are cleaved at two sites by two membrane-bound proteases, site-1 protease (S1P) encoded by MBTPS1 gene and site-2 protease (S2P) encoded by MBTPS2 gene, and release the active $NH_2$-terminal domains that translocate to the nucleus and activate lipid metabolism genes, such as HMGCR and the LDLR (35, 36, 37) (Figure 1.1).

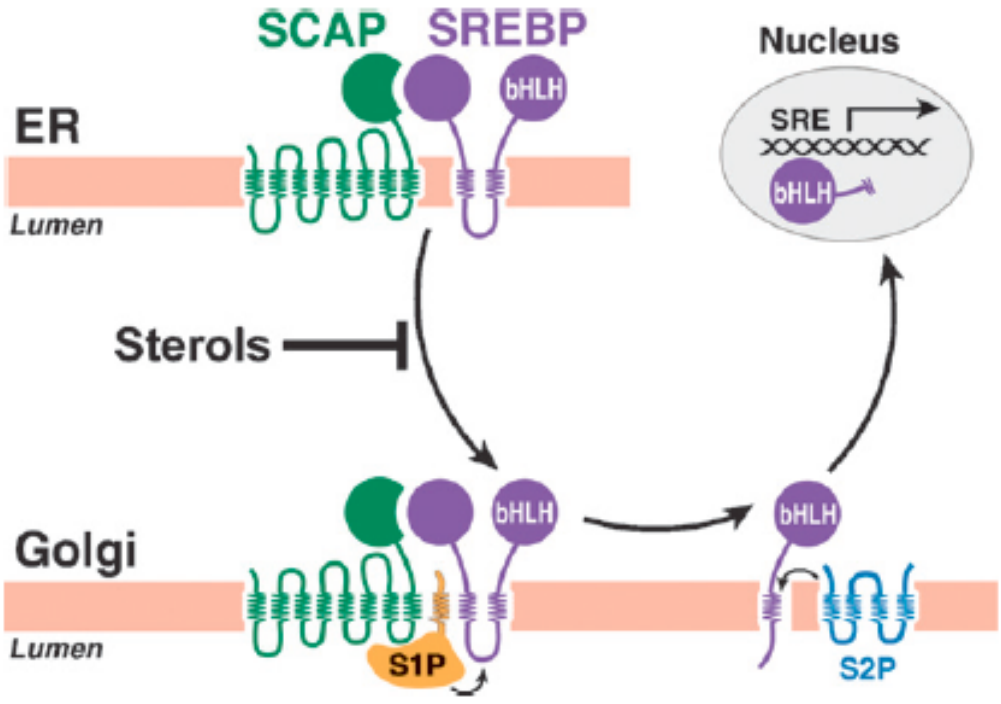


***Figure 1.1. The SREBP pathway.*** Following synthesis in the RE, SREBP transcriptional factors are retained at the membrane as a complex with SCAP. Both of the N- and C-terminus of SREBPs point toward the cytoplasm to form a hairpin structure. In response to sterol depletion, SCAP serves as an escort protein that directs SREBPs to transport vesicles, and subsequently, to the Golgi. In the Golgi, SREBPs undergoes two steps of proteolysis mediated by S1P and S2P, Golgi-located proteases. S1P cleaves the luminal loop between two membrane-spanning helices of SREBPs, whereas S2P separates the N-terminal bHLH-Zip domain from the membrane-spanning region. This second cleavage releases soluble SREBPs that translocate to the nucleus and transcriptionally activate the expression of critical genes in lipid metabolism. Image taken from Brown and Goldstein (2009) (27).

In addition to regulation at the processing level, SREBP activity can be controlled in numerous other ways. For example, in the absence of sterols, SREBP-2 and SREBP-1c can activate the expression of their own genes in a feed-forward manner via the sterol response elements (SRE) located in their respective promoter regions (29). Nuclear SREBPs can also be modified by ubiquitination, leading to their degradation by the 26S proteasome or by SUMO-1 to repress transcriptional activity (38, 39). Recently, it has been shown that sirtuin 1 (SIRT1), a $NAD^+$-dependent deacetylase, can decrease the stability of these transcriptional factors via deacetylation (40). In contrast, the acetylation of SREBP-1a and SREBP-1c by the transcriptional activator, p300, stabilizes their structures, resulting in significant increases of the expression of target genes (29).

## 1.2 LDLR and LDL uptake

### 1.2.1 LDLR

An important component of cholesterol homeostasis is the SREBP-2 – regulated cell surface LDLR. LDLR serves as the principal receptor for cellular cholesterol uptake, mediating the endocytic removal of cholesterol-containing particles (VLDL, VLDL remnants and LDL) from the circulation (41, 42).

*Domain organization of LDLR*: First discovered by Brown and Goldstein in 1974, the mature LDLR is a modular, trans-membrane glycoprotein of 839 amino acids (42). The amino terminus of the receptor contains seven adjacent LDLR type-A (LA) modules that act in combination to bind to various lipoproteins, including LDL and β-VLDL particles. Among the LA repeats, LA3 to LA7 are responsible for binding to LDL (43, 44, 45). Immediately C-terminal to these ligand-binding repeats of the LDLR is the epidermal growth factor (EGF)-precursor homology domain, including two EGF-like modules (EGF-A and EGF-B),

followed by a YWTD β-propeller domain and a third EGF-like module (EGF-C). This homologous region of the LDLR is involved in the release of bound lipoproteins at low pH as well as the receptor-recycling to the cell surface. Several studies confirmed that despite maintaining binding to β-VLDL and to a lesser extent, LDL, deletion of the entire EGF-homology domain not only eliminates the acid-dependent lipoprotein release but also inhibits the efficient receptor-recycling (46, 47, 48). The importance of this EGF precursor domain is also further highlighted by the fact that more than 50% of human familial hypercholesterolemia (FH) point mutations occur in this region (49).

Following the EGF homology domain, a region that is rich in serine as well as threonine and undergoes O-linked glycosylation serves as a spacer isolating the functional domains of the LDLR from the cell surface. The glycosylated region is followed by a transmembrane segment and a 50-residue cytoplasmic tail, which plays a necessary role in receptor localization into clathrin-coated pits as well as receptor endocytosis (50, 51).

*LDLR processing:* Aiming at adjusting the number of LDLRs to provide sufficient cholesterol for metabolic needs without producing cholesterol over-accumulation, LDLR expression is subjected to feedback regulation via SREBP-2 (42). After synthesis, the 120kDa precursor form of LDLR undergoes several folding processes in the ER (52) (Figure 1.2). The receptor-associated protein (RAP) functions not only as a chaperone for the correct folding of N-terminal LA repeats but also as an inhibitor of the premature binding of co-expressed ligands (53); whereas a second kind of chaperone proteins (called Boca in Drosophila) is thought to bind the β-propeller domain in order to facilitate its proper folding (54). Briefly, each LA repeat in the ligand-binding domain contains two loops connected by three disulfide bonds, of which the second loop carries four highly conserved acidic residues

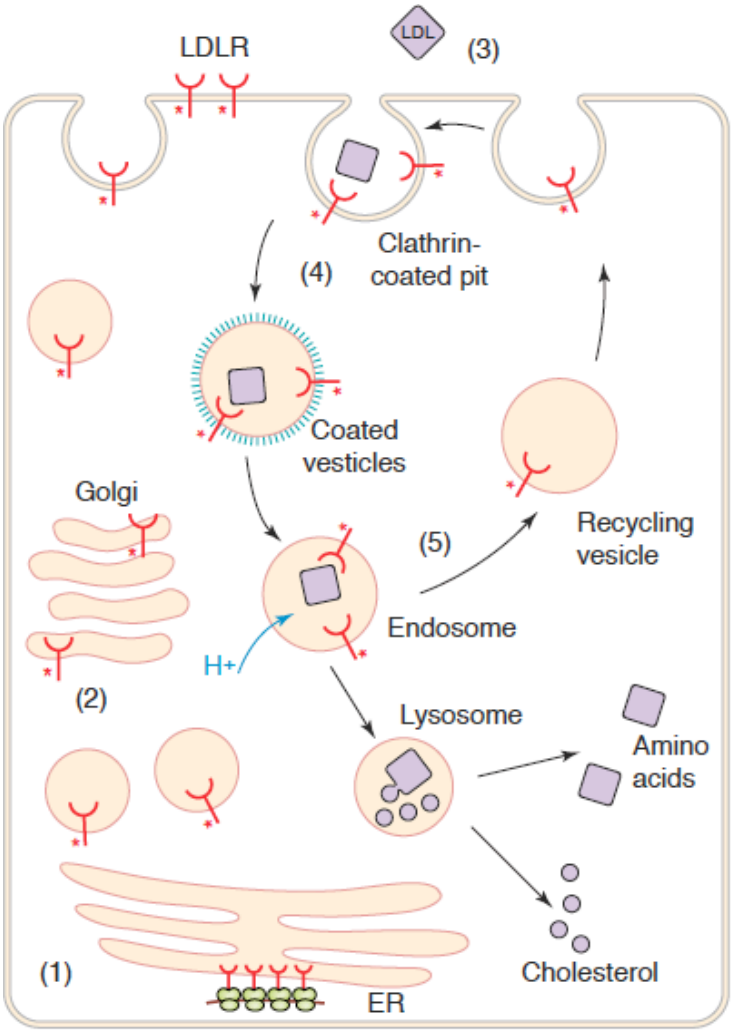


***Figure 1.2. Cellular itinerary of the LDLR.*** (1) The precursor form of the LDLR is synthesized and subjected to several folding steps in the ER. (2) After being transported to the Golgi where it undergoes extensive glycosylation, the LDLR is translocated to the cell membrane as a mature functional form. (3) At the cell membrane, the LDLR binds to circulating lipoproteins, especially LDL containing the single copy of apoB. (4) Subsequently, the receptor-ligand complex is endocytosed into clathrin-coated pits, mediated by the adaptor protein ARH, and delivered to endosomes. (5) In early endosomes where the low pH environment triggers release of the bound lipoprotein particle, the receptor separates from the ligand and recycles back to the cell surface for another round, while the released lipoprotein proceeds to lysosomes where its cholesterol esters are hydrolyzed. Images borrowed from Beglova and Blacklow (2005)(58).

near the C-terminal end of the module. These acidic residues are required to maintain the structure of cysteine-rich repeats through forming a calcium-binding site with the consensus sequence (55, 56). In the absence of calcium, the structural integrity as well as the lipoprotein-binding capacity of LA repeats is impaired (57). In addition to the ligand-binding repeats, the EGF-like modules, including EGF-A, EGF-B, and EGF-C, also contain three disulfide bonds and a calcium ion in their calcium-binding sites each (56). Finally, the LDLR precursor is transported to the Golgi where it undergoes extensive O-linked glycosylation to form the mature 160kDa receptor found at the cell surface (52).

### 1.2.2 LDLR-mediated LDL uptake pathway

*LDL uptake pathway (Figure 1.2)*: Binding of the LDLR to circulating lipoproteins, including LDL – the most important physiological ligand, occurs at the cell surface. The LDLR binds LDL via a single copy of the 550kDa ApoB, which accounts for the 1:1 stoichiometry between LDL and the LDLR (59, 60). In the ligand recognition of LDLR, the C-terminal acidic residues on each LA repeat form a discrete patch of electron-negative surface that interacts with positive charges on ApoB. Indeed, selective chemical modifications of conserved basic residues on ApoB completely disrupted the LDLR binding to LDL (61, 62).

Upon ligand binding, the receptor-ligand complexes are endocytosed into clathrin-coated pits (63). Endocytosis of the LDLR requires the participation of a NPXY sequence in the cytoplasmic tail and an adaptor protein called autosomal recessive hypercholesterolemia (ARH) in hepatocytes. ARH contains a PTB domain that can simultaneously bind the NPXY sequence of LDLR and components of the endocytic machinery, including a canonical clathrin-binding sequence LLDLE and a sequence recognized by the β2-adaptin subunit of adaptor protein AP-2 (64). The complexes are then delivered to endosomes, where the low

pH as well as low calcium environment triggers the release of bound lipoprotein particles. After this dissociation, the receptors recycle back to the cell surface while the released lipoproteins proceed to lysosomes where its cholesterol esters are hydrolyzed (42, 65). The LDLR makes one round trip every 10 minutes whether it is carrying bound lipoproteins or not, and had a total of several hundred trips during its 20-hour lifespan (66).

*Critical conformational rearrangements for lipoprotein release by the LDLR*: Dissociation of LDL particles from the LDLR at low pH results from the formation of two interfaces described below. The primary interactions required for LDL release are the contacts between LA4 and LA5 repeats with the β-propeller domain, in which the propeller domain acts as an alternative intramolecular ligand for the central lipoprotein-binding repeats at acidic pH instead of LDL. In this structure, the calcium-binding loops of both LA4 and LA5 dock side by side to the six-bladed sheet of the β-propeller domain, providing this domain with 14 major residues to form an interface mediated by hydrophobic and charged interactions. Among these residues, three histidine residues (H190, H562, and H586) serve as pH sensors to promote closure of the receptor at acidic conditions (49, 56, 58).

Structural studies also revealed another interface related to release of LDL particles at low pH. Along with the terminal ligand-binding repeat LA7, the EGF-A module forms a pH-invariant scaffold, functioning as an anchor to limit central ligand-binding repeats to a smaller conformation search space and to help them easily dock into the propeller domain. By this way, the elbow-shaped scaffold facilitates the intracellular closure of LDLR at low pH, and then the release of bound lipoprotein particles as well as the receptor-recycling to the cell surface by converting the receptor from an open ligand-binding active conformation to a closed ligand-binding inactive conformation (49, 58).

## 1.3 PCSK9: a new player in cholesterol metabolism

The PCSK9 story started in February 2003 when Nabil Seidah, a biochemist at the Clinical Research Institute of Montreal, and his colleagues discovered a new member of the proprotein convertase family called neural apoptosis regulated convertase 1 (NARC-1) as well as its coding gene located on the short arm of chromosome 1 (67). Mutations in this newly discovered gene, whose name was changed to *PCSK9* later, were found in two French families with hypercholesterolemia in whom previous investigations failed to identify mutations in either *LDLR* or *ApoB* genes (68). Especially, Kara Maxwell and Jay Horton not only identified *PCSK9* as a novel SREBP-regulated gene in mice but also uncovered its role in regulating cholesterol via a previously unknown pathway (4, 69, 70). Since then, PCSK9 has become the most promising target for several hundred studies related to hypercholesterolemia and CHD.

### 1.3.1 Structure and processing of PCSK9

*Structure:* PCSK9 is the ninth known member of the proteinase K subfamily of subtilisin-related serine endoproteases, which is predominantly expressed in liver, intestine and kidney (71). PCSK9 mRNAs are also present in the developing brains (67). The human *PCSK9* gene, which is located on chromosome 1p32.3, is about 22kb-long and consists of 12 exons encoding a 692 amino acid glycoprotein (4, 5, 67).

Like other members of this family, PCSK9 shares the general structure that consists of a signal sequence, followed by a prodomain (residues 31-152), a subtilisin-like catalytic domain (residues 153-447) that contains a conserved triad of residues (Asp-186, His-226, and Ser-386), and a variable C-terminal domain (residues 452-692) (72) (Figure 1.3). The prodomain functions not only as a chaperone required for the correct folding of the catalytic domain in the ER but also as an inhibitor of catalytic activity (67).

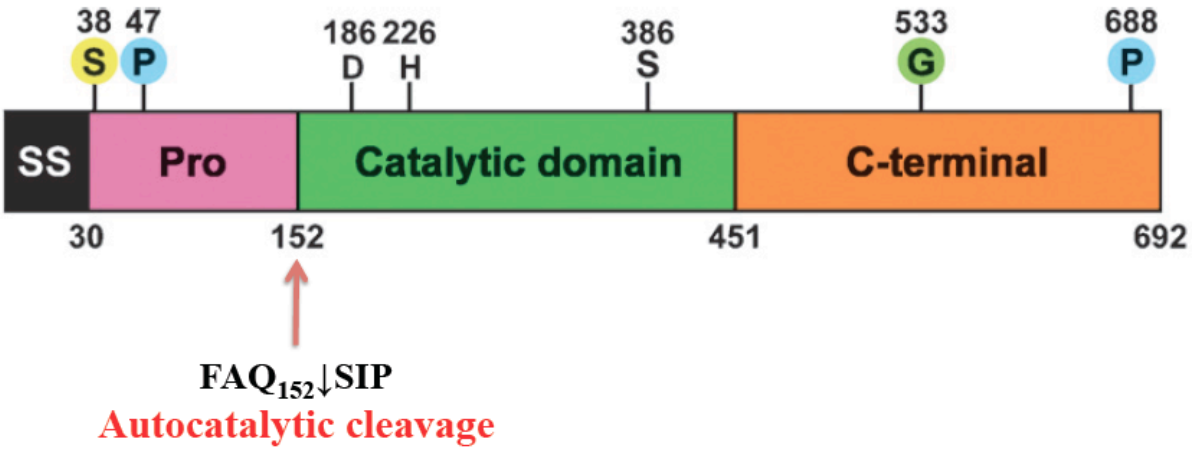


***Figure 1.3. Structure of PCSK9.*** Like other members of the proprotein convertase family, PCSK9 consists of a 30-amino acid signal sequence, followed by a prodomain (residues 31-152), a subtilisin-like catalytic domain (residues 153-451), and a variable C-terminal domain (residues 452-692) that is rich in histidine and cysteine. The catalytic domain contains a conserved triad of residues, including aspartate-186, histidine-226, and serine-386. PCSK9 is cleaved after a non-basic residue, between residues 152 and 153 ($FAQ_{152}\downarrow SIP$), producing a 14-kDa prodomain and a 60-kDa fragment. Posttranscriptional modifications of PCSK9 in the Golgi are also shown, in which the yellow circle represents sulfation at tyrosine-38, the blue circles represent phosphorylation at serine-47 and serine-688, whereas the green circle symbolizes glycosylation at asparagine-533. Images modified from Horton, Cohen, and Hobbs (2009)(72).

*Cellular itinerary of PCSK9:* PCSK9 is synthesized as an inactive 74kDa precursor that undergoes intramolecular cleavage at the boundary between the prodomain and the catalytic domain in the ER. While the first seven known convertases are typically cleaved after a basic residue, PCSK9 is cleaved after a non-basic residue, between residues 152 and 153 ($FAQ_{152}\downarrow$SIP), producing a 14-kDa prodomain and a 60-kDa fragment (5, 67, 73). However, after cleavage, the separated prodomain remains associated with the catalytic/C-terminal domains, and its last four amino acids occlude the catalytic triad (74, 75). Subsequently, this noncovalent complex is transported to the Golgi where it goes through a series of posttranslational modifications, including glycosylation, phosphorylation and tyrosine sulfation (72). PCSK9 is then rapidly secreted from the liver as a stable complex with its prosegment. Another difference between PCSK9 and other family members is that most proprotein convertases undergo a second proteolytic processing within the prodomain to generate active proteases, no evidence of the second cleavage as well as no other protein substrates for PCSK9, except itself in an autocatalytic manner, has been yet identified. Structural studies have shown that PCSK9 lacks a typical loop structure that is required for the second cleavage event (74, 76, 77).

### 1.3.2 The crystal structure of PCSK9

Three separate crystal structures of apo-PCSK9 have recently been published, revealing a tightly bound prodomain that makes the active site inaccessible to exogenous substrates as well as a C-terminal domain with a previously unknown fold (74, 78, 79). The PCSK9 prodomain comprises two α helices and a four-stranded antiparallel β sheet, of which the β sheet forms the interface between the prodomain and the catalytic domain via hydrophobic and electrostatic interactions. Particularly, the four C-terminal amino acids of

the prodomain (residues 149-152) bind the catalytic site as a β strand, in an analogous fashion to an inhibitory peptide. Gln-152 forms hydrogen bonds with His-226 and occupies the oxyanion hole located between the Ser-386 backbone nitrogen and the Asn-317 side chain amide. Furthermore, extra stabilization of the inhibitory peptide in this position, provided by a 14- amino acid extension at the N-terminus of the prodomain, further blocks access to the catalytic triad (74, 79).

The central part of the catalytic domain is composed of a seven-stranded parallel β sheet, flanked on both sides by α helices. Of note, the N-terminal α helix undergoes a considerable conformational shift following autocatalytic cleavage of pro-PCSK9, moving more than 25Å from Gln-152, and is found in a position similar to that observed in other mature subtilases. This change in conformation is thought to be a consequence of autocatalysis and necessary for secretion (78, 79). Similar to other proprotein convertases, the two α helices are involved in the interface with the inhibitory prodomain. Three disulfide bonds are also identified in this domain. Although minor differences can be observed in their positions, resulting from differences in the surrounding amino acid residues, the catalytic triad of PCSK9 is highly conserved and superimposable when compared to other subtilases. Asn-137 forms the oxyanion hole that has been proposed to be critical for catalysis (79). However, it should be noted that, different from other members, the substrate-binding groove of PCSK9, which governs the substrate specificity, is mostly neutral in lieu of being negatively charged (74).

The C-terminal cysteine-rich domain is mainly composed of three subdomains of antiparallel β strands folded in a truncated jellyroll motif. Each subdomain is stabilized by three internal disulfide bonds between the first and six cysteines, the second and fifth

cysteines, and the third and fourth cysteines cross-linking β-sheets (β1 – β6, β2 – β6, and β3 – β5, respectively). This domain is also rich in histidine residues, with the majority of them cluster on a surface between subdomains 2 and 3 (78, 79).

### 1.3.3 Regulation of PCSK9

Several findings have connected PCSK9 to cholesterol metabolism and CHD risk. In fact, a causative association was established between two nonsense mutations of *PCSK9* (Y142X and C679X) and low plasma LDL-C levels. Individuals who carry these mutations have 28% less LDL-C compared with non-carriers, which is accompanied by an astonishing 88% lower risk of developing heart diseases. Except from lower levels of total cholesterol, mainly LDL-C and triglycerides, no other clinical phenotypes such as high-density lipoprotein (HDL) cholesterol levels are identified in this population. Likewise, European people who carry the R46L missense mutation in *PCSK9* gene also exhibit significantly lower LDL-C levels, which are associated with 47% reduction in CHD risk (8, 80). In contrast, two gain-of-function alleles (S127R and F216L) that act in a dominant fashion are implicated in autosomal dominant hypercholesterolemia (ADH) in French families. ADH is an inherited disorder characterized by a selective increase of LDL-C levels in plasma and leading to cardiovascular complications. Importantly, a gain-of function mutation Asp-374-Tyr (D374Y) leads to significantly higher serum total cholesterol levels (even levels of total cholesterol on treatment with statins), which is accompanied by 10-year earlier development of premature CHD in British and Norwegian families when compared with typical heterozygous FH patients with known mutations in *LDLR* (5, 68).

Because of its importance role in LDL metabolism, it seems clinically relevant to measure circulating levels of PCSK9 in humans. Several studies have developed ELISA

assays to measure PCSK9 concentrations in human plasma, which vary over a very wide range (from 33 ng/ml to 4 μg/ml) among normal and apparently healthy individuals (84, 85, 86). The dissimilar results between these assays are likely attributable to differences in specificities among antibodies to bind plasma PCSK9 and the recombinant PCSK9 standards used in ELISA. More recently, PCSK9 plasma levels have been shown to be mirror markers of hepatic cholesterol metabolism, with increased levels following refeeding and furthermore following a diurnal rhythm (75). Thus different methods of blood collection may at least partially explain previous observations of PCSK9 variance in human plasma samples.

Like other genes involved in cholesterol metabolism such as *LDLR*, *PCSK9* is also regulated primarily at the transcriptional level by SREBPs (69, 70). SREBP binding sites, such as SRE and Sp1, were characterized in the promoter of human, mouse, and rat *PCSK9* genes. Although SREBP-1c has been suggested to be responsible for the increased PCSK9 expression in response to liver X receptor (LXR) agonists, SREBP-2 appears to play a more central role under physiological conditions. Hepatic expression of PCSK9 was significantly decreased by long-term fasting, which suppressed SREBP-2 activity, and was restored by re-feeding, which activated SREBP-2 (81, 82, 83). It was shown that PCSK9 was also down-regulated by fenofibrate, an agonist of the nuclear peroxisome proliferator-activated receptor α (PPARα), and up-regulated by cholestyramine, the bile acid-binding resin that stimulates the clearance of circulating LDL (76). The physiological importance of these regulators requires further studies.

### 1.4 PCSK9-mediated LDLR degradation

Soon after its discovery, several studies demonstrated that PCSK9 regulates LDL-C levels in human plasma by targeting the LDLR for degradation. Early studies showed that

adenovirus-mediated overexpression of *PCSK9* in mice resulted in a dramatic increase in circulating LDL particles, which was dependent on the LDLR since no effects on LDL levels were observed in LDLR null mice (4, 5, 6). In converse experiments, *PCSK9*$^{-/-}$ mice exhibited a 2.8-fold increase in liver LDLR levels compared with the wild-type animals, which were associated with a significant hypocholesterolemia profile of VLDL and LDL (87). Also, PCSK9 when added to the medium of culture cells such as human hepatoma cells (HepG2 and HuH7) or human embryonic kidney cells (HEK-293) significantly reduced LDLR levels (6, 88, 89). Particularly, the results of parabiosis studies in wild-type mice and *PCSK9* transgenic mice provided clear evidence that circulating PCSK9 could function to degrade LDLR in liver. It was reported that gain-of-function mutations of *PCSK9* decreased cell surface levels of the LDLR by 23% and LDL internalization by 38% as compared with wild-type PCSK9, whereas loss-of-function mutations resulted in a 16% increase of cell surface LDLRs and a 35% increase of LDL internalization (90). Through directly interacting with the LDLR, PCSK9 inhibits the receptor recycling and induces the redistribution of LDLR to late endosomes/lysosomes for degradation. However, the precise mechanisms by which this occurs have yet been fully defined (Figure 1.4).

### 1.4.1 Crystal structure of LDLR/PCSK9 complex

*Wild type PCSK9:* Biomedical studies showed that PCSK9-induced LDLR degradation involved the binding of PCSK9 to the first repeat in the EGF-precursor homology domain of the LDLR (91) (Figure 1.5). This binding to EGF-A module occurs with a 1:1 stoichiometry at a $K_d$ of 170-750 nM at the neutral pH of plasma (92, 93, 94), and appears to be calcium-dependent because the EGF-A interaction was completely abolished by sequestration of divalent cations using EDTA (91). In contrast to the binding of LDL particles to the LDLR,

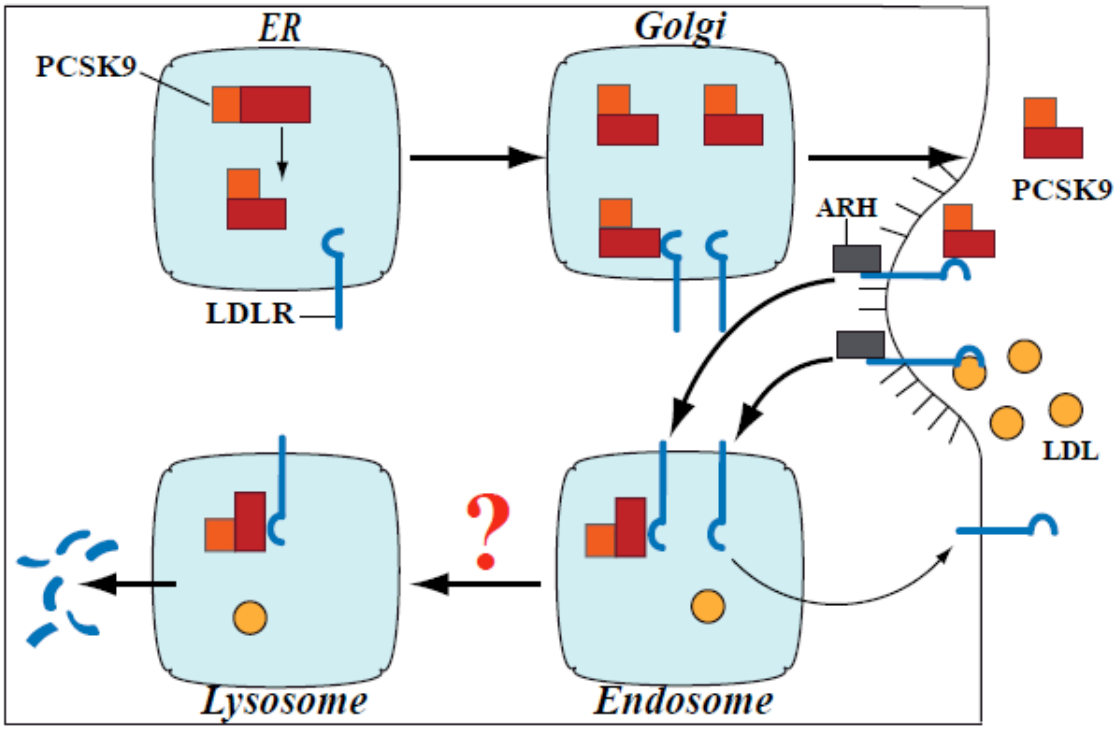


***Figure 1.4. Model of LDLR degradative pathway mediated by secreted PCSK9 in hepatic cells.*** Like the LDLR, PCSK9 is synthesized as an inactive precursor in the ER. After undergoing the autocatalytic cleavage, the separated prodomain remains associated with the catalytic/C-terminal domains, and its last four amino acids occlude the catalytic triad. Afterward, this noncovalent complex is transported to the Golgi where it goes through several posttranslational modifications, and rapidly secreted from liver. PCSK9 interacts directly with the LDLR on the cell surface, followed by the endocytosis of the complexes via the adaptor protein ARH. Different from LDL particles that release from the LDLR in early endosomes, PCSK9 still maintains the binding to the LDLR with substantially higher affinity, and then routes the receptor to lysosomes for degradation by an unknown mechanism. Images modified from Horton, Cohen, and Hobbs (2009)(72).

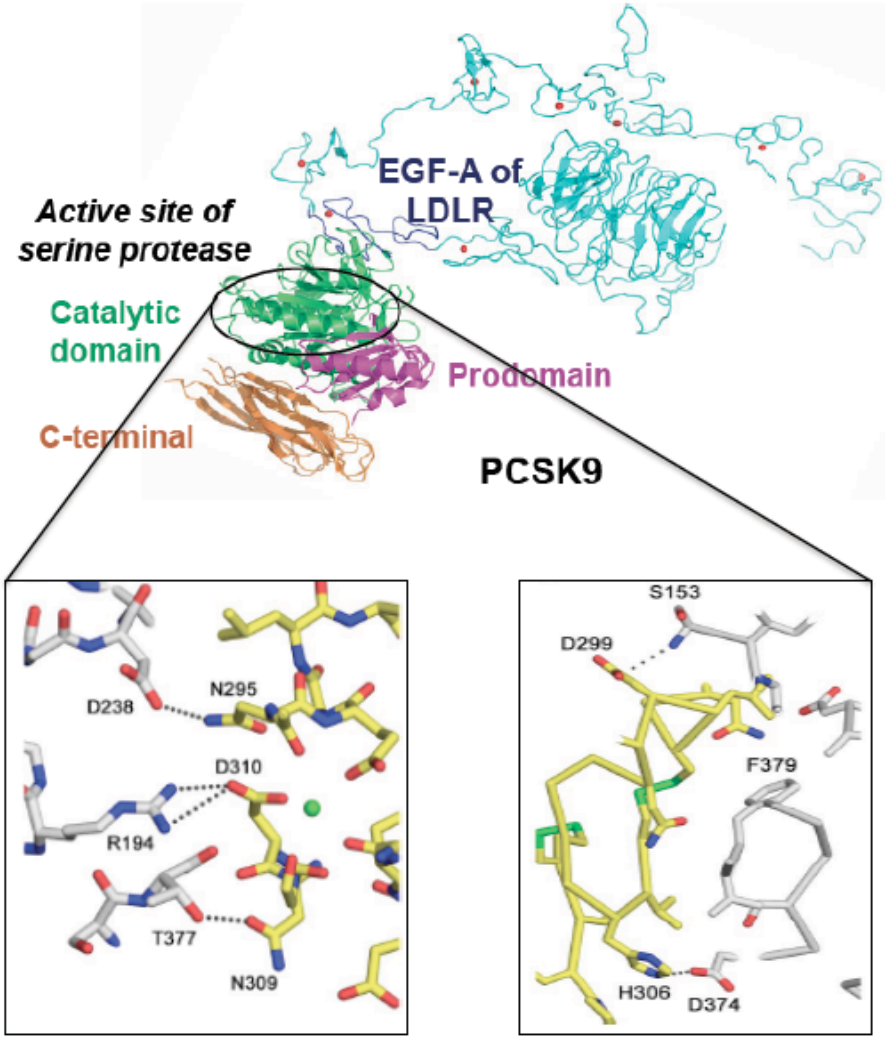


***Figure 1.5. The LDLR-PCSK9 complex at acidic pH.*** PCSK9-mediated LDLR degradation involves the binding of PCSK9 to the first EGF-homology domain of the LDLR. The affinity between PCSK9 and the LDLR is significantly enhanced in the acidic environment of endosomes. Here, three major domains of PCSK9 are shown in different color, whereas the LDLR is shown in light blue and the EGF-A domain is shown in dark blue. In this structure, phenylalanine-379 serves as a critical residue at the center of the hydrophobic surface. Several hydrogen bonds, which include interactions between (PCSK9)Aspartate-238 and (EGF-A)Asparagine-295 as well as (PCSK9)Threonine-377 and (EGF-A)Asparagine-309, are important for the specificity of the structure. Essential salt bridges between such as (PCSK9)Serine-153 and (EGF-A)Aspartate-299 , (PCSK9)Arginine-194 and (EGF-A)Aspartate-310, and (PCSK9)Aspartate-374 and (EGF-A)Histidine-306 are also shown. Images modified from Kwon et al. (2008) (96).

under acidic pH conditions of endosomes, the affinity between PCSK9 and the LDLR is substantially higher (up to 170-fold) (74, 79, 92). His-306 of the EGF-A domain serves as an important residue to help increase the binding affinity toward PCSK9 by moving from >9Å away, at neutral pH, to 4Å away from PCSK9 – Asp-374 at acidic pH, forming an intermolecular salt bridge (95). Also, it has been proposed that the prodomain as well as the histidine-rich region of the C-terminus of PCSK9 might be also responsible for the pH-dependent increase in affinity toward the LDLR (96, 97, 98).

The binding interface between PCSK9 and EGF-A is >20Å from the catalytic site of PCSK9, mainly containing residues 367-381. The prodomain and the C-terminal domain of PCSK9 are not involved in the binding to the EGF-A, whereas PCSK9 mainly contacts the N-terminal region of the EGF-A domain, but not the C-terminus. Key residues that contribute to the hydrophobic interface between PCSK9 and EGF-A include Phe-379, which is located at the center of this surface and makes a number of contacts to EGF-A, and Cys-378, which contacts an important residue of EGF-A (Leu-318) for specific binding between PCSK9 and the LDLR. Besides, other polar interactions surrounding the interface are also important for the specificity of PCSK9 binding to the EGF-A domain such as a hydrogen bond between PCSK9 – Asp-238 and EGF-A – Asn-295 or a salt bridge between PCSK9 – Ser-153 to EGF-A – Asp-299 (96). The conformational shift of PCSK9 – Ser-153 after autocatalysis, moving more than 25Å from Gln152 as mentioned above, is required for forming a salt bridge to EGF-A – Asp-299, which accounts for the incompetence of uncleaved PCSK9 in binding to the LDLR (79). Mutation of these critical contacts in either PCSK9 or the LDLR completely decreased the binding affinity between PCSK9 and the receptor (91). Most importantly, in the structure of this complex, Arg-194 of PCSK9 forms a salt bridge with EGF-A – Asp-310, a calcium-coordinating residue in the EGF-A repeat (96).

The specificity of this interaction was highlighted by studies in which Asp-310 residue of EGF-A or PCSK9 – Arg-194 was changed into Glutamine. These modifications significantly reduced the binding of PCSK9 to the LDLR by >90% (91). Because Asp-310 is involved in the salt bridge with Arg-194, it just contributes one of its side-chain oxygen atoms for the calcium coordination. The other calcium ligands in the EGF-A module consist of the side-chain oxygen from Glu-296; the carbonyl oxygens of Thr-294, Leu-311, and Gly-314; and a water molecule, forming a classic pentagonal bipyramid. Besides, there is a seventh ligand, the carbonyl oxygen of Cys-292 (96).

*Gain-of-function mutation D374Y:* Among natural mutations of *PCSK9*, D374Y was characterized to be about 10-fold more active than wild-type PCSK9 in degrading LDLRs (7) because of 5 to 30-fold greater affinity in binding to the LDLR when compared with the wild-type PCSK9. At neutral pH, Tyr-374 in lieu of Asp-374 forms a hydrogen bond with the backbone carbonyl atom of EGF-A – Cys-319, resulting in a considerable increase in total buried surface at the interface due to packing of the aromatic side chain of PCSK9 – Tyr-374 against EGF-A – Leu-318 (93). At acidic pH, the hydroxyl group of Tyr-374 is ~3Å from EGF-A – His-306, forming a favorable hydrogen bond. These additional interactions account for the enhanced affinity of PCSK9 – Tyr-374 toward the LDLR, thus providing a molecular basis for the severe hypercholesterolemia associated with the gain-of-function mutation D374Y in humans (96).

### 1.4.2 Molecular characterization of PCSK9-mediated LDLR degradation

Although many aspects of PCSK9 as well as PCSK9-mediated LDLR degradation have not been completely understood, over the last decade the research interests surrounding this protein have dramatically grown, and mechanistic along with molecular studies related

to it have gained significant achievements. Numerous elegant works have provided us deeper insights into underlying mechanisms for PCSK9-mediated LDLR degradation.

*PCSK9 internalization requires the LDLR:* In hepatocytes, secreted PCSK9 or purified PCSK9 added to culture medium directly contacts with the LDLR on the cell surface. PCSK9 is then internalized into the cells as a complex with the LDLR, and traffics to endosomes/lysosomes to direct the receptor for degradation. PCSK9 endocytosis was mediated by the LDLR as LDLR deficiency in hepatocytes from LDLR-null mice as well as RNA interference-mediated knockdown of LDLR markedly reduced PCSK9 endocytosis (7, 99). Moreover, McNutt et al. (95) showed that addition of the LDLR(H306Y) subfragment, which abolished the interaction of purified PCSK9 and the LDLR on the cell surface due to the increased binding affinity toward PCSK9, completely blocked uptake of PCSK9 in HuH7 cells. In addition, several studies showed that PCSK9 also binds to very low-density lipoprotein receptor (VLDLR) and apolipoprotein E receptor 2 (ApoER2), also known as low-density lipoprotein receptor-related protein 8 (LRP8), with significantly lower affinity when compared to LDLR interaction. For example, PCSK9 failed to bind cells that expressed VLDLRs after 2-hour treatment (91); however, overnight incubation resulted in an increased association of PCSK9 to these cells (110). VLDLR and ApoER2 receptors are not highly expressed in hepatic cells, and they also do not contain Leu-318 residue shown to be important for PCSK9 interaction. When Leu-318 was introduced into the VLDLR, this construct was able to bind to PCSK9 equally compared to the LDLR (91), thus confirming the defined molecular basis for the specificity of binding to the LDLR EGF-A domain.

*Clathrin-mediated endocytosis is necessary for PCSK9 to degrade LDLRs*: Clathrin-mediated endocytosis is the major route of entry for many cargos in cells. Clathrin also participates in the delivery of proteins from the Golgi to the cell surface (100). RNA

interference-mediated knockdown of clathrin heavy chain significantly abolished PCSK9-mediated LDLR degradation without affecting the enrichment of LDLRs on the cell surface (101, 102). So, PCSK9 uses the same endocytic machinery that imports LDL to promote LDLR degradation.

*The catalytic activity of PCSK9 is not required for its function:* Replacement of catalytic histidine residue in PCSK9 by alanine completely abolished its autocatalytic cleavage, and resulted in PCSK9 remaining sequestered in the ER. So, autocatalytic activity seems necessary for PCSK9 proper folding as well as secretion. However, it is not required for PCSK9-mediated LDLR degradation (103). To overcome the requirement of PCSK9 catalytic activity for its maturation, a PCSK9 construct lacking its prodomain and containing an inactive catalytic residue (Ser-386-Ala) was expressed *in trans* with the prodomain, which yielded the catalytically inactive PCSK9 secreted in a manner similar to wild-type PCSK9. Interestingly, this catalytic-dead version of PCSK9 degraded LDLRs to the same extent as a catalytically active counterpart in HepG2 cells.

*PCSK9 directs the LDLR to lysosome for degradation via a mechanism that is not related to ubiquitination as well as proteasomes, autophagy, and canonical ESCRT pathway:* Cell fractionation and imaging studies confirmed that PCSK9 interfered with the LDLR recycling to the cell surface, and routed the receptor to lysosomes for degradation. Moreover, treatment of HuH7 cells with the lysosomal protease inhibitor E64d completely inhibited PCSK9-mediated LDLR degradation (7, 102, 101). Some cell surface receptors, including the LDLR, also undergo degradation via ligand-induced ubiquitination of lysine residues in their cytoplasmic tails. These ubiquitinated receptors are then targeted to lysosomes or proteasomes for degradation. IDOL is an E3 ubiquitin ligase that is transcriptionally activated by LXR agonists, instead of SREBP transcriptional factors. Several studies showed

that by promoting the ubiquitination of the LDLR, IDOL targeted the receptor for lysosomal degradation (13). However, mutation of lysine and cysteine residues in the cytoplasmic tail of the LDLR failed to interrupt PCSK9-mediated receptor degradation, suggesting that PCSK9 did not promote the LDLR ubiquitination. Besides, using proteasome inhibitors did not affect the ability of PCSK9 to reduce LDLR levels in hepatic cells. So, PCSK9 acts independently of ubiquitination and proteasomes to degrade LDLRs (102).

Several integral membrane proteins such as EGF receptor and ATP-binding cassette transporter ABCA1 are delivered from endosomes to the multivesicular bodies (MVBs) and then lysosomes by the endosomal sorting complex required for trafficking (ESCRT) pathway. Inactivation of the initial components of the ESCRT machinery such as hepatocyte growth factor-regulated Tyr-kinase substrate (HRS) and tumor susceptibility gene 101 (TSG101) did not inhibit PCSK9-mediated LDLR degradation in many cell types. However, it is still possible that silencing RNA-mediated knockdown of HRS and TSG101 do not completely inactivate the ESCRT pathway. Furthermore, PCSK9-induced LDLR degradation may not require first components to enter the ESCRT pathway (102). These results still need to be confirmed in future studies. Finally, depletion of Atg5 and Atg7, core components required for autophagosome formation, failed to abolish LDLR degradation mediated by PCSK9, indicating that PCSK9 did not use the basic molecular machinery of autophagy to degrade LDLRs.

*Structural requirements for PCSK9-mediated LDLR degradation:* As mentioned above, PCSK9 binds specifically to the EGF-A module of the LDLR in a calcium-dependent manner (91). While other regions, including the β-propeller domain and at least three ligand-binding repeats, are not required for PCSK9 binding or LDLR internalization, they play

important roles in PCSK9-mediated LDLR degradation. Similarly, the C-terminal domain of PCSK9 is also essential for its activity on LDLRs although this domain does not bind the receptor. Actually, it was suggested that the C-terminus might either prevent the LDLR from binding to proteins required for recycling to the cell surface or provide a site for interaction with other proteins that direct the receptor to lysosomes for degradation (104, 105). Further studies are needed to define the functional role of these domains in PCSK9-mediated LDLR degradation.

*PCSK9 disrupts the acid-dependent change in LDLR conformation:* Under acidic conditions of endosomes, the LDLR changes from an open ligand-binding active conformation to a closed ligand-binding inactive conformation, which facilitates the release of LDL particles (49, 58). PCSK9 was shown to prevent the pH-dependent change in LDLR conformation; however, disrupting this conformation shift of the receptor was not sufficient for explaining PCSK9 activity since the LA4 and LA5 repeats were not required for PCSK9-mediated LDLR degradation. Besides, PCSK9 efficiently degraded the mutant LDLR lacking four ligand-binding repeats, but not the LDLR lacking five ligand-binding repeats although both forms disrupted the pH-dependent conformational change of the LDLR (104).

### 1.4.3 Sites of action

Although the intracellular itineraries of PCSK9 and the LDLR are similar, their paths become diverged at the cell surface, where the LDLR still attaches to the cell membrane and PCSK9 is rapidly secreted into the circulation (58, 72). Secreted PCSK9 from transgenic mice was able to reduce hepatic LDLR levels in recipient wild-type mice when it was transferred via shared circulation in parabiosis experiments (7). In addition, single injection or continuous infusion of recombinant human PCSK9 (32μg) to mice decreased hepatic

LDLR levels by ~90% within 60 minutes or 2 hours, respectively (106), supporting the extracellular mechanism of PCSK9-mediated LDLR degradation. In this pathway, PCSK9 is secreted from cells and directly interacts with the LDLR on the cell surface; subsequently, extracellular PCSK9 is internalized together with the LDLR and directs the receptor for lysosomal degradation. The extracellular mechanism requires the presence of ARH, an adaptor protein necessary for the endocytosis process of the LDLR in hepatocytes. In fact, PCSK9 failed to decrease surface LDLR levels, and the LDLRs were visualized almost entirely on the cell surface in hepatocyes derived from $Arh^{-/-}$ mice (7, 99). However, a previous study demonstrated that adenovirus-mediated PCSK9 overexpression promoted similar hepatic LDLR degradation in ARH knockout and control mice (6). Additionally, PCSK9 enhanced degradation of mature LDLRs as well as precursor forms of the LDLR in post-ER compartments of HepG2 cells (107), indicating that PCSK9 might also act on the LDLR before it reached the cell surface. Support for an intracellular mechanism is also derived from a study in which Nassoury et al. identified the ER-localized proform of PCSK9 bound to the LDLR in the early secretory pathway when both proteins were overexpressed in cultured cells (101). This may involve other domains of the LDLR since, as mentioned previously, structural studies strongly support that the interaction of PCSK9 with the EGF-A domain requires autocatalytic cleavage in order to create the binding interface of PCSK9. Moreover, present data from HepG2 cells and mouse primary hepatocytes preferred a model in which, depending on incubation time and concentrations, endogenous PCSK9 promoted both extra- and intracellular degradation of the LDLR (108). Nevertheless, around the same time, by addition of LDLR(H306Y) subfragments, which had increased binding affinity toward PCSK9, to block the extracellular pathway, McNutt et al. recovered LDLRs in cells overexpressing PCSK9 to levels approximating to those of control cells. They concluded that

if the intracellular pathway existed, it could only play a minor role in LDLR degradation promoted by PCSK9 (95). However, further studies are still needed to clearly address the relative contributions of intra- and extracellular mechanisms to PCSK9-mediated LDLR degradation under both physiological and pathological conditions.

### 1.5 Research objectives

PCSK9 mainly acts as a secreted protein, and circulating PCSK9 can mediate degradation of LDLRs in the liver. However, it is not clear to what extent PCSK9 affects LDLRs in tissues other than the liver. Therefore, our objective for the first part of this study was to assess PCSK9 activity on LDLR levels of hepatic and fibroblast cell lines. Studies in mice demonstrated that although PCSK9 in plasma was capable of decreasing hepatic LDLRs, no changes in LDLR levels were observed in the adrenal glands, proposing a cell-type specific manner of PCSK9 activity (106). Moreover, Lagace et al. (2006) showed that exogenous PCSK9 failed to degrade LDLRs in mouse embryonic fibroblasts despite its normal LDLR-dependent uptake into these cells (7). Recently, it was also found that stable levels of LDLR were similar in the brains of wild type, PCSK9-knockout and human PCSK9-overexpressing mice (117). Based on these data, we hypothesized that PCSK9 degrades LDLR in a cell-type dependent manner.

In the second part of this study, our objective was to better understand the underlying mechanisms for dissimilar responses to PCSK9-mediated LDLR degradation in hepatic and fibroblast cells. Particularly, we wanted to gain further insights into the trafficking of PCSK9 after being internalized in responsive and nonresponsive cells. In PCSK9-responsive cells, exogenous PCSK9 was endocytosed as a complex with the LDLR, followed by the delivery of whole LDLR/PCSK9 complex to lysosome for degradation. However, it was shown that PCSK9 failed to decrease LDLR levels in PCSK9-nonresponsive cells despite normal

cellular uptake; however, the fate of PCSK9 after binding to the LDLR in these cells was still unknown. Illuminating the fate of PCSK9 in responsive and nonresponsive cells allowed us to explore potential factors that might affect PCSK9-induced LDLR degradation in these cell types.

To summarize, understanding how fibroblast cells are resistant to PCSK9-mediated LDLR degradation will help us gain important information relevant to the elucidation of molecular mechanisms by which PCSK9 degrades LDLRs as well as to the development of PCSK9 inhibitors for treatment of CHD.

## 2. Materials and Methods

### 2.1 Materials

#### 2.1.1 Chemicals and reagents

Cell culture medium DMEM, fetal bovine serum (FBS), newborn calf serum, and human transferrin were obtained from Gibco – Life Technologies. LysoTracker® Red DND-99, AlexaFluor® 488 protein labeling kit, and AlexaFluor® 647 human transferrin were purchased from Molecular Probes – Life Technologies. We also obtained E-64 N-[N-(L-3-trans-carboxyoxirane-2-carbonyl)-L-leucyl]-agmatine and EDTA-free Complete™ Protease Inhibitor Tablets from Roche; EZ-Link™ Sulfo-NHS-SS-Biotin from Thermo Scientific; Lipofectamine 2000 from Invitrogen – Life Technologies; PureProteome™ Streptavidin Magnetic Beads from Millipore; and IRDye® 800CW Streptavidin from LI-COR Biosciences. All other chemicals and reagents were obtained from Sigma unless otherwise specified.

#### 2.1.2 Antibodies

Monoclonal anti-LDLR antibody C7 was purified by Protein G affinity chromatography from conditioned medium of cultured mouse hybridomas purchased from Cerdalane Laboratories (ACTT); rabbit anti-serum 3143 against the C-terminal 14 amino acids of LDLR was the kind gift of Joachim Herz (University of Texas Southwestern Medical Center, Dallas, TX); a mouse antihuman transferrin receptor (mbv) antibody was purchased from Life Technologies; monoclonal anti-actin antibody (AC-10) and monoclonal anti-FLAG M2 antibody were from Sigma-Aldrich. Secondary IRDye-labeled goat anti-mouse and anti-rabbit IgG antibodies were from LI-COR Biosciences.

## 2.2 Protein assay

Protein assay was performed using Pierce™ BCA Protein Assay Kit (Thermo Scientific) according to the manufacturer's instructions. BCA Reagent A consists of sodium carbonate, sodium bicarbonate, bicinchoninic acid and sodium tartrate in 0.1M sodium hydroxide, whereas BCA reagent B contains 4% cupric sulfate. Reagent B was mixed with reagent A in a 1:50 ratio to prepare the BCA working reagent, which is stable as a clear and green solution. The sample was diluted with $ddH_2O$ to a final volume of 50 μl, in which the sample volume depends on its predicted concentration. Standard curves were prepared using a bovine albumin serum (BSA) reagent with concentrations ranging from 4-32 μg/ml. 1 ml of the BCA working reagent was added to all samples that were then incubated at 37°C for 30 minutes. Absorbance was read at 562 nm on a BIOWAVE II (Biochrom Ltd.) and plotted against the determined standard curve.

## 2.3 Purification of human wild-type PCSK9 and PCSK9(D374Y)-FLAG fusion proteins

FLAG epitope-tagged recombinant human wild-type PCSK9 and PCSK9 containing the gain-of-function D374Y mutation were produced in stably transfected HEK293S cells and purified similar to previously described (7). Briefly, HEK293S cells stably expressing FLAG-tagged wild-type PCSK9 or PCSK9-D374Y were cultured in suspension without $CO_2$ in UltraDOMA™ hybridoma serum-free growth medium (Lonza) supplement with 10% (v/v) FBS, 2 mM L-Glutamine, 100 U/ml penicillin, and 100 μg/ml streptomycin sulfate. Recombinant PCSK9 was purified from the conditioned medium of HEK293S by using anti-FLAG M2 affinity gel (Sigma) chromatography according to the manufacturer's instructions, followed by size-exclusion chromatography on a Tricorn high performance column

(Superdex 200 10/300 GL-GE Healthcare). Fractions containing PCSK9 peak were concentrated approximately 8-fold using Amicon Ultra-4 Centrifugal Filter Units (10 kDa-molecular weight cut-off) (Millipore). Protein concentration was identified by protein assay, and protein purity was monitored by SDS-PAGE along with Coomassie Brilliant Blue R-250 Staining (Bio-Rad).

### 2.4 Tissue culture medium

Medium A contained DMEM and 4.5 g/l glucose, supplemented with 100 U/ml penicillin and 100 μg/ml streptomycin sulfate. Medium B contained medium A supplemented with 10% (v/v) FBS. Medium C contained medium A with 5% (v/v) newborn calf lipoprotein-deficient serum (NCLPDS), 50 μM sodium mevalonate, and 10 μM pravastatin. Medium D contained medium A with 5% (v/v) NCLPDS, 1 μg/ml 25-hydroxycholesterol, and 10 μg/ml cholesterol. Medium E contained DMEM and 1 g/l glucose, supplemented with 100 U/ml penicillin and 100 μg/ml streptomycin sulfate. Medium F contained medium E supplemented with 10% (v/v) FBS. Medium G contained medium E with 5% (v/v) NCLPDS, 50 μM sodium mevalonate, and 10 μM pravastatin. Medium H contained medium E with 5% (v/v) NCLPDS, 1 μg/ml 25-hydroxycholesterol, and 10 μg/ml cholesterol.

### 2.5 Protein labeling

#### 2.5.1 AlexaFluor® 488- labeled proteins

Recombinant human wild-type PCSK9 along with PCSK9-D374Y, and C7 antibody were labeled according to the manufacturer's instructions. Briefly, the protein was diluted to 2 mg/ml in HEPES-buffered saline buffer, supplemented with 2 mM $CaCl_2$ (HBS-C), and was subsequently mixed with 50 μl of 1M bicarbonate. The protein solution was transferred

to the vial of reactive dye that contained a magnetic stir bar, and was suspended a few times to completely dissolve the dye. The reaction mixture was allowed to sit for 1 hour at room temperature, followed by the separation of labeled proteins from unincorporated dye using size-exclusion chromatography. Protein concentration was identified by protein assay, and labeled proteins were stored in aliquots at -80$^{o}$C.

### 2.5.2 Biotin-labeled proteins

Recombinant human wild-type PCSK9 as well as PCSK9-D374Y, and human transferrin were diluted to 2 mg/ml in HBS-C buffer. 40 μl of 0.67M borate buffer was added to each protein solution to get 50 mM final concentration. A 10 mM solution of Sulfo-NHS-SS-Biotin was prepared by dissolving 6mg of reagent in 1 ml of dd$H_2O$. The appropriate volume of biotin solution added to each protein solution was calculated according to the manufacturer's instructions. The reactions were incubated on ice for 2 hours; subsequently, was stopped by quenching buffer (25 mM Tris-HCl, pH 7.4; 192 mM Glycine). Labeled proteins were purified by size-exclusion chromatography, and protein concentration was determined by protein assay.

## 2.6 PCSK9 cellular uptake assay

SV589 human skin fibroblasts were grown in medium B to ~80% confluence, and then were cultured in sterol-depleting medium C and sterol-supplemented medium D for 18 hours to up-regulate and down-regulate LDLR expression, respectively. Similarly, HepG2 human hepatoma cells were grown in low-glucose medium F to ~80% confluence, and then were cultured in medium sterol-depleting G and sterol-supplemented medium H for 18 hours. These mediums were supplemented with E64 to inhibit lysosomal degradation (102). Following 1 hour of incubation with AlexaFluor® 488-labeled PCSK9-D374Y (1 μg/ml),

the medium was replaced with stripping buffer (100 mM Na 2-mercapto-ethanesulfonate; 50 mM Tris, pH 8.6; 100 mM NaCl; 1 mM EDTA; 0.2% BSA). Cells were collected and filtered through a 70 μM sterile cell strainer (BD Biosciences). An additional 0.5 ml of sterile phosphate-buffered saline (PBS) was used to collect excess cells from the wells. Samples were spun at 1,000 rpm for 5 minutes and resuspended in 300 μl of PBS, followed by the analysis on BD FACSAria flow cytometer and cell sorter (BD Biosicences).

**2.7 Biotinylation and immunoblot analysis**

SV589 cells were grown in medium B to ~80% confluence, and then were cultured overnight in sterol-depleting medium C to induce LDLR expression prior to treatment with purified wild-type PCSK9 or PCSK9-D374Y. Similarly, HepG2 cells were grown in medium F to ~80% confluence, and then were cultured overnight in medium G prior to treatment with PCSK9. The cells were incubated with PCSK9 for 6 hours, except the overnight experiments, in which the cells were treated with PCSK9 for 18 hours.

Cell surface proteins were biotinylated as previously described (7). Whole cell extracts were prepared with Tris lysis buffer (50 mM Tris-Cl, pH 7.4; 150 mM NaCl; 1% Nonidet P-40 (EMD Biosciences); 0.5% sodium deoxycholate; 5 mM EDTA; 5 mM EGTA; Complete$^{TM}$ protease inhibitor cocktail; 1 mM phenylmethylsulfonyl fluoride (PMSF)). Three quarters of each cell lysate was added to the mixture of Tris lysis buffer and 50 μl streptavidin magnetic beads to bring the final volume to 500 μl. The mixture was rotated overnight at 4$^{o}$C. The pellets were then precipitated, and washed three times in lysis buffer. Cell surface proteins were eluted from the beads by adding 1X SDS loading buffer (50 mM Tris-HCl, pH 6.8; 1% SDS; 5% glycerol; 10 mM EDTA; 0.0032% bromophenol blue) and incubating for 10 minutes at 96$^{o}$C. Proteins were subjected to 8% SDS-PAGE and

transferred to nitrocellulose membranes (Bio-Rad) for immunoblot analysis. Secondary infrared dye (IRDye800)-labeled antibodies were used for detection on a LI-COR Odyssey infrared imaging system (LI-COR Biosciences). Band intensity was quantified using Odyssey 2.0 software.

### 2.8 LDLR degradation assay on 917 and HuH7 cells

Similarly, 917 human foreskin fibroblasts and HuH7 human hepatoma cells were cultured in medium B to ~80% confluence, and then were incubated in lipoprotein-deficient medium C for 18 hours to up-regulate LDLR expression prior to treatment with purified wild-type PCSK9 (5, 10, 20 μg/ml) or PCSK9-D374Y (2 μg/ml) for 6 hours. After PCSK9 treatment, cells were washed twice with PBS immunofluorescence buffer (PBS-IF; 10 mM $Na_2HPO_4$, 225 mM NaCl, 2 mM $MgCl_2$, 0.1 mM $CaCl_2$, pH 7.4), and fixed with 3.7% formaldehyde in PBS-IF for 15 minutes. Cells were then incubated for 5 minutes with 1% glycine (w/v) in PBS-IF and rewashed three times with PBS-IF, followed by the standard staining procedure as described. Briefly, cells were blocked with 1% BSA (w/v) in PBS-IF for >30 minutes at room temperature prior to overnight incubation with the primary antibody, AlexaFluor® 488-labeled C7 antibody. C7 antibody was used at 20 μg/ml to detect cell surface LDLRs. At the final steps, cells were subjected to three 10-minute washes in 1% BSA (w/v) in PBS-IF, and collected for flow cytometry as described above. Samples were analyzed on BD FACSAria flow cytometer and cell sorter (BD Biosicences).

### 2.9 $^{125}$I-radiolabeled PCSK9 degradation assay

SV589 cells were grown in medium B to ~80% confluence, and the medium was then switched to medium C. Similarly, HepG2 cells were grown in medium F to ~80% confluence, and the medium was then switched to medium G. After 18 hours, the cells were

washed with PBS and incubated in 1 ml of medium A containing ~5 μg/ml $^{125}$I-labeled wild-type PCSK9 or ~1 μg/ml $^{125}$I-labeled PCSK9-D374Y for 1 hour. In negative control, 100 μM chloroquine was added to culture medium 30 minutes prior to and during later incubation to inhibit lysosomal degradation of internalized PCSK9. The medium was removed and the cells were washed with ice-cold PBS for 5 minutes. The cells were then incubated in 1.5 ml of medium A for 6 hours at 37$^{o}$C. The amounts of $^{125}$I-mono-iodotyrosine as a catabolic product when internalized $^{125}$I-labeled PCSK9 was degraded in lysosomes were determined in the medium as previously described (104). Briefly, the medium was collected and spun at 3,000 rpm for 5 minutes to remove unattached cells. 1.3 ml of the medium was transferred to new tubes, followed by the addition of 130 μl of 100% trichloroacetic acid (TCA) to obtain a TCA final concentration of 10% (v/v). Samples were incubated on ice for more than 30 minutes and spun at 13,000 rpm for 15 minutes to precipitate residual $^{125}$I-labeled PCSK9 that had not been internalized and released from the cell surface into the medium. 1 ml of supernatant was removed to 13x100mm glass tubes, and was mixed with 10 μl of 40% KI. 40 μl of 30% hydrogen peroxide was added, and the mixture was extensively vortexed. Samples were allowed to stand for 10 minutes at room temperature. 2 ml of chloroform were added, followed by 15-minute incubation at room temperature. These steps aimed at removing any free iodide. Finally, sample tubes were spun at 2,500 rpm for 2 minutes, and 700 μl of the upper aqueous layer was removed to test tubes for γ counting. The amounts of $^{125}$I-mono-iodotyrosine were normalized to protein levels determined by protein assay, and were corrected for negative controls.

## 2.10 Recycling assay

### 2.10.1 Transferrin

SV589 cells were cultured in medium B to ~80% confluence using 12-well plates, and then were cultured in serum-free medium A for >1 hour to deplete endogenous transferrin prior to incubation with labeled complexes. For monensin-treated wells, 50 μM monensin was added to culture medium more than 1 hour prior to and during later incubation to inhibit recycling of internalized Transferrin. Biotin-labeled transferrin was incubated with IRDye® 800CW Streptavidin in medium A for 1 hour at 37$^{o}$C, and the complexes were then added to the cells. After 1 hour, the cells were incubated with 20 mM Tris(2-carboxyethyl)phosphine hydrochloride (TCEP) in buffer B (PBS, 0.1 mM $CaCl_2$, 2 mM $MgCl_2$, 0.5% BSA (w/v)) for 20 minutes at 4$^{o}$C to remove cell surface labeled complexes before being subjected to two 10-minute washes with 5 mg/ml Iodoacetamide in buffer B. The cells were rewashed with buffer B as well as PBS-CM (PBS, 0.1 mM $CaCl_2$, 2 mM $MgCl_2$), and then incubated in medium A, supplemented with 20 mM TCEP, for 2 hours at 37$^{o}$C. The plate was directly scanned on the LI-COR system at the indicated time intervals to visualize internalized transferrin. Signal intensity was quantified using Odyssey 2.0 software, corrected for background using untreated wells, and normalized to DNA levels stained by DRAQ5$^{TM}$ (Cerdalane Laboratories, Canada) (1:10,000).

### 2.10.2 PCSK9

SV589 cells were grown in medium B to ~80% confluence using 12-well plates, and then were cultured in medium C, supplemented with 150 μM E-64, for 18 hours. The recycling assay was performed as described above, with the exception that the internalized complexes were chased for 6 hours in the continuous presence of both TCEP and E-64.

## 2.11 Live cell imaging for co-localization studies

### 2.11.1 PCSK9 and LysoTracker

SV589 cells were cultured in medium B to ~80% confluence using μ-slide 8-well plates, and then were cultured in medium C1 (medium C supplemented with 150 μM E-64) for 18 hours. HepG2 cells were seeded in medium F using μ-slide 8-well plates to 80% confluence, and then were cultured overnight in medium G1 (medium G supplemented with 150 μM E-64). The medium was replaced with medium C1 (or G1) containing 30 μg/ml AlexaFluor® 488-labeled wild-type PCSK9 or 5 μg/ml AlexaFluor® 488-labeled PCSK9-D374Y, and the cells were incubated for 1 hour at 37°C. The cells were washed two times with medium A before internalized AlexaFluor® 488-labeled PCSK9 was chased for 6 hours at 37°C in medium C1 (or G1). LysoTracker® Red DND-99 was used as per the manufacturer's instructions. Briefly, the stock solution of 1mM probe was diluted to the final working concentration (200 nM) in medium C1 (or G1). The cells were then incubated with LysoTracker for 2 hours prior to being washed twice with medium A and directly observed on a microscope at the indicated time intervals. Images were taken using the confocal microscope Fluoview FV1000 version 2.1 (Olympus), in which PCSK9 was visualized using a 488nm laser, and a 543nm laser was used for LysoTracker. The percentage of co-localization was quantified using Image J (http://rsb.info.nih.gov/ij/), and corrected for background using negative images.

### 2.11.2 PCSK9 and transferrin

SV589 cells were grown in medium B to 80% confluence using μ-slide 8-well plates, and then were cultured in medium C1 for 18 hours. Following >1 hour incubation in serum-free medium A1 (medium A supplemented with 150 μM E-64) to deplete endogenous

transferrin, cells were treated with AlexaFluor® 488-labeled PCSK9-D374Y (or AlexaFluor® 488-labeled wild-type PCSK9) and AlexaFluor® 647-labeled transferrin for 1 hour at 37$^{o}$C. The cells were then washed two times with PBS-IF, and chased for 2 hour in medium A1. Images were directly taken on the confocal microscope Fluoview FV1000 version 2.1 (Olympus) using the 488nm laser for PCSK9 and a 633nm laser for transferrin.

### 2.11.3 Transferrin and Rab4 (RAS-related GTP-binding protein 4)

SV589 cells were cultured in medium B using glass bottom dishes. When reaching 60% confluence, cells were transiently transfected with N-terminal tRFP-tagged Rab4 expression plasmid (OriGene Technologies) using Lipofectamine 2000 according to the manufacturer's protocols. After 20 to 24 hours, the cells were incubated in serum-free medium A for >1 hour, followed by the addition of 100 μg/ml AlexaFluor® 647-labeled transferrin for 1 hour at 37$^{o}$C. The cells were then washed two times with PBS-IF, and chased for 2 hour in medium A. Images were taken using the confocal microscope Fluoview FV1000 version 2.1 (Olympus), in which Rab4 was visualized using the 543nm laser, and the 633nm laser was used for Transferrin.

## 2.12 Mutagenesis

A pCMV4 vector that contains the full-length sequence encoding human LDLR (pLDLR17) was used as a template for mutagenesis. Mutagenesis was carried out using a modified protocol of QuickChange$^{TM}$ site-directed mutagenesis kit (Stratagene, La Jolla, CA) (109). Briefly, primers were designed to contain extended non-overlapping sequences at the 3' end, which has a melting temperature ($T_{m\ no}$) 5 to 10$^{o}$C higher than that of primer-primer complementary sequences at the 5' end ($T_{m\ pp}$). The mutation sites could be placed either in the overlapping region or the complementary region. A 50 μl PCR reaction consists of 50 ng

templates, 0.3 μM each primer, 0.3 mM dNTPs and 1 unit Phusion DNA polymerase (New England Biolabs). The PCR cycles were initiated at 95$^{o}$C for 5 minutes, followed by 25 amplification cycles. Each cycle includes 95$^{o}$C for 1 minute, 76$^{o}$C for 1 minute and 72$^{o}$C for 15 minutes. The cycles were finished with an annealing step at 75$^{o}$C for 1 minute and an extension step at 72$^{o}$C for 30 minutes. The following steps were performed according to the instructions of the QuickChange$^{TM}$ site-directed mutagenesis kit.

### 2.13 Transient transfection

SV589 cells were grown in 100-mm dishes using medium B. HepG2 cells were grown in 60-mm dishes using medium F. When reaching ~70% confluence, cells were transfected with wild-type LDLR, LDLR(E296Q) or LDLR(EGF66) expression plasmids using Lipofectamine 2000 as per the manufacturer's protocols. After 5 hours, cells were incubated overnight in sterol-supplemented medium D to suppress endogenous LDLR expression prior to treatment with wild-type PCSK9 or PCSK9-D374Y for 6 hours. Cell surface proteins were isolated by biotinylation as previously described (7). Whole cell extracts as well as cell surface proteins were prepared for SDS-PAGE and immunoblot analysis as mentioned above.

### 2.14 Statistical analysis

All presented values are mean ± standard deviation. Statistical analysis was determined by Student's t-test and GraphPad Prism 5 software.

## 3. Results

### 3.1 Exogenous PCSK9 significantly decreased LDLR levels in HepG2 hepatic cells, not in SV589 fibroblast cells

#### 3.1.1 PCSK9 at physiological concentrations

Although it caused robust degradation of membrane hepatic LDLRs during continuous infusion into wild-type mice, purified PCSK9 had minimal effects on cell surface LDLRs in the adrenals (106), suggesting that PCSK9-mediated LDLR degradation was cell-type specific. To test this hypothesis, we assessed the effects of exogenous added PCSK9 on LDLR levels of HepG2 hepatic cells and SV589 fibroblast cells.

Both of these cell types were incubated in sterol-depleting medium containing statin (pravastatin) for 18 hours before PCSK9 treatment to up-regulate LDLR expression. Recombinant purified PCSK9, including wild-type PCSK9 and the mutant PCSK9-D374Y, was added to the medium of cultured cells at physiological concentrations and incubated for 6 hours. As discussed in the introduction, PCSK9 concentrations in human plasma range from 33 ng/ml to 4 μg/ml among healthy individuals (84, 85, 86). Therefore, we treated the cells with wild-type PCSK9 at 2.5 μg/ml and 5 μg/ml, whereas PCSK9-D374Y was used at 10-fold lesser concentration because this mutant has been characterized to be about 10-fold more active than wild-type PCSK9 in degrading LDLRs as mentioned above (7).

Immunoblot analyses of whole cell proteins as well as cell surface proteins showed that in response to PCSK9 addition, LDLR levels didn't significantly change in SV589 fibroblast cells despite a dramatic decrease of LDLRs in HepG2 hepatic cells, compared to control untreated cells (Figure 3.1). Particularly, cell surface LDLRs became nearly undetectable

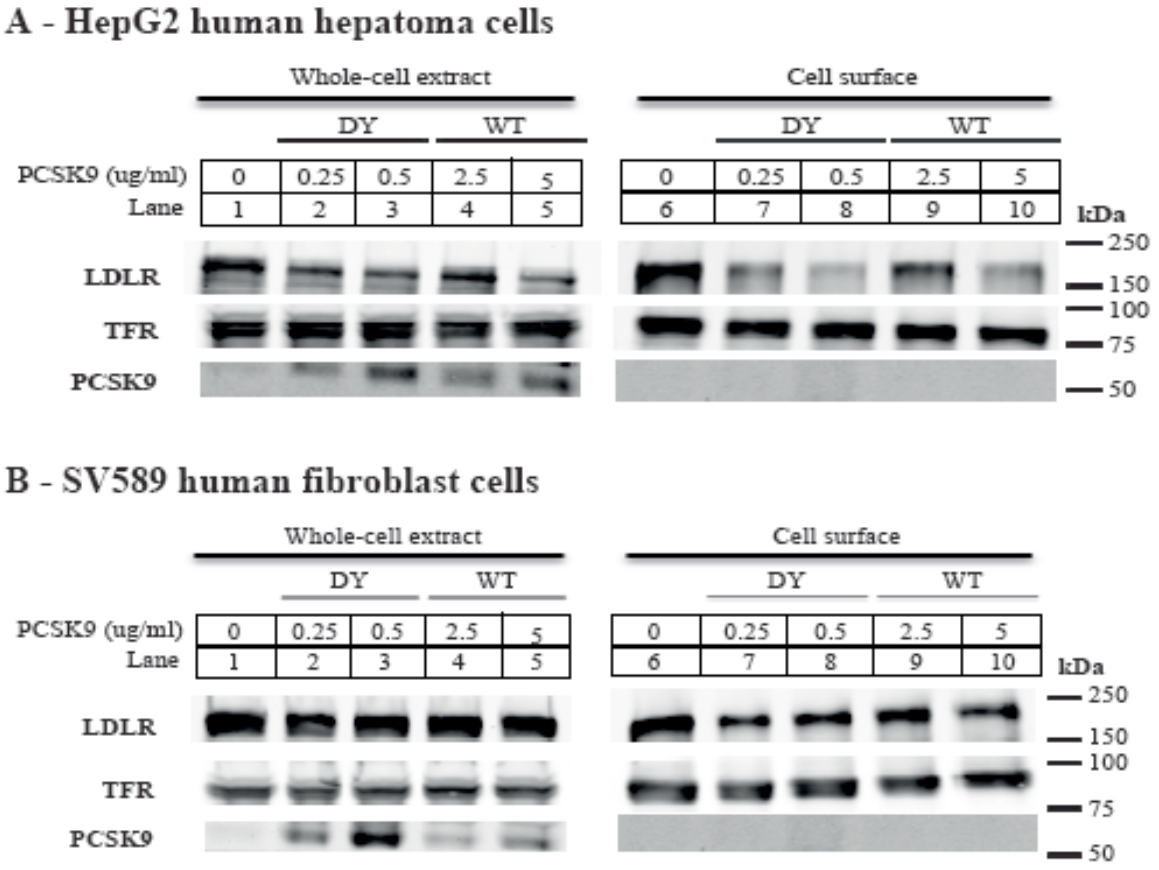


***Figure 3.1. Addition of PCSK9 at physiologically relevant concentrations causes robust LDLR degradation in HepG2 human hepatoma cells, but not SV589 human fibroblast cells.*** (A) HepG2 cells were cultured to ~80% confluence in medium F. The medium was then switched to sterol-depleting medium G, and the cells were incubated for 18 hours to induce LDLR expression. Wild-type PCSK9 at 2.5 μg/ml and 5 μg/ml along with PCSK9-D374 at 10-fold lesser concentrations were added to the medium for 6 hours. Cell surface proteins were isolated by biotinylation as described in *Materials and Methods*. Whole cell lysates and streptavidin-precipitated proteins were subjected to 8% SDS-PAGE followed by immunoblot analysis of LDLR, PCSK9 and TFR. Secondary infrared dye (IRDye800)-labeled antibodies were used for detection on the LI-COR Odyssey infrared imaging system. (B) SV589 cells were cultured to ~80% confluence in medium B, and then were incubated in sterol-depleting medium C for 18 hours to induce LDLR expression. SV589 cells were treated with PCSK9 and whole cell proteins as well as cell surface proteins were analyzed as described in Panel *A*. All experiments were performed twice with similar results.

when HepG2 cells were incubated with either 5 μg/ml of wild-type PCSK9 (lane 10) or 0.5 μg/ml of PCSK9-D374Y (lane 8), while whole cell LDLRs were decreased in a lesser extent (lane 2-5). Nevertheless, although there was a minor reduction of membrane LDLRs resulted from PCSK9 treatment (lane 7-10), no differences were observed in whole cell LDLRs of SV589 fibroblast cells (lane 2-5), indicating that a portion of cell surface LDLRs might be internalized, but not degraded as well as not recycled yet.

Exogenous PCSK9 was detected in a concentration-dependent manner in whole cell extracts (lane 2-5), whereas no PCSK9 was observed in cell surface proteins. Therefore, most of the cell-associated PCSK9 was internalized normally in both HepG2 hepatic cells and SV589 fibroblast cells. Levels of internalized PCSK9-D374Y were significantly higher in these cells when being compared with wild-type PCSK9 perhaps due to its 5 to 30-fold greater affinity in binding to the LDLR.

### 3.1.2 PCSK9 at higher concentrations

Importantly, when purified PCSK9 was added to the medium at higher concentrations compared with physiological levels, SV589 fibroblast cells were still resistant to PCSK9-mediated LDLR degradation (Figure 3.2). Wild-type PCSK9 at 5 μg/ml or 10 μg/ml didn't considerably affect the number of both whole cell (lane 3-4) and cell surface (lane 8-9) LDLRs in SV589 fibroblast cells. When the dose was increased up to 20 μg/ml of wild-type PCSK9, whole cell LDLRs fell by ~20% compared to the control (lane 5), but it should be noted that this concentration is remarkably higher than the physiological levels of PCSK9 in human plasma, which range from 33 ng/ml to 4 μg/ml (84, 85, 86). Notably, PCSK9-D374Y at 2 μg/ml dramatically reduced LDLR levels on the cell surface (lane 7) despite no changes

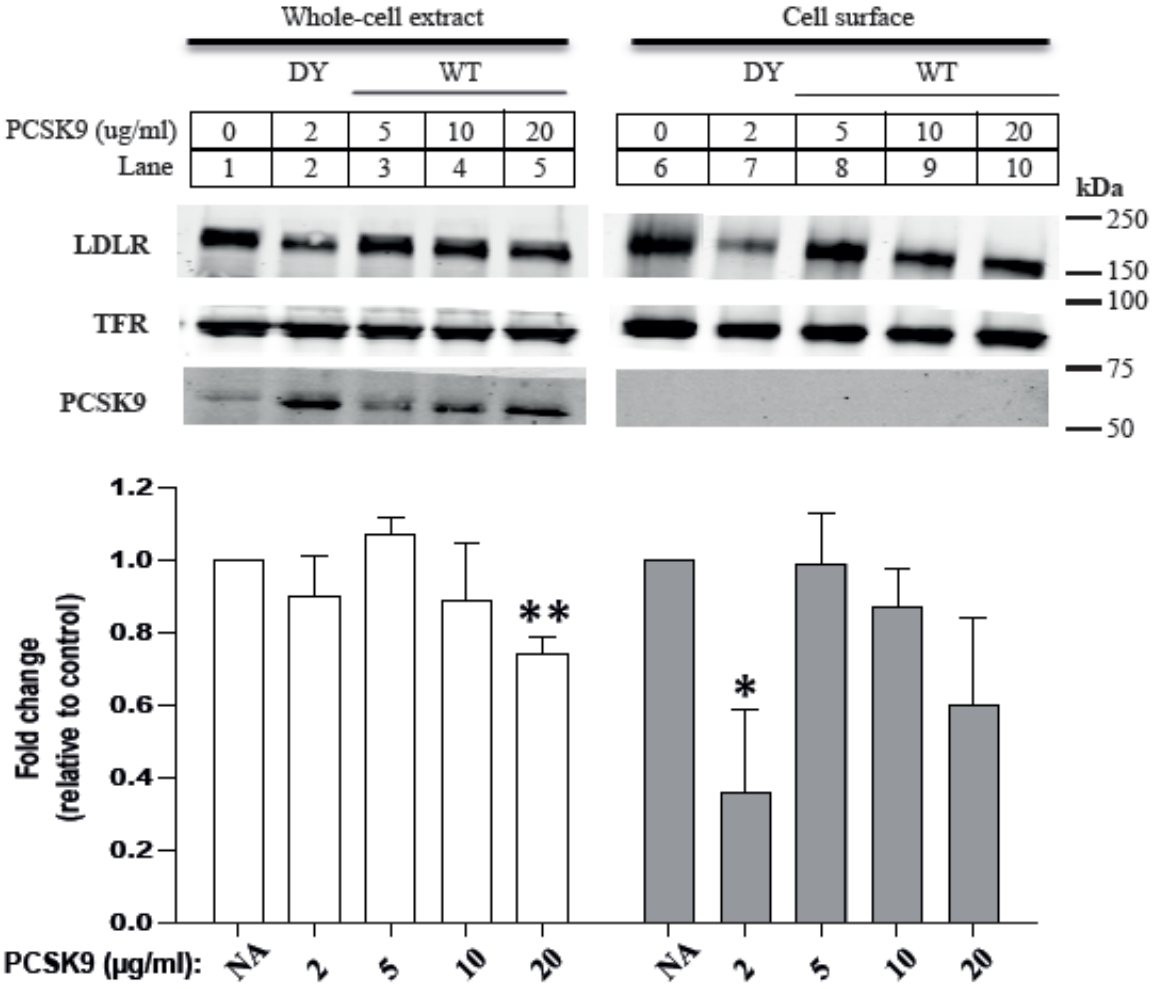


***Figure 3.2. Changes of endogenous LDLR levels in SV589 human fibroblast cells when PCSK9 was added at higher concentrations.*** SV589 cells were grown in medium B to ~80% confluence, and then were cultured overnight in lipoprotein–deficient medium C to induce LDLR expression. Wild-type PCSK9 (5, 10, and 20 μg/ml) and PCSK9-D374Y (2 μg/ml) were added to the medium for 6 hours. Cell surface proteins were biotinylated as described in *Materials and Methods*. Whole cell lysates and membrane proteins were subjected to 8% SDS-PAGE followed by immunoblot analysis of LDLR, PCSK9 and TFR. Secondary detection used infrared dye (IRDye800)-labeled antibodies. Blots were visualized and quantified using the LI-COR Odyssey infrared imaging system. LDLR levels were normalized to TFR expression and expressed relative to control cells (no addition – NA). Graphs represent the means ± standard deviation from three independent experiments. * indicates a statistical difference between columns with significance $p < 0.05$ by Student's t-test; ** $p < 0.005$.

in the levels of whole cell LDLRs (lane 2), therefore again, suggesting that LDLR might be rapidly taken up into the cells, but not degraded or recycled.

In contrast, higher doses of exogenous PCSK9 resulted in a more significant reduction of LDLRs in HepG2 hepatic cells (Figure 3.3). Especially, whole cell as well as cell surface LDLRs were decreased in a PCSK9 concentration-dependent manner. Incubation of HepG2 cells for 6 hours with 5 μg/ml wild-type PCSK9 degraded LDLR levels by approximately 50% for whole cell proteins (lane 3), and by approximately 80% for cell surface proteins (lane 8). Especially, it was hard to detect LDLRs in both whole cell and cell surface proteins when the cells were incubated with 20 μg/ml wild-type PCSK9 (lane 5 and lane 10) or 2 μg/ml PCSK9-D374Y (lane 2 and lane 7), in which the mutant at 2 μg/ml was as effective as 20 μg/ml of wild-type PCSK9 in reducing LDLR levels.

### 3.2 Long incubation time did not interfere with the resistance of SV589 fibroblast cells to PCSK9-mediated LDLR degradation

A report demonstrated that upon 2-hour incubation, PCSK9 failed to bind cells that expressed VLDLRs, a close ortholog of the LDLR (91); whereas a recent study showed that overnight incubation with purified added PCSK9 led to an increased association of PCSK9 to these cells, and subsequently, an enhanced degradation of VLDLRs (110). Therefore, to confirm that PCSK9 has minimal effects on LDLR levels of SV589 fibroblasts and to eliminate the contribution of different uptake time to the observed resistance of SV589 fibroblast cells to PCSK9-mediated LDLR degradation, we decided to increase incubation time with both of wild-type PCSK9 and PCSK9-D374Y.

SV589 and HepG2 cells were cultured as described in the above experiment, with the exception that these cells were incubated with PCSK9 for 18 hours. In HepG2 cells, overnight

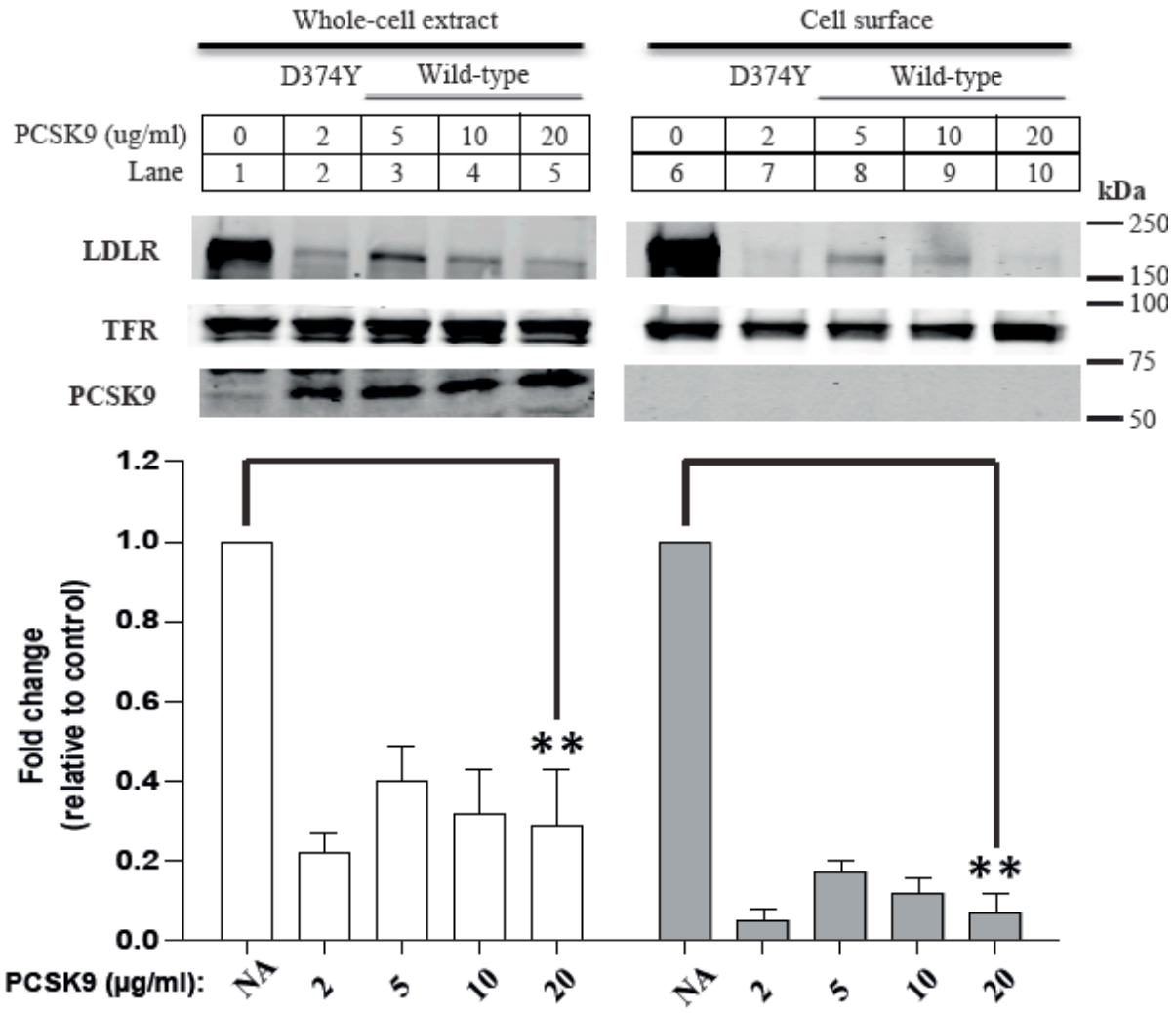


***Figure 3.3. Changes of endogenous LDLR levels in HepG2 human hepatoma cells when PCSK9 was added at higher concentrations.*** HepG2 cells were grown in medium F to ~80% confluence, and then were cultured in sterol–depleted medium G for 18 hours to induce LDLR expression. Wild-type PCSK9 (5, 10, and 20 µg/ml) and PCSK9-D374Y (2 µg/ml) were added to the medium for 6 hours. Cell surface proteins were biotinylated as described in *Materials and Methods*. Whole cell lysates and membrane proteins were subjected to 8% SDS-PAGE followed by immunoblot analysis of LDLR, PCSK9 and TFR. Secondary detection used infrared dye (IRDye800)-labeled antibodies. Blots were visualized and quantified using the LI-COR Odyssey infrared imaging system. LDLR levels were normalized to TFR expression and expressed relative to control cells (no addition – NA). Graphs represent the means ± standard deviation from three independent experiments. ** indicates a statistical difference between columns with significance $p < 0.005$ by Student's t-test.

treatment with exogenous purified PCSK9 made cell surface as well as whole cell LDLR levels became undetectable (lane 2-5 and 6-10), even with 5 μg/ml of wild-type PCSK9 (Figure 3.4). However, SV589 fibroblasts were still highly resistant to PCSK9 upon overnight treatment. The number of LDLRs in cells incubated with 20 μg/ml wild-type PCSK9 was similar to those in untreated cells (lane 5). LDLRs significantly decreased in response to overnight treatment with 2 μg/ml PCSK9-D374Y for cell surface proteins (lane 7), and in a lesser extent for whole cell proteins (lane 2).

Internalized wild-type PCSK9 was also detected in a concentration-dependent manner (lane 2-5) while PCSK9-D374Y at 2 μg/ml was taken up into cells as effectively as 20 μg/ml wild-type PCSK9.

### 3.3 PCSK9 was ineffective to degrade LDLRs in another fibroblast cell line, 917 foreskin fibroblasts

To further confirm that PCSK9 significantly down-regulated the number of LDLRs in hepatic cells while it did not in several different cells, we assessed PCSK9 activity in another hepatic (HuH7) and fibroblast (917) cells (Figure 3.5).

Similarly, wild-type PCSK9 and the mutant PCSK9-D374Y was added to the medium of cells cultured in LDLR expression-induced medium. After 6-hour incubation, cells were collected and subjected to flow cytometry using AlexaFluor® 488-labeled C7 antibody to detect LDLRs. C7 antibody specifically binds to the first cysteine-rich repeat of the LDLR ligand-binding domain (111). Although permeabilization steps were not performed, we could not completely exclude the possibility that C7 antibody might go into the cells and recognize endocytosed LDLRs. So, LDLR levels in this experiment were considered as whole cell proteins.

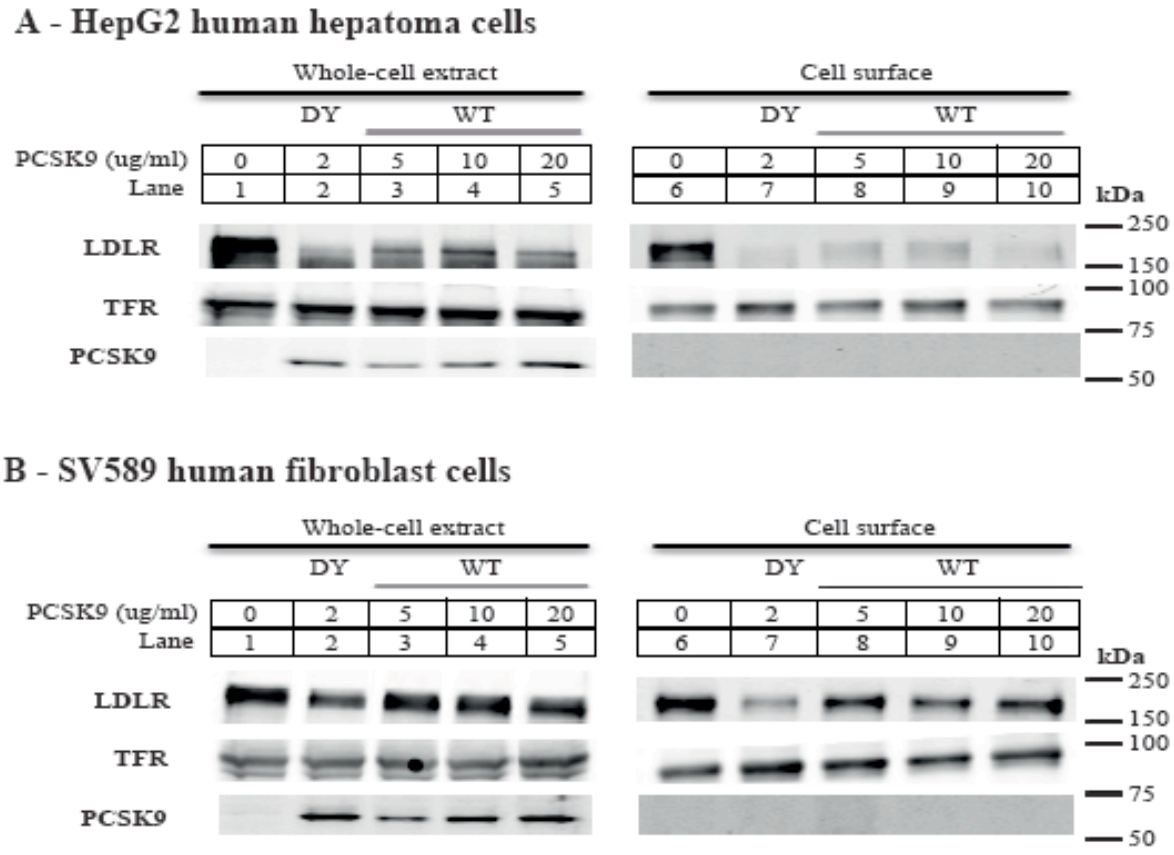


***Figure 3.4. Increased incubation time with PCSK9 had no effects on the resistance of SV589 human fibroblast cells to PCSK9-mediated LDLR degradation.*** (A) HepG2 cells were cultured to ~80% confluence in medium F. The medium was then switched to sterol-depleting medium G to induce LDLR expression. Wild-type PCSK9 (5, 10, and 20 μg/ml) and PCSK9-D374Y (2 μg/ml) were added to the medium for 18 hours. Cell surface proteins were biotinylated as described in *Materials and Methods*. Whole cell lysates and streptavidin-precipitated proteins were subjected to 8% SDS-PAGE followed by immunoblot analysis of LDLR, PCSK9 and TFR. Secondary infrared dye (IRDye800)-labeled antibodies were used for detection on the LI-COR Odyssey infrared imaging system. (B) SV589 cells were cultured to ~80% confluence in medium B, and then were incubated overnight in sterol-depleting medium C to induce LDLR expression. SV589 cells were treated with PCSK9 and whole cell proteins as well as cell surface proteins were analyzed as described in Panel *A*. All experiments were performed twice with similar results.

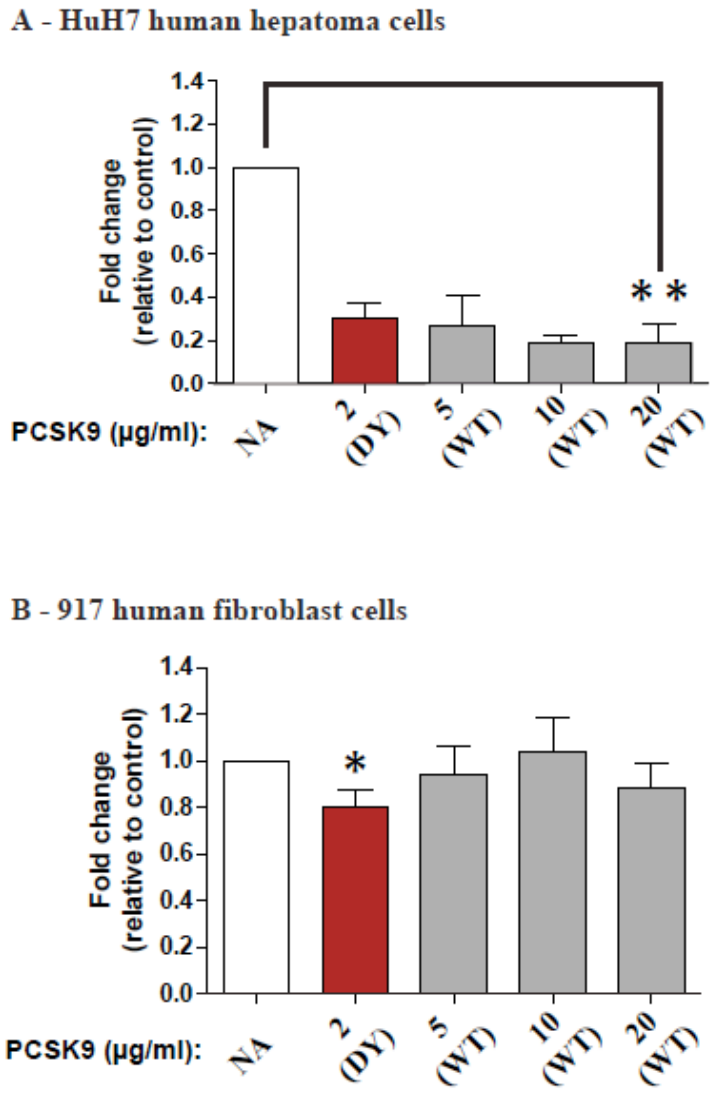


***Figure 3.5. PCSK9-mediated LDLR degradation assay in HuH7 human hepatoma cells and 917 human fibroblast cells.*** (A) HuH7 cells were cultured in medium B to ~80% confluence, and the medium were subsequently switched to lipoprotein-deficient medium C for 18 hours to induce LDLR expression. Following wild-type PCSK9 (5, 10, 20 µg/ml) and PCSK9-D374Y (2 µg/ml) incubation for 6 hours, cells were fixed as described in *Materials and Methods.* AlexaFluor® 488-labeled C7 antibody was used to detect cell surface LDLRs, and the cells were incubated overnight before being collected. (B) 917 human fibroblast cells were treated and samples were prepared as described in Panel *A*. Samples were analyzed on BD FACSAria flow cytometer to quantify the signal of LDLRs in each population. LDLR levels were corrected to background, and values were expressed relative to control cells (no addition – NA). Graphical representations are the average and standard deviation from 3 different experiments. * indicates a statistical difference between columns with significance $p < 0.05$ by Student t-test; ** $p < 0.005$.

Treatment of HuH7 cells with 5 μg/ml wild-type PCSK9 lowered LDLR levels by ~60% whereas LDLRs in cells treated with 20 μg/ml wild-type PCSK9 were 80% less than untreated cells. Here, we were unable to observe the PCSK9 concentration-dependent manner of LDLR decrease in response to exogenous purified PCSK9 as well as the exact 10-fold greater activity of the mutant PCSK9-D374Y in degrading LDLRs, perhaps due to association of C7 antibody to a portion, not whole, of internalized LDLRs in addition to cell surface LDLRs.

However, PCSK9 failed to degrade LDLRs in fibroblast cells again. When 917 fibroblast cells were incubated with either 20 μg/ml wild-type PCSK9 or 2 μg/ml PCSK9-D374Y, LDLR levels were not notably reduced compared to untreated cells.

### 3.4 PCSK9 endocytosis were LDLR-dependent in both hepatic and fibroblast cells

It was shown that PCSK9 internalization in hepatic cells required the LDLR (7, 99). Moreover, the above results showed that the mutant PCSK9-D374Y, which was identified to have 5 to 30-fold greater affinity in binding to the LDLR (93, 96), was taken up more efficiently than wild-type PCSK9 in both hepatic and fibroblast cells, suggesting the requirement of the LDLR for PCSK9 uptake in these cell types. To assess the role of the LDLR in PCSK9 internalization, we measured AlexaFluor® 488-labeled PCSK9 uptake in the absence and presence of the LDLR.

For this and subsequent experiments, HepG2 cells were used as a representative model for hepatic cells whereas SV589, which are referred to fibroblast cells from now, represented fibroblasts. These cell types were incubated either in medium containing statin (pravastatin) to induce LDLR expression or in medium containing sterols (cholesterol and 25-hydroxycholesterol) to suppress LDLR expression for 18 hours. AlexaFluor® 488- labeled

PCSK9-D374Y (1 μg/ml) was allowed to be taken up for 1 hour in the continuous presence of E64 before the cells were washed with stripping buffer to remove cell surface labeled PCSK9. E64 is a potent and highly selective cysteine protease inhibitor that was shown to completely abolish PCSK9-mediated LDLR degradation in lysosomes (102). Samples were then subjected to flow cytometry to measure the overall population of cells that had positive signal for internalized labeled PCSK9.

After 1-hour incubation, AlexaFluor® 488-labeled PCSK9-D374Y was detectable in approximately 70% of fibroblast cells expressing LDLRs while the amount of internalized PCSK9-D374Y was dramatically reduced in fibroblast cells lacking LDLR expression (Figure 3.6). Similarly, abundant labeled PCSK9 was found to associate with approximately 50% of hepatic cells expressing LDLRs, and PCSK9 endocytosis was significantly abolished in these cells when LDLR expression was suppressed. However, a small amount of AlexaFluor® 488-labeled PCSK9-D374Y was still detectable in either hepatic or fibroblast cells deficient in LDLRs, perhaps due to incomplete sterol-dependent suppression of LDLR expression. Also, it was possible that another receptor might play only a minor role while internalization of exogenous PCSK9 in hepatic and fibroblast cells was mostly dependent on the LDLR.

To further confirm the importance of LDLR in PCSK9 endocytosis, we next tested PCSK9 association/uptake into cells expressing either wild-type LDLR or a PCSK9 binding-defective LDLR (LDLR-E296Q). This mutation, which would presumably decrease calcium-affinity of the LDLR EGF-A domain more extensively according to the equivalent residue in coagulation factor IX (112), failed to bind PCSK9 at neutral pH as well as at acidic

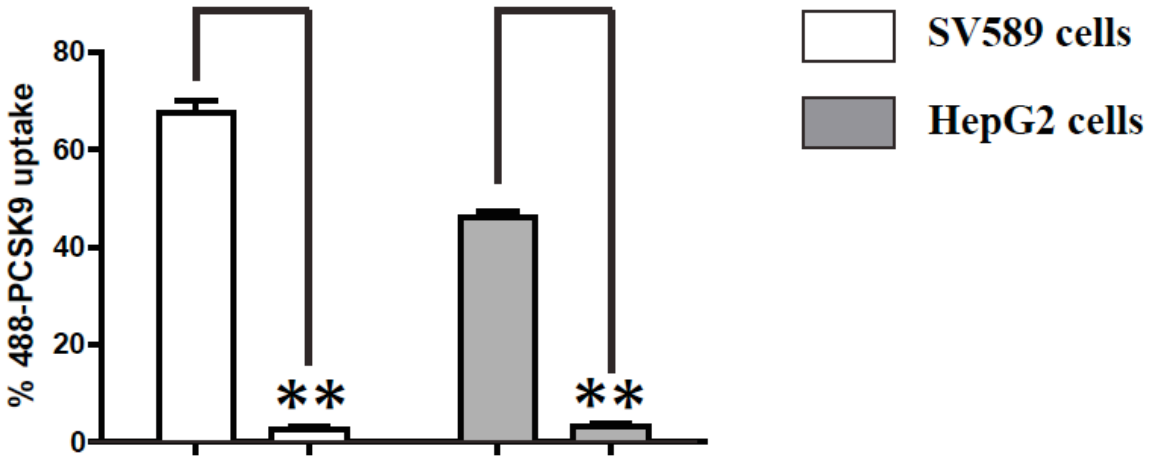


***Figure 3.6. PCSK9 uptake in the presence and absence of LDLRs in HepG2 human hepatoma cells and SV589 human fibroblast cells.*** SV589 cells were grown in medium B to ~80% confluence, and then were cultured overnight in sterol-depleting medium C or medium D containing sterols (25-hydroxycholesterol/cholesterol) to up-regulate and down-regulate LDLR expression, respectively. Similarly, HepG2 cells were cultured in sterol-depleting medium G or medium H containing sterols (25-hydroxycholesterol/cholesterol) for 18 hours. These mediums were supplemented with 150 μM E64 to inhibit lysosomal degradation. AlexaFluor® 488-labeled PCSK9-D374Y was added to the medium at 1 μg/ml for 1 hour before the medium was replaced with stripping buffer to wash cell surface PCSK9. Cells were collected and subjected to analysis using the BD FACSAria flow cytometer. The signal of internalized PCSK9 in each population was quantified and corrected to background. Graphical representations are the average and standard deviation from 3 different experiments. ** indicates a statistical difference between columns with significance $p < 0.005$ by Student t-test.

pH in *in vitro* binding studies (data not shown) because the interaction between PCSK9 and the LDLR EGF-A domain is calcium-dependent as stated in the introduction (91). LDLR-transfected cells were treated overnight with sterols (25-hydroxycholesterol and cholesterol) to suppress endogenous LDLR expression prior to incubation with 1 μg/ml purified PCSK9-D374Y for 6 hours. E64 was used to inhibit lysosomal degradation of internalized PCSK9.

PCSK9 association and uptake occurred normally in cells expressing wild-type LDLR, but was completely negligible in cells expressing the mutant LDLR-E296Q although both the wild-type LDLR (lane 7-8) and the mutant LDLR-E296Q (lane 5-6) were expressed normally on the cell surface (Figure 3.7). Purified added PCSK9 was detected in whole cell extracts (lane 4), but not in cell surface proteins (lane 8) of cells expressing wild-type LDLR, suggesting that most of cell-associated PCSK9 was internalized as usual. Particularly, not only hepatic cells but also fibroblast cells expressing wild-type LDLR could normally associate and then uptake exogenous purified PCSK9 after a 6-hour incubation (lane 4). Nevertheless, no traces of PCSK9 were detected in either whole cell lysates (lane 2) or membrane proteins (lane 6) of hepatic and fibroblast cells expressing the binding-defective mutation (LDLR-E296Q), indicating that PCSK9 failed to associate as well as be taken up into these cells in the absence of LDLR/PCSK9 interaction. Combined together, these data strongly confirmed the LDLR-dependent manner of PCSK9 endocytosis in both hepatic and fibroblast cells.

### 3.5 Both wild-type PCSK9 and the mutant PCSK9-D374Y trafficked to lysosomes in hepatic cells

To elucidate the mechanisms responsible for different responses to PCSK9-mediated LDLR degradation in hepatic and fibroblast cells, first we wanted to determine the fate of

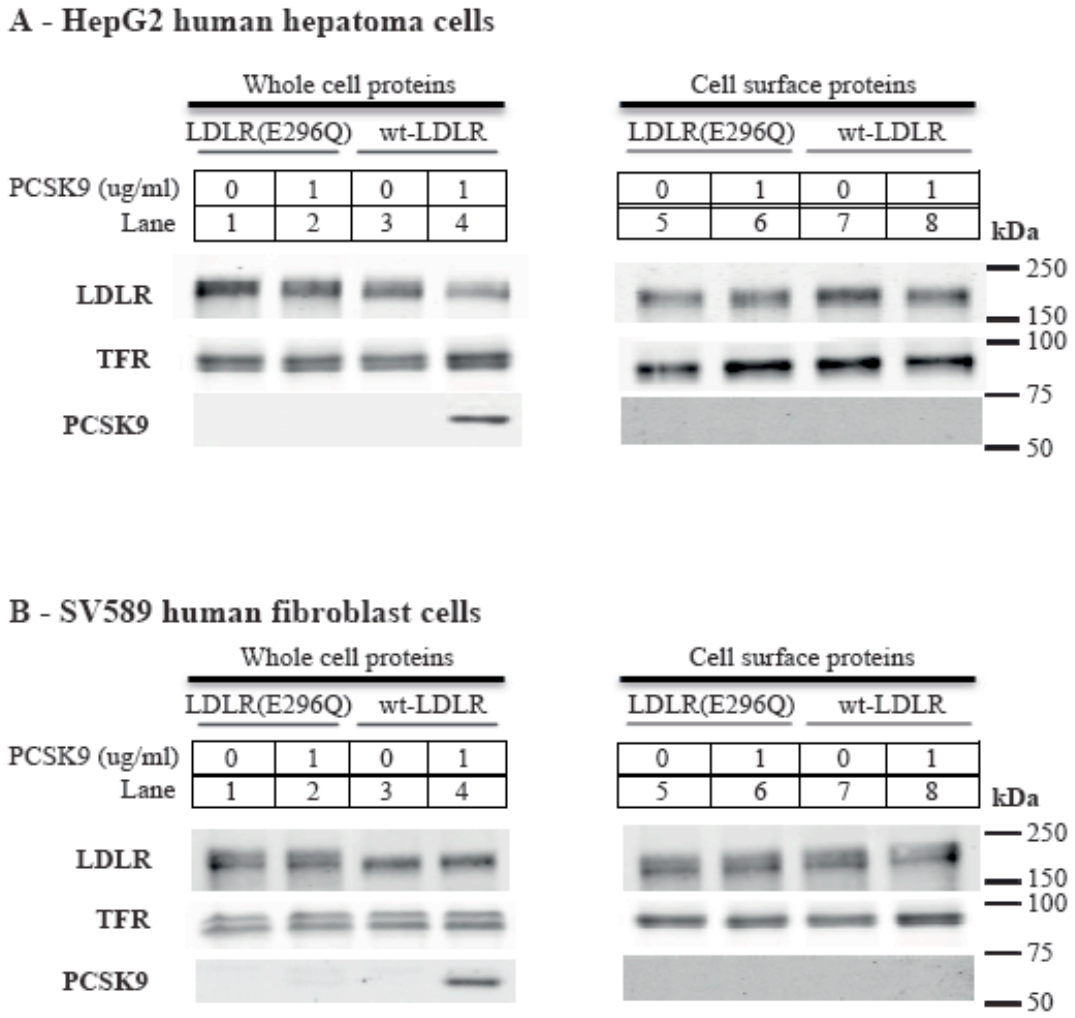


***Figure 3.7. PCSK9 uptake in cells expressing either wild-type LDLR or a PCSK9 binding-defective mutation.*** (A) HepG2 cells were grown in medium F to ~60-70% confluence. The cells were then transiently transfected with wild-type LDLR or LDLR-E296Q expression vectors, and incubated overnight in sterol-supplemented medium (25-hydroxycholesterol/cholesterol) to suppress endogenous LDLR expression. PCSK9-D374Y (1 μg/ml) was incubated for 6 hours in the continuous presence of 150 μM E64. Cell surface proteins were isolated by biotinylation as described in *Materials and Methods*. Whole cell lysates and membrane proteins were subjected to immunoblot analysis of LDLR, PCSK9 and TFR. Secondary infrared dye (IRDye800)-labeled antibodies were used for detection on the LI-COR Odyssey infrared imaging system. (B) SV589 cells were cultured to ~60% confluence in medium B. The cells were treated and whole cell proteins as well as cell surface proteins were analyzed as described in Panel *A*. All experiments were performed twice with similar results.

PCSK9 after binding to the LDLR in these cells.

PCSK9 internalization, which depended on its interaction with the LDLR on the cell surface, led to a dramatic reduction of LDLRs in hepatic cells through routing the receptor to lysosomes for degradation (7, 99, 102), possibly along with PCSK9. PCSK9 trafficking was characterized using $^{125}$I-labeled PCSK9 degradation assay along with co-localization studies. Hepatic cells were cultured in sterol-deficient medium supplemented with statin (pravastatin) for 18 hours prior to radioisotope-labeled PCSK9 incubation. We monitored the fate of both wild-type PCSK9 and the mutant PCSK9-D374Y, which was used at 5-fold lesser concentration compared to the wild-type. After 1-hour incubation, residual cell surface PCSK9 was removed, and fresh medium was added. Following 6-hour chase of internalized $^{125}$I-labeled PCSK9, the amount of mono-iodotyrosine radioactivity (TCA-soluble) in the medium was measured as a catabolic product of $^{125}$I-labeled PCSK9 degradation in lysosomes. C7 monoclonal antibody, which is taken up by the LDLR, and subsequently, dissociates from the receptor in early endosomes and proceeds for degradation in lysosomes, was used as a positive control for lysosomal degradation (111).

After 6 hours, TCA-soluble counts were significantly increased in the medium for both wild-type PCSK9 and the mutant PCSK9-D374Y (Figure 3.8). The levels of $^{125}$I-mono-iodotyrosine released into the medium reach ~4,000 cpm/mg protein for wild-type PCSK9, similar to those of the mutant PCSK9-D374 (~3,800 cpm/mg protein). Of note, labeled PCSK9-D374Y was used at concentrations 5-fold less than those of wild-type PCSK9. Degradation of $^{125}$I-labeled C7 antibody attained ~15,000 cpm/mg protein after 6 hours, confirming lysosomal degradation was effective under these conditions. These data indicated that in hepatic cells, wild-type PCSK9 and the mutant PCSK9-D374Y were internalized and delivered to lysosomes for degradation, in which the mutant was degraded more effectively.

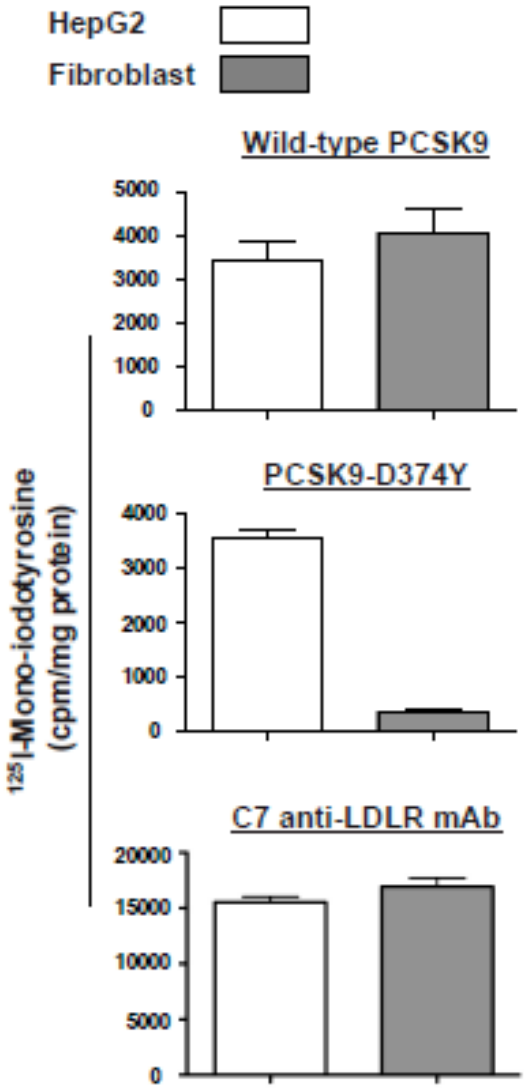


***Figure 3.8.*** ***$^{125}$I-labeled PCSK9 degradation assay.*** HepG2 cells were cultured to ~80% confluence in medium F. The medium was switched to sterol-depleting medium G, and the cells were incubated for 18 hours to induce LDLR expression. Similarly, SV589 cells were cultured in sterol-depleting medium C. Medium A containing ~5 μg/ml $^{125}$I-labeled wild-type PCSK9 or ~1 μg/ml $^{125}$I-labeled PCSK9-D374Y was then added to the cells for 1 hour. In negative controls, the cells were treated with 100 μM chloroquine 30 minutes prior to and during later incubation to inhibit lysosomal degradation. The medium was removed, and the cells were incubated in label-free medium A for 6 hours after being washed extensively. The amounts of $^{125}$I-mono-iodotyrosine were determined in the medium as described in *Materials and Methods.* TCA-soluble counts were normalized to protein levels, and corrected to negative controls. Graphs represent the means ± standard deviation from three independent experiments.

Co-localization studies between PCSK9 and lysosomal markers also demonstrated that in hepatic cells, both wild-type PCSK9 and the mutant D374Y trafficked to lysosomes after being taken up into these cells via the LDLR (Figure 3.9). In this experiment, following incubation in sterol-depleting medium containing statin (pravastatin), cells were treated with AlexaFluor® 488-labeled PCSK9 for 1 hour and then washed extensively. Labeled PCSK9 were chased for 6 hours in the continuous presence of E64 while LysoTracker, the lysosome marker, was added 2 hours before being directly observed on the confocal microscope. E64 served as a lysosomal protease inhibitor to inhibit degradation of internalized labeled PCSK9 (102). Addition of AlexaFluor® 488-labeled PCSK9 to the medium supplemented with E64 resulted in the diffuse localization of these proteins in big punctate perinuclear structures of hepatic cells. Notably, a significant amount of these structures overlapped with LysoTracker signal after 6 hours for both labeled wild-type PCSK9 and the mutant PCSK9-D374Y, suggesting that these proteins proceeded to lysosomes for degradation after binding to the LDLR.

### 3.6 Wild-type PCSK9, not the mutant PCSK9-D374Y, was completely degraded in fibroblast cells

Above results showed that PCSK9 failed to degrade LDLRs in fibroblast cells despite its normal LDLR-dependent cellular uptake; however, the fate of PCSK9 after binding to the LDLR had been still unknown. To explore whether PCSK9 was degraded in fibroblast cells as it is in hepatic cells whereas the LDLR recycled to the cell surface, we also performed $^{125}$I-labeled PCSK9 degradation assay.

Fibroblast cells were cultured as described above. Figure 3.8 showed that following 6-hour chase of internalized $^{125}$I-labeled wild-type PCSK9, the levels of TCA-soluble proteins

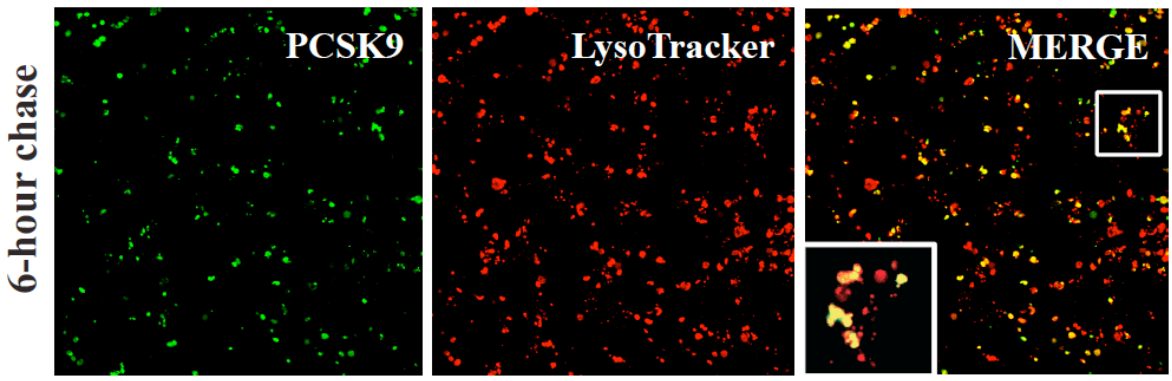


***Figure 3.9. Co-localization of PCSK9 and the lysosome marker (LysoTracker) in HepG2 human hepatoma cells.*** HepG2 cells were seed in μ-slide 8-well plates to ~80% confluence, and then were cultured overnight in lipoprotein-deficient medium G supplemented with 150 μM E-64. The medium was replaced with medium containing 5 μg/ml AlexaFluor® 488-labeled PCSK9-D374Y, and the cells were incubated for 1 hour. Internalized AlexaFluor® 488-labeled PCSK9 was then chased for 6 hours in label-free medium G containing 150 μM E-64 to inhibit lysosomal degradation. LysoTracker® Red DND-99 was diluted to the final working concentration (200 nM), and incubated for 2 hours prior to two washes with label-free medium E and direct observation on microscope at the indicated time. Images were taken using the confocal microscope Fluoview FV1000 Version 2.1 (Olympus), in which PCSK9 was visualized using the 488nm laser, and the 543nm laser was used for LysoTracker.

released in the medium reached ~4,500 cpm/mg protein, equivalent to those of hepatic cells. Therefore, wild-type PCSK9 was internalized as well as degraded equally in both hepatic and fibroblast cells, indicating dissociation of wild-type PCSK9 from the recycling LDLR in fibroblast cells. Nevertheless, only trace amount of $^{125}$I- mono-iodotyrosine (<500 cpm/mg protein) was detected in the medium of fibroblast cells treated with radioisotope-labeled PCSK9-D374Y. Particularly, this amount was considerably lower than the amount of $^{125}$I-mono-iodotyrosine observed in hepatic cells treated with labeled PCSK9-D374Y, suggesting that high percentage of internalized PCSK9-D374Y was degraded in hepatic cells, but not in fibroblast cells. Moreover, C7 antibody was degraded to the same extent (~15,000-16,000 cpm/mg protein) in both of hepatic and fibroblast cells, verifying that lysosomal degradation functioned properly in these cells. Combined together, these data suggested that different from hepatic cells, wild-type PCSK9 separated from the recycling LDLR and went to lysosomes for degradation in fibroblast cells whereas the mutant PCSK9-D374Y seemed to maintain the binding to the receptor and recycle to the cell surface. Another possibility is that similar to wild-type PCSK9, the mutant also dissociated from the recycling LDLR in fibroblast cells, but still stuck in endocytic compartments instead of proceeding to lysosomes for degradation.

### 3.7 More internalized PCSK9-D374Y proteins recycled to the cell surface

#### 3.7.1 Recycling assay

For further determination of PCSK9-D374Y fate in fibroblast cells, we turned to a recycling assay based on on-cell western to quantify the percentage of recycled and intracellular PCSK9 compared to total internalized proteins (Figure 3.10).

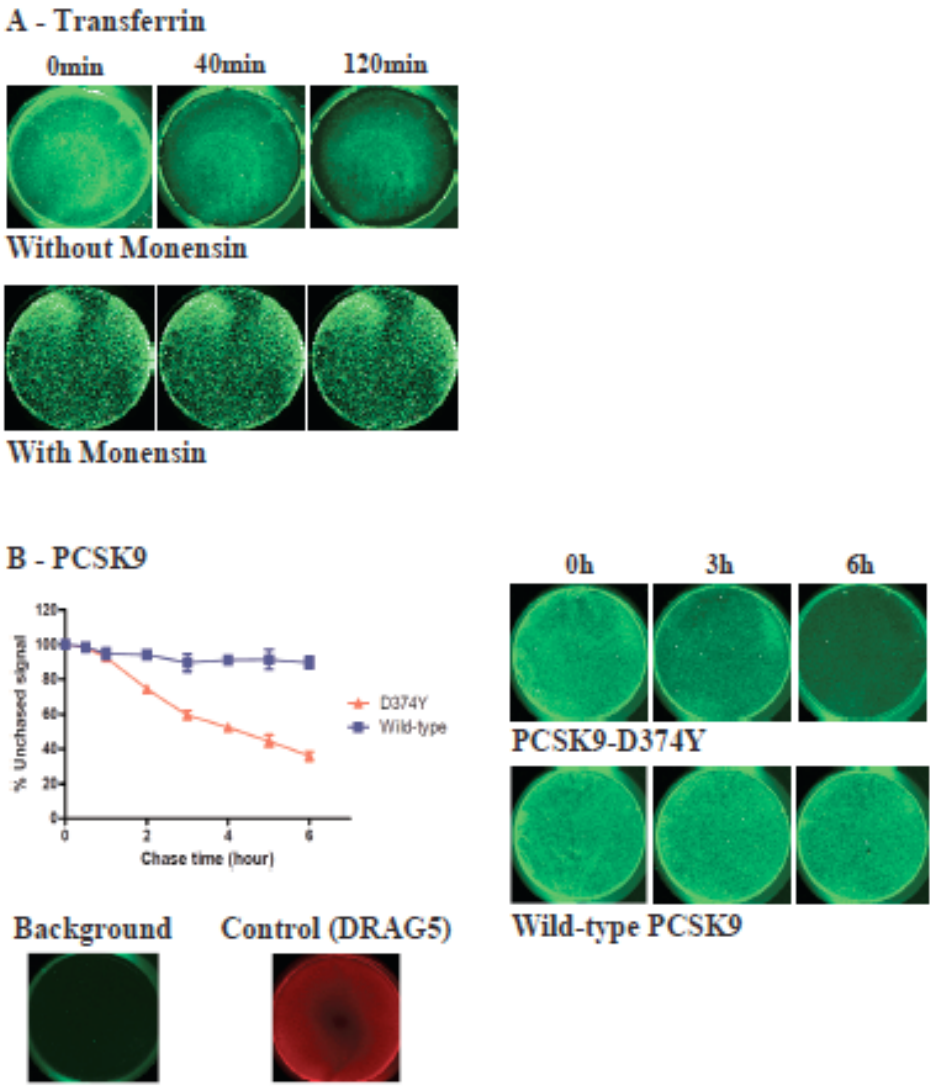


***Figure 3.10. Recycling assay of wild-type PCSK9 and PCSK9-D374Y in SV589 human fibroblast cells.*** (A) SV589 cells were cultured in 12-well plates to ~80% confluence, and then were incubated in serum-free medium A for >1 hour to deplete endogenous transferrin. For monensin-treated wells, the cells were also treated with 50 μM monensin for >1 hour prior to and during later incubation to inhibit the recycling process. Biotin-labeled transferrin was incubated with IRDye® 800CW Streptavidin in medium A for 1 hour at 37°C, and the complexes were added to the cells for 1 hour. Subsequently, the cells were washed at 4°C with 20 mM TCEP to remove cell surface labeled complexes before incubation in medium A supplemented with 20 mM TCEP for 2 hours. The plate was directly scanned on the LI-COR Odyssey infrared imaging system at the indicated time intervals. (B) The recycling assay was performed as described above, with the exception that the internalized complexes were chased for 6 hours in the medium continuously containing TCEP and E-64. Signal intensity was quantified using Odyssey 2.0 software. PCSK9 levels were normalized to DNA levels stained by DRAQ5™ (1:10,000), and corrected for background using untreated wells. Graphs represent the means ± standard deviation from three independent experiments.

After incubation in lipoprotein-deficient medium supplemented with statin to induce LDLR expression, cells were allowed to uptake IRDye® 800CW-Streptavidin/Biotin-PCSK9 complexes for 1 hour, and then washed extensively at 4$^{o}$C to remove remaining complexes from the cell surface. Internalized PCSK9 was directly visible in fibroblast cells due to the IRDye® 800CW tag of streptavidin as well as the interaction between streptavidin and biotin particles attached to PCSK9. The signal of internalized PCSK9 was chased in the medium continuously containing E64 and TCEP, and was measured at various intervals over the ensuing 6 hours. E64 was used to inhibit lysosomal degradation whereas TCEP served as a reducing agent that disrupted the disulfide bond between PCSK9 and biotin particles, leading to cleavage of the IRDye® 800CW-Streptavidin-Biotin tag from PCSK9. Therefore, if PCSK9 recycled to the cell surface, we would see the incremental loss of signal over time. In contrast, if PCSK9 still stayed in the cells, we would see no changes in the signal of internalized PCSK9.

Transferrin, a well-known recycling protein, was used as a positive control to verify the preciseness of this experiment. Exogenous diferric transferrin specifically binds the transferrin receptor on the cell surface, and the complexes are subsequently internalized via the receptor-mediated endocytosis. At the reduced pH in early endosomes, iron dissociates from transferrin and still stays within the cells while transferrin remains bound to the transferrin receptor and is recycled to the cell surface (113). Consistent with this scenario, our recycling assay showed that during the chase period in the continuous presence of TCEP, the signal of internalized transferrin dropped gradually in fibroblast cells (Figure 3.10). Particularly, almost the entire signal was lost after 120 minutes, indicating recycling of transferrin to the cell surface. Moreover, this incremental decrease in signal was completely

abolished when fibroblast cells were treated with 50 μm monensin, a recycling inhibitor (114).

For wild-type PCSK9, no significant changes were observed in the intensity of internalized proteins after a 6-hour chase in the medium continuously supplemented with TCEP, suggesting that higher percentage of internalized wild-type PCSK9 remained inside fibroblast cells, instead of recycling to the cell surface. Here, although IRDye® 800CW was not usually degraded, but accumulated in the cells, we still used E64 on the safe side to inhibit lysosomal degradation of internalized PCSK9. This was consistent with the results of $^{125}$I-labeled PCSK9 degradation assay, which indicated that wild-type PCSK9 separated from the recycling LDLR and trafficked to lysosomes for degradation. Recycling assay showed that only <10% of wild-type PCSK9 signal was lost during 6 hours, which might represent the release of residual labeled complexes from the cell surface into the medium. In contrast, >60% of PCSK9-D374Y signal was lost following 6-hour chase, suggesting that higher percentage of internalized PCSK9-D374Y still bound the LDLR and recycled to the cell surface along with the receptor.

### 3.7.2 Co-localization studies

Co-localization studies that showed both wild-type PCSK9 and mutant PCSK9-D374Y co-localized with LysoTracker in fibroblast cells further confirmed the above results. However, PCSK9-D374Y also overlapped with transferrin in recycling compartments while wild-type PCSK9 did not.

In imaging studies between AlexaFluor® 488-labeled PCSK9 and LysoTracker, fibroblast cells were cultured as described above, with the exception that the percentage of overlapped pixels was quantified at intervals during a 6-hour chase in the medium

supplemented with E64. In fibroblast cells, wild-type PCSK9 (Figure 3.11) and the mutant PCSK9-D374Y (Figure 3.12) overlapped with LysoTracker in large punctate vacuoles, and PCSK9 co-localization with LysoTracker increased time-dependently. Especially, 2-hour chase resulted in ~50% of intracellular PCSK9 that overlapped LysoTracker, whereas the percentage of co-localization between PCSK9 and LysoTracker reached >80% after 6-hour chase. Although the above results showed that more than half of PCSK9-D374Y recycled to the cell surface in fibroblast cells, the percentage of co-localization between PCSK9-D374Y and LysoTracker over time was roughly equal to that of wild-type PCSK9. One explanation is that recycled PCSK9-D374Y could release into the medium and be eventually removed whereas the percentage of co-localization with LysoTracker was quantified based on the intracellular signal of labeled PCSK9. The majority of PCSK9-D374Y signal overlapped with LysoTracker was intracellular PCSK9 that did not recycle to the cell surface.

For labeling recycling compartments, we used AlexaFluor® 647-labeled transferrin. Cells were pulsed with labeled transferrin and PCSK9 for 1 hour following incubation in serum-free medium to deplete endogenous transferrin. Labeled proteins were subsequently chased in the medium supplemented with E64 to block lysosomal degradation of internalized PCSK9. After 2-hour chase, AlexaFluor® 647-labeled transferrin concentrated in clusters of small vacuoles, which significantly overlapped with the signal of labeled PCSK9-D374Y (Figure 3.13). No significant co-localization between wild-type PCSK9 and transferrin was observed in fibroblast cells under similar conditions. Furthermore, we also used Rab4, a well-known early endosome marker, as a control to indicate that AlexaFluor® 647-labeled transferrin was chased out of early endosomes after 2-hour chase, and that the co-localization

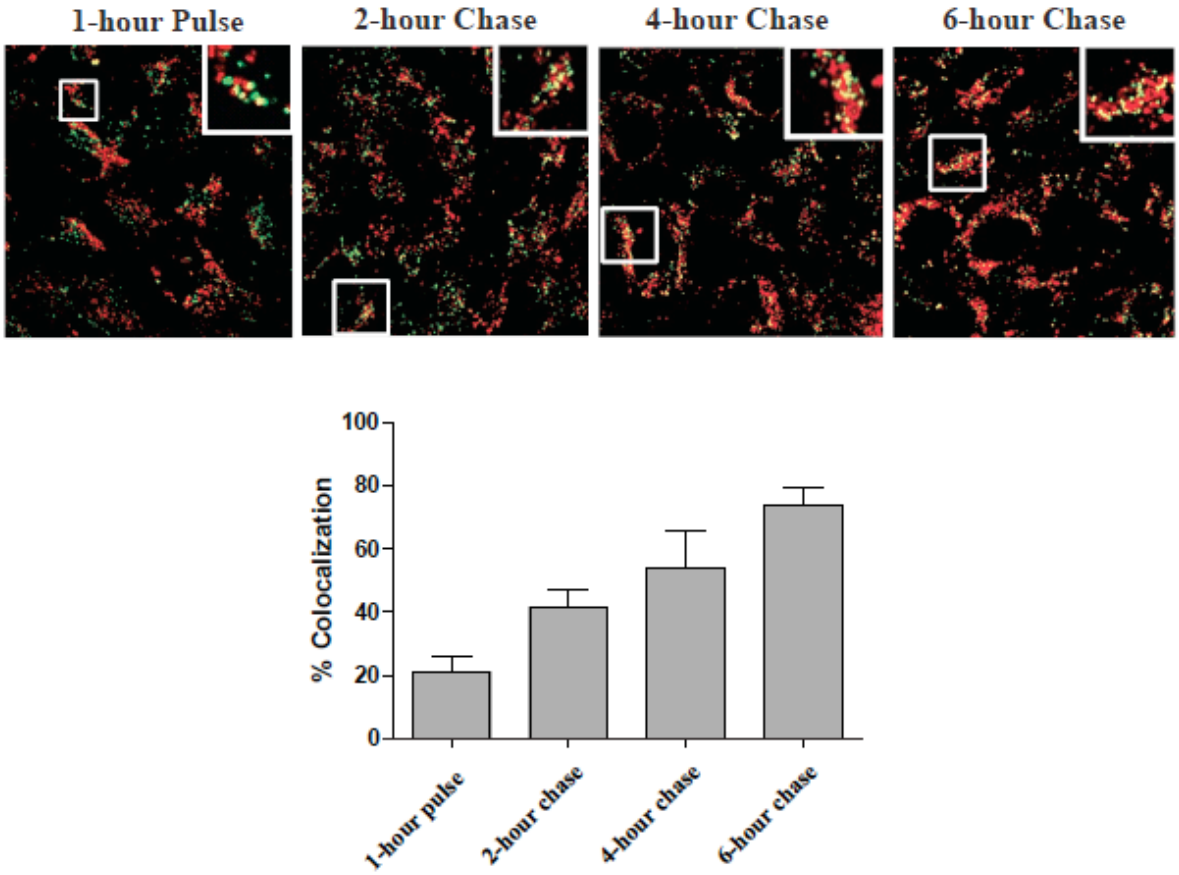


***Figure 3.11. Co-localization of wild-type PCSK9 and the lysosome marker (LysoTracker) in SV589 human fibroblast cells.*** SV589 cells were cultured in μ-slide 8-well plates to ~80% confluence, and then were incubated overnight in sterol-depleting medium C supplemented with 150 μM E-64. 30 μg/ml AlexaFluor® 488-labeled wild-type PCSK9 was added to the medium for 1 hour. Internalized labeled PCSK9 was then chased for 6 hours in label-free medium C containing 150 μM E-64. LysoTracker® Red DND-99 was diluted to the final working concentration (200 nM), and incubated for 2 hours prior to direct observation on microscope at the indicated time. Images were taken on the confocal microscope Fluoview FV1000 Version 2.1 (Olympus), in which PCSK9 was visualized using the 488nm laser and the 543nm laser was used for LysoTracker. The percentage of co-localization was quantified using Image J (http://rsb.info.nih.gov/ij/), and corrected for background using negative images. A minimum of 3 fields was analyzed per indicated time. Graphs represent the means ± standard deviation from three independent experiments.

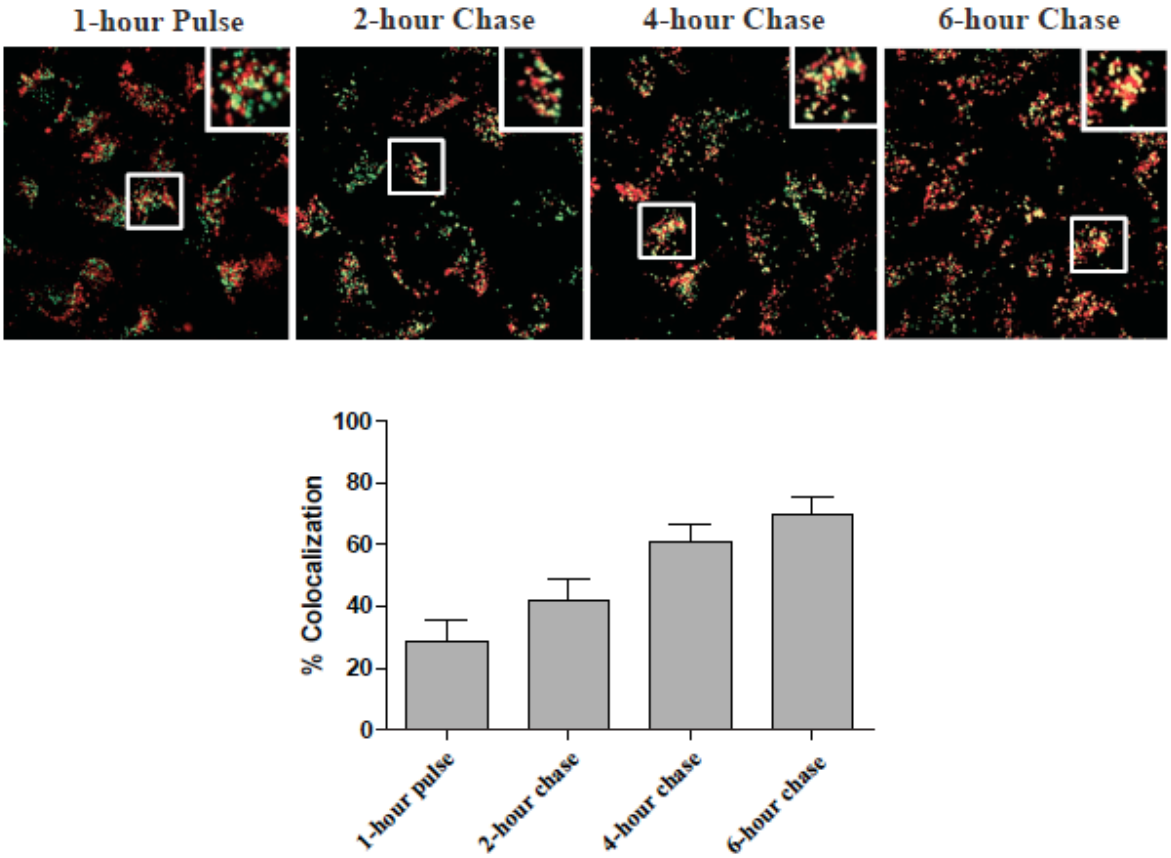


***Figure 3.12. Co-localization of PCSK9-D374Y and the lysosome marker (LysoTracker) in SV589 human fibroblast cells.*** SV589 cells were cultured in μ-slide 8-well plates to ~80% confluence, and were incubated overnight in sterol-depleting medium C supplemented with 150 μM E-64. 5 μg/ml AlexaFluor® 488-labeled PCSK9-D374Y was added to the medium for 1 hour. Internalized labeled PCSK9 was then chased for 6 hours in label-free medium C containing 150 μM E-64. LysoTracker® Red DND-99 was diluted to the final working concentration (200 nM) and incubated for 2 hours prior to direct observation on microscope at the indicated time. Images were taken on the confocal microscope Fluoview FV1000 Version 2.1 (Olympus), in which PCSK9 was visualized using the 488nm laser and the 543nm laser was used for LysoTracker. The percentage of co-localization was quantified using Image J (http://rsb.info.nih.gov/ij/), and corrected for background using negative images. A minimum of 3 fields was analyzed per indicated time. Graphs represent the means ± standard deviation from three independent experiments.

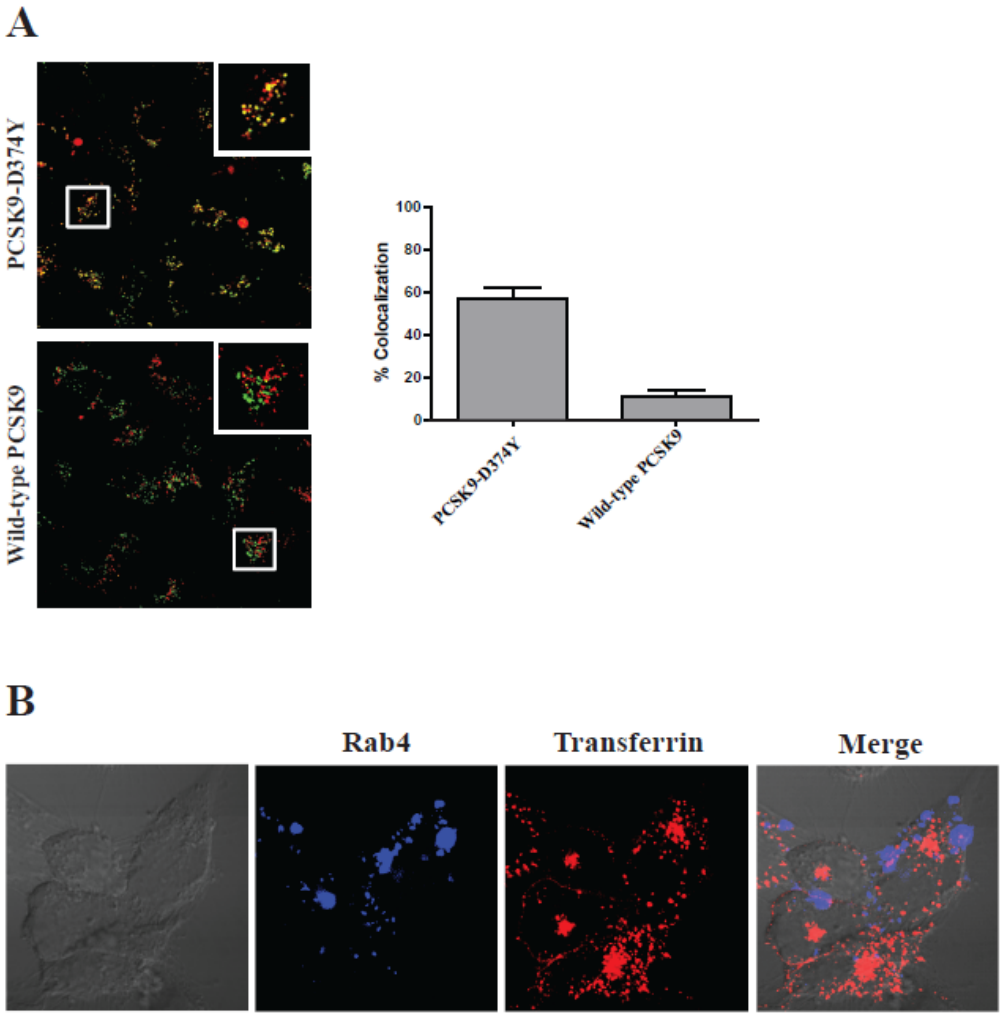


***Figure 3.13. Co-localization of the mutant PCSK9-D374Y and transferrin in recycling compartments of SV589 human fibroblast cells.*** (A) SV589 cells were grown in μ-slide 8-well plates to ~80% confluence, and were cultured overnight in medium C supplemented with 150 μM E-64. Following >1 hour incubation in serum-free medium A to deplete endogenous transferrin, cells were treated with AlexaFluor® 488-labeled PCSK9-D374Y (or AlexaFluor® 488-labeled wild-type PCSK9) and AlexaFluor® 647-labeled transferrin for 1 hour. The labeled proteins were then chased for 2 hour in label-free medium A. (B) SV589 cells were transiently transfected with tRFP tagged Rab4 expression plasmid using Lipofectamine 2000. After 20 to 24 hours, the cells were incubated in serum-free medium A for >1 hour, followed by the addition of AlexaFluor® 647-labeled transferrin for 1 hour. The cells were then chased for 2 hours in label-free medium A. Images were directly taken on the confocal microscope Fluoview FV1000 Version 2.1 (Olympus) using the 488nm laser for PCSK9, the 543nm laser for Rab4, and the 633nm laser for transferrin. The percentage of co-localization was quantified using Image J (http://rsb.info.nih.gov/ij/), and corrected for background using negative images. Graphs represent the means ± standard deviation from three independent experiments.

between the mutant PCSK9-D374Y and transferrin really happened in recycling compartments, but not in early endosomes.

### 3.8 LDLR-EGF66 variant that binds PCSK9 in a calcium-independent manner could restore wild-type PCSK9 activity in fibroblast cells

PCSK9 failed to promote LDLR degradation in fibroblast cells despite its normal uptake into these cells. Above results showed that in fibroblast cells, wild-type PCSK9 dissociated from the recycling receptor and proceeded to lysosomes for degradation whereas the mutant PCSK9-D374Y, which has higher affinity in binding to the LDLR, seemed to maintain the binding to the LDLR in early endosomes and recycle to the cell surface along with the receptor. However, the mechanisms responsible for different PCSK9 fate in hepatic and fibroblast cells had not been molecularly defined.

As discussed in the introduction, PCSK9 binds to the LDLR in a calcium-dependent manner (91). Here, we examined PCSK9 activity in fibroblast cells transiently overexpressing either wild-type LDLR or a special LDLR variant (LDLR-EGF66) that binds PCSK9 in a calcium-independent manner. This variant contains five single-site mutations in the EGF-A domain of the LDLR, including Aspartate-299-Alanine, Asparagine-301-Leucine, Valine-307-Isoleucine, Asparagine-309-Arginine, and Aspartate-310-Lysine. All of them are involved in PCSK9 binding, and therefore isolated EGF66 exhibits >10-fold stronger binding affinity toward PCSK9 compared to the wild type EGF-A domain. Especially, it should be noted that the interaction of LDLR-EGF66 with PCSK9 would no longer be dependent on calcium (115). LDLR-transfected cells were treated with sterols (25-hydroxycholesterol and cholesterol) to suppress endogenous LDLR expression prior to 6-hour incubation with wild-type PCSK9 (10 μg/ml) or PCSK9-D374Y (2 μg/ml). Non-

transfected cells were used as controls for the resistance of fibroblast cells to PCSK9-mediated LDLR degradation.

As shown in Figure 3.14, fibroblast cells expressing either wild-type LDLR or the LDLR-EGF66 variant were still highly resistant to LDLR degradation promoted by PCSK9-D374Y, whereas LDLR(EGF66)-transfected cells became partially responsive to wild-type PCSK9. Following PCSK9-D374Y incubation, LDLR protein levels were not significantly decreased (only ~10% compared to untreated cells) in fibroblast cells expressing wild-type LDLR (lane 5) or LDLR-EGF66 (lane 8). LDLR levels in non-transfected cells were approximately 20% less than those of untreated cells as usual (lane 2). Similarly, no reduction in cellular LDLRs was detected in non-transfected cells (lane 3) as well as cells expressing wild-type LDLR (lane 6) after treatment with wild-type PCSK9. However, approximately half of LDLR levels were decreased in cells expressing the LDLR-EGF66 variant (lane 9) when these cells were incubated with 10 μg/ml wild-type PCSK9. Both wild-type PCSK9 and the mutant PCSK9-D374Y occurred at similar levels in cells expressing wild-type LDLR or LDLR-EGF66, indicating that PCSK9 binding and uptake was mediated equally by either construct.

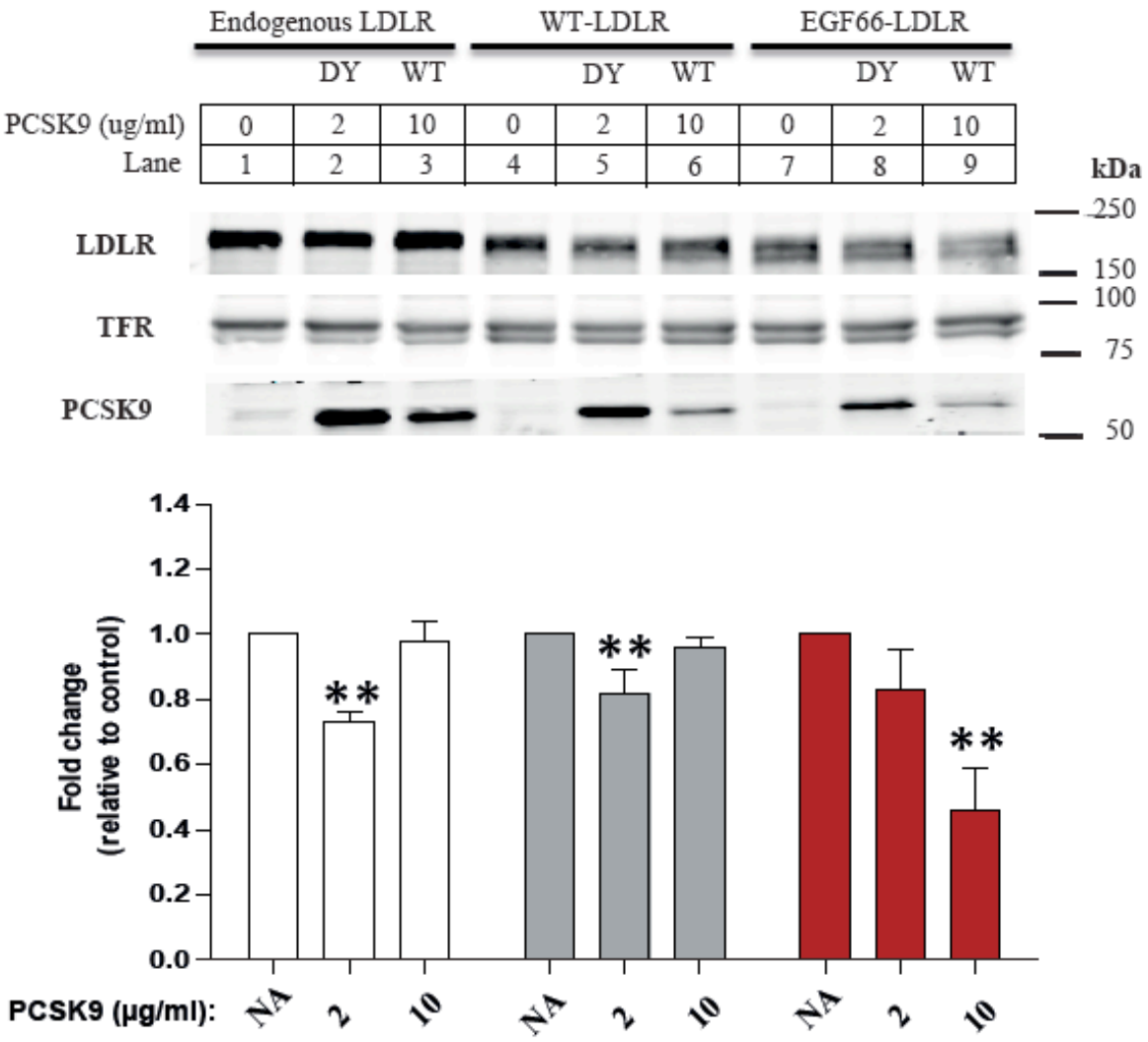


***Figure 3.14. Wild-type LDLR and LDLR-EGF66 degradation mediated by PCSK9 in SV589 human fibroblast cells.*** SV589 cells were grown in medium B to ~60-70% confluence. The cells were then transiently transfected with wild-type LDLR or LDLR-EGF66 expression vectors, and incubated overnight in sterol-supplemented medium (25-hydroxycholestrol/cholesterol) to suppress endogenous LDLR expression. Wild-type PCSK9 (10 μg/ml) and PCSK9-D374Y (2 μg/ml) was incubated for 6 hours. Whole cell lysates were subjected to 8% SDS-PAGE followed by immunoblot analysis of LDLR, PCSK9 and TFR. Secondary detection used infrared dye (IRDye800)-labeled antibodies. Blots were visualized and quantified using the LI-COR Odyssey infrared imaging system. LDLR levels were normalized to TFR expression and expressed relative to control cells (no addition – NA). Graphs represent the means ± standard deviation from three independent experiments. * indicates a statistical difference between columns with significance $p < 0.05$ by Student's t-test; ** $p < 0.005$.

## 4. Discussion

Increased plasma levels of LDL-C represent the greatest risk factor of CHD (1). The LDLR that mediates the endocytic uptake of LDL particles into cells is the major determinant of plasma LDL-C concentrations (42, 58). The discovery of PCSK9, a secreted protein that promotes LDLR degradation in liver, has opened a new era not only for our understanding of cholesterol metabolism but also for the treatment of cardiovascular diseases. Particularly, the strikingly low levels of LDL-C found in individuals who carry loss-of-function mutations in *PCSK9* have inspired researchers to investigate the mechanisms responsible for PCSK9-mediated LDLR degradation (8). In the present study, we determined PCSK9 activity on LDLR levels of several cell lines, including hepatic cells and fibroblast cells. Our hypothesis is that PCSK9 has cell-type specificity, in which hepatic cells are the most responsive cells. We also illuminated the fate of PCSK9 after binding to the LDLR in nonresponsive cells, which might allow us to explore potential mechanisms that lead to dissimilar responses to PCSK9-mediated LDLR degradation in hepatic and fibroblast cells. These mechanisms could be targeted to inhibit PCSK9 activity and preserve LDLR function in the liver.

### 4.1 PCSK9 degrades LDLRs in a cell-type dependent manner

It was shown that injection of human recombinant PCSK9 into mice and adenovirus-mediated overexpression of PCSK9 in mice resulted in a dramatic reduction of LDLRs in liver as well as LDLRs in kidney, ileum and lung, in a lesser extent. However, no changes in LDLR levels were observed in brains (67, 71, 116, 117). Particularly, even when PCSK9 was specifically overexpressed in kidney, LDLR levels in this tissue were still reduced to a lower degree than those in liver (118). In addition, purified PCSK9 introduced into the circulation of wild-type mice at physiological concentrations induced robust degradation of hepatic

LDLRs whereas it was completely ineffective to promote LDLR degradation in the adrenal glands (106), which also have the highest LDLR expression in the body for cholesterol uptake and are the main places to produce steroid hormones in humans (119). These findings, when taken together, suggested that not all tissues respond equally to circulating PCSK9, in which liver is most responsive. Here we showed that incubation of liver-derived cell-lines with purified PCSK9 caused dramatic degradation of cell surface as well as whole cell LDLRs (Figure 3.3 and 3.5), whereas PCSK9 only had minimal effects on LDLRs in several lines of fibroblast cells (Figure 3.2 and 3.5). Thus, PCSK9 degrades LDLRs in a cell-type specific manner. Our data are consistent with those reported that recombinant human PCSK9 added to the medium did not significantly affect the protein levels of LDLR in mouse embryonic fibroblasts whereas it promoted LDLR degradation in hepatocytes (7). Particularly, addition of purified PCSK9 to the medium at levels comparable with those in human plasma induced LDLR degradation in hepatic cells, but not in fibroblast cells (Figure 3.1), confirming that cell-type specificity of PCSK9 does occur physiologically. Besides, SV589 cells were still highly resistant to PCSK9-mediated LDLR degradation after overnight incubation with exogenous PCSK9 (Figure 3.4). Therefore, it is not likely that dissimilar responses to PCSK9 in hepatic and fibroblast cells mainly result from different association and uptake time of PCSK9 in these cells.

However, it was shown that although PCSK9 was not involved in the degradation of LDLRs in adult mouse brain, PCSK9 seemed to affect LDLR levels in brain during development and following transient ischemic stroke (120). Therefore, the effect of PCSK9 on LDLRs might be not the same under different conditions. Studies using more cell lines under a wide range of conditions will help to further address this hypothesis.

## 4.2 PCSK9 association/uptake is LDLR-dependent in both of hepatic and fibroblast cells

Purified PCSK9 injected into wild-type mice had a half-life of 5 minutes whereas this interval was increased to 15 minutes in $LDLR^{-/-}$ mice, suggesting that functional LDLRs might play an important role in mediating PCSK9 clearance (106). Complementing this experiment, numerous studies have demonstrated that PCSK9 internalization in hepatic cells is mediated by the LDLR. LDLR deficiency in hepatocytes from LDLR-null mice as well as RNA interference-mediated knockdown of LDLR significantly inhibited PCSK9 endocytosis (99, 101). As indicated in LDLR degradation assay, PCSK9 failed to degrade LDLRs in fibroblast cells despite its normal uptake into the cells (Figure 3.1, 3.2, and 3.4). However, it could be argued that PCSK9 was taken up via different receptors, which led to the lack of PCSK9-mediated LDLR degradation in fibroblast cells. To rule out this possibility, we examined the contribution of LDLR to PCSK9 association/uptake in hepatic as well as fibroblast cells. A high percentage of exogenous labeled PCSK9 was internalized in hepatic and fibroblast cells expressing LDLRs whereas the amount of endocytosed PCSK9 was completely abolished when LDLR expression was suppressed in these cells (Figure 3.6). Moreover, no cell-associated PCSK9 along with internalized PCSK9 were detected in either hepatic or fibroblast cells expressing a binding-defective LDLR (LDLR-E296Q) (Figure 3.7). This mutation, which presumably decreased calcium-affinity of the LDLR EGF-A domain more extensively, failed to bind PCSK9 (data not shown) because of the calcium-dependent manner of PCSK9 binding to the LDLR (91, 112). Combined together, these data confirmed that PCSK9 association/uptake is LDLR-dependent in hepatic and fibroblast cells. Similar to our results, it was shown that purified added PCSK9 was taken up by mouse embryonic fibroblasts in a manner that depended on the LDLR (7). Besides, PCSK9 failed to

internalize into cells expressing a mutant LDLR missing the EGF-A domain, which is necessarily required for the interaction between PCSK9 and the LDLR (91). However, these data, when taken together, argued against a recent study that reported PCSK9 was endocytosed in an LDLR-independent manner in HepG2 cells (121).

### 4.3 PCSK9 in hepatic cells

To explore the potential mechanisms underlying dissimilar responses to PCSK9-mediated LDLR degradation in hepatic and fibroblast cells, we examined the fate of PCSK9 after binding to the LDLR in these cell lines.

Previous work demonstrated that after being secreted from liver as a stable complex with its prosegment (72), PCSK9 binds to the LDLR on the cell surface (7, 101). The LDLR/PCSK9 complex is then internalized via the same endocytic machinery importing LDL, which requires the endocytic adaptor protein ARH (7, 99). However, different from bound lipoprotein particles that release from the LDLR in the low pH and low calcium environment in early endosomes (42, 58, 65), PCSK9 still binds to the LDLR with considerably increased affinity (92), prevents the receptor from recycling to the cell surface, and directs it to lysosomes where the whole complex, including the LDLR and PCSK9, is degraded (7, 102, 104) (Figure 1.4).

Results obtained in our studies confirmed this scenario in hepatic cells. PCSK9 degradation assay revealed that the levels of mono-iodotyrosine radioactivity were significantly increased in the medium following 6-hour chase of internalized $^{125}$I-labeled wild-type PCSK9 and PCSK9-D374Y, implicating that both of wild-type PCSK9 and the mutation were delivered to lysosomes for degradation in hepatic cells. Particularly, PCSK9-D374Y was degraded more effectively than wild-type PCSK9 (about 5-fold) as indicated by the different concentrations of labeled proteins added to the medium and the nearly equal

amounts of TCA-soluble counts released in the medium (Figure 3.8). In addition, wild-type PCSK9 and the mutant PCSK9-D374Y co-localized with the lysosome marker (LysoTracker) in live cell imaging, confirming the trafficking of PCSK9 to lysosomes in hepatic cells (Figure 3.9). Therefore, in hepatic or responsive cells, both of wild-type PCSK9 and PCSK9-D374Y were internalized and delivered to lysosomes for degradations.

**4.4 PCSK9 in fibroblast cells**

However, the fate of PCSK9 is not the same for wild-type PCSK9 and the mutant PCSK9-D374Y in fibroblast cells. A significant amount of $^{125}$I-labeled wild-type PCSK9 was delivered to lysosomes for degradation in fibroblast cells, following the chase period in PCSK9 degradation assay, whereas $^{125}$I-labeled PCSK9-D374Y was degraded at lower levels in fibroblast. Particularly, wild-type PCSK9 was internalized and degraded equally in both of hepatic and fibroblast cells (Figure 3.8), thus suggesting that wild-type PCSK9 separated from the recycling receptor after being internalized in fibroblasts since the LDLR was not readily degraded whereas PCSK9 was. Furthermore, almost no wild-type PCSK9 that recycled to the cell surface was detected in PCSK9 recycling assay, confirming dissociation of wild-type PCSK9 from the LDLR in fibroblast cells. However, consistent with the results of PCSK9 degradation assay, recycling assay showed that higher percentage of internalized PCSK9-D374Y recycled to the cell surface along with the LDLR, instead of directing the receptor to lysosomes for degradation (Figure 3.10). Live cell imaging confirmed that both of wild-type PCSK9 and PCSK9-D374Y co-localized with the lysosome marker (LysoTracker) in fibroblast cells (Figure 3.11 and 3.12) while only the PCSK9-D374Y mutation also overlapped with labeled transferrin in endocytic recycling compartments (Figure 3.13). These data implied that even with persistent binding, PCSK9 might have reduced activity to route the LDLR to lysosomal degradation in fibroblast cells. Similarly, it was shown that a

mutant PCSK9 lacking the C-terminal domain also failed to promote LDLR degradation in hepatic cells although it still maintained the binding to the LDLR (104). The deficiency of this mutation in degrading LDLRs has not been fully characterized. In fact, the C-terminal domain of PCSK9 has been reported to interact with endocytic adaptor protein(s) that are required for lysosomal targeting and PCSK9-mediated LDLR degradation (94, 105). If so, then perhaps these same proteins or processes might be less expressed in fibroblast cells compared to in hepatocytes. Therefore, it would be interesting to determine if C-terminal domain truncated PCSK9 recycles in hepatocytes, similar to PCSK9-D374Y recycling in fibroblasts.

Based on these results, our studies provide the first description of PCSK9 trafficking in non-responsive cells, which may allow us to illuminate potential factors as well as mechanisms that help these cells be resistant to PCSK9-mediated LDLR degradation. The fate of PCSK9 in fibroblast cells can be described as follow. After the LDLR/PCSK9 complex is endocytosed in an LDLR-dependent manner, the LDLR does not traffic to lysosomes for degradation, but recycles to the cell surface instead. In the case of wild-type PCSK9, PCSK9 dissociates from the LDLR in early endosomes following internalization, and proceeds to late endosomes/lysosomes for degradation while the receptor recycles to the cell surface, resulting in no significant changes of LDLR levels in response to wild-type PCSK9 (Figure 4.1). In contrast, the mutant PCSK9-D374Y has 5 to 30-fold greater affinity in binding to the LDLR compared with wild-type PCSK9 (93, 96), so higher percentage of PCSK9-D374Y still maintains the binding to the receptor in early endosomes. The LDLR/PCSK9 complex then either goes to lysosomes for degradation or recycles to the cell surface (Figure 4.2). It accounted for a small reduction of LDLRs (approximately <20%) in response to the mutant PCSK9-D374Y.

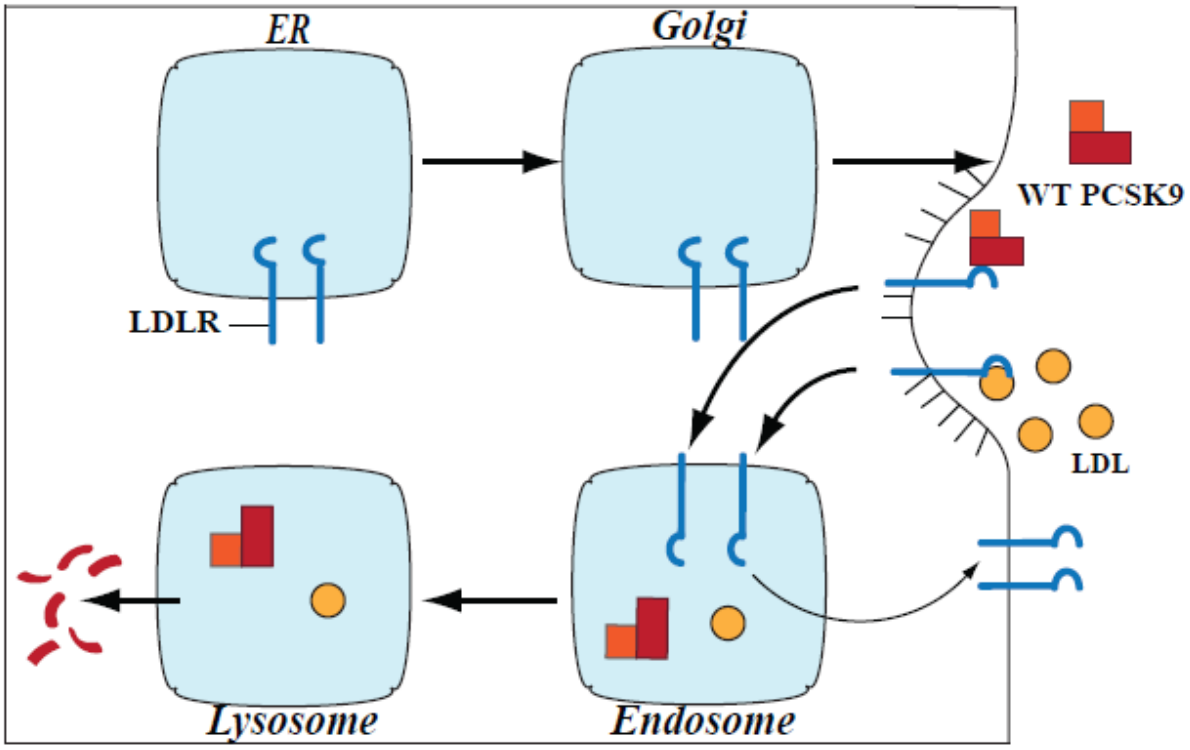


***Figure 4.1. Model of wild-type PCSK9 in fibroblast cells.*** Wild-type PCSK9 directly binds the LDLR on the cell surface, and is internalized in an LDLR-dependent manner. However, different from PCSK9 fate in hepatic cells, wild-type PCSK9 dissociates from the LDLR in early endosomes, and proceeds to late endosomes/lysosomes for degradation while the receptor recycles to the cell surface. Images modified from Horton, Cohen, and Hobbs (2009)(72).

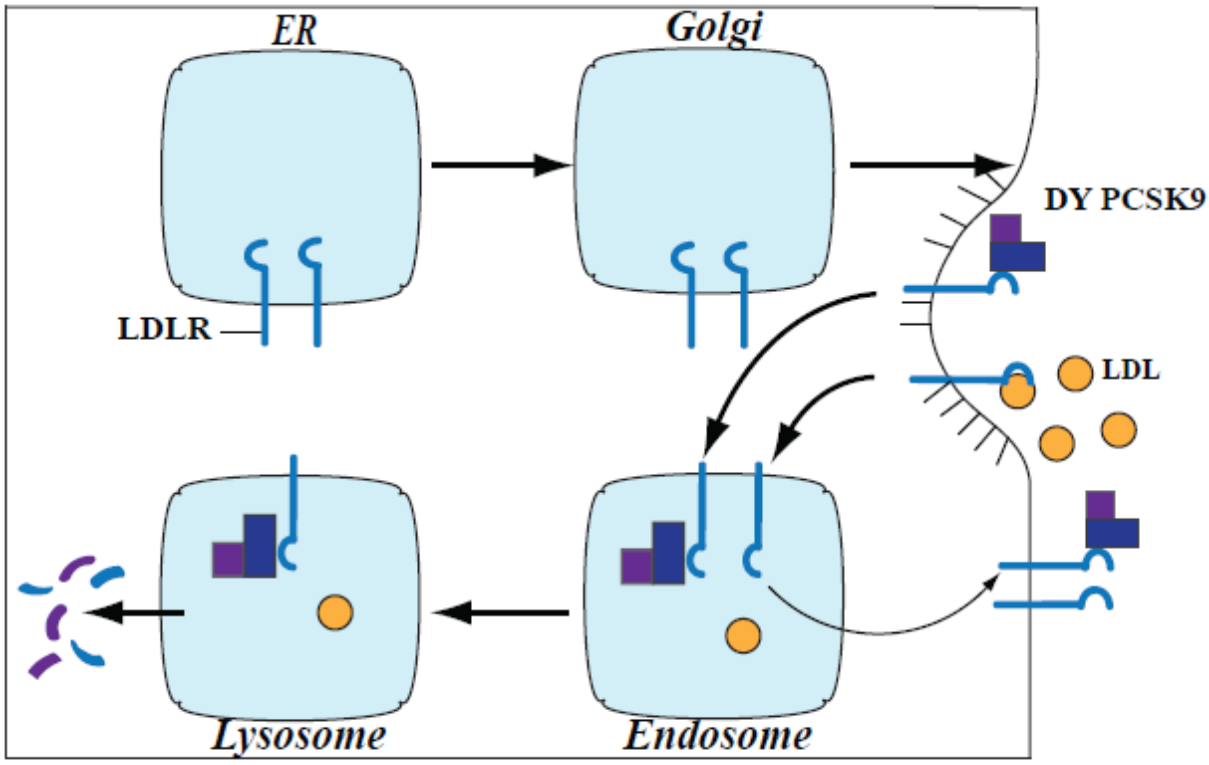


***Figure 4.2. Model of PCSK9-D374Y in fibroblast cells.*** PCSK9 directly binds the LDLR on the cell surface, and is internalized in an LDLR-dependent manner. When the LDLR/PCSK9 complexes reach early endosomes, high percentage of PCSK9-D374Y does not separate from the LDLR, but maintain the binding to the receptor due to 5 to 30-fold greater binding affinity (93, 96). Subsequently, the complex then either goes to lysosomes for degradation or recycles to the cell surface. Images modified from Horton, Cohen, and Hobbs (2009)(72).

## 4.5 A possible role of endosomal calcium concentrations in PCSK9-mediated LDLR degradation

As discussed in the introduction, PCSK9-mediated LDLR degradation involves the binding of PCSK9 to the first repeat in the EGF-precursor homology domain of LDLR. This binding to the EGF-A module is calcium-dependent and enhances in the acidic environment of early endosomes (91, 92). In the structure of this complex, due to its involvement in the salt bridge with Arg-194 of PCSK9, Asp-310, which is a calcium-coordinating residue in the EGF-A repeat, just contributes one of its side-chain oxygen atoms for the calcium coordination (96). Especially, the calcium coordination observed in the LDLR EGF-A domain when binding to PCSK9 has similar geometry to the coordination in the EGF-like domain of C1s, the homologous complement serine proteases (122). However, in the EGF-like module of coagulation factor IX, the equivalent aspartate residue (Asp-64) coordinates calcium by both of its side-chain oxygen atoms (123) (Figure 4.3). Moreover, previous work reported that mutations causing Asp-64 to Asn change in factor IX, which altered the contribution of residue 64 for the calcium coordination from two side-chain oxygens to one side-chain oxygen, resulted in approximately 1000-fold lower calcium-affinity of the EGF-like domain compared to the wild-type, and subsequently, led to a functionally defective factor IX in hemophilia B patients (112, 124).

Thus, we hypothesize that through forming a salt bridge between its Arg-194 residue and the side-chain oxygen of LDLR – Asp-310, PCSK9 might induce a conformation change in the calcium-binding site, which affects titration of calcium of the EGF-A domain in early endosomes. Especially, it was shown that the measured calcium-affinity in the LDLR EGF-A domain was closely tuned to endosomal calcium concentrations. The plasma calcium concentration is ~2 mM, which decreases about 50- to 200-fold within endosomal compartments

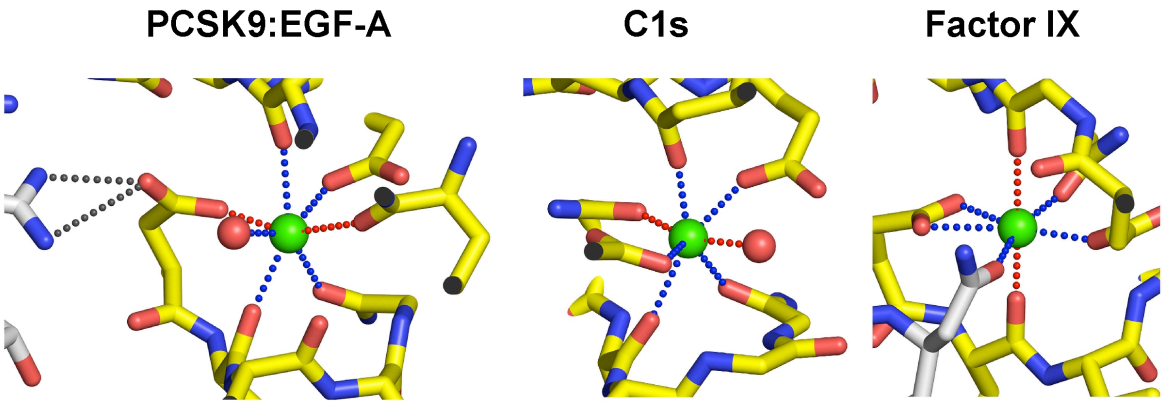


***Figure 4.3: Binding of PCSK9-R194 to LDLR-D310 in the calcium-binding site of the LDLR EGF-A domain.*** The calcium coordination within the PCSK9:EGF-A complex are shown. In the structure of this complex, Arg-194 of PCSK9 forms a salt bridge with EGF-A – Asp-310, a calcium-coordinating residue in the EGF-A repeat. Therefore, Asp-310 just contributes one of its side-chain oxygen atoms for the calcium coordination. The other calcium ligands in the EGF-A module consist of side-chain oxygen from Glu-296; the carbonyl oxygens of Thr-294, Leu-311, and Gly-314; and a water molecule, forming a classic pentagonal bipyramid. Besides, there is a seventh ligand, the carbonyl oxygen of Cys-292 (96). The calcium coordination observed in EGF-A when bound to PCSK9 has the similar geometry to the coordination in the EGF-like domain of C1s (122). However, in the EGF-like module of coagulation factor IX, the equivalent aspartate residue (Asp-64) coordinates calcium by both of its side-chain oxygens (123). Calcium is shown as a green sphere and water molecules are shown as red spheres. The equatorial ligands are indicated by blue dots and the axial ligands are indicated by red dots.

depending on the cell-types (125, 126). Therefore, differences in endosomal calcium concentrations could account for dissimilar responses to PCSK9-mediated LDLR degradation in hepatic and fibroblast cells. Our working model is that if PCSK9-responsive cells had higher endosomal calcium concentrations than PCSK9-nonresponsive cells, it would lead to more LDLRs in which the EGF-A domain is still calcium loaded and PCSK9-binding competent because PCSK9 binding to the LDLR is calcium-dependent. So, PCSK9 would be able to promote LDLR degradation by maintaining the stable interaction to the receptor in hepatic cells. While changed calcium titration in the LDLR EGF-A domain due to PCSK9 binding, which combined with the relatively lower calcium concentrations in early endosomes of fibroblast cells, could cause loss of calcium from the EGF-A domain and wild-type PCSK9 dissociation from the LDLR, allowing the receptor to recycle to the cell surface in these cells. However, the mutant PCSK9-D374Y might dissociate less frequently in fibroblast cells due to 5 to 30-fold greater affinity in binding to the LDLR versus wild-type PCSK9.

We expected that changing the interaction between PCSK9 and the LDLR from calcium-dependent to calcium-independent would allow PCSK9 to maintain the binding to the receptor, and subsequently, to be effective in degrading LDLRs in fibroblast cells. In the present study, fibroblast cells expressing the LDLR mutation (LDLR-EGF66) that binds PCSK9 in a calcium-independent manner (115) did become responsive to wild-type PCSK9 although still in a lesser extent compared with hepatic cells. Surprisingly, addition of the mutant PCSK9-D374Y to the medium of culture fibroblasts expressing either wild-type LDLR or LDLR-EGF66 did not result in a significant difference of LDLR levels between these cells. Instead, they responded equally to PCSK9-D374Y (Figure 3.14). These data implicated that the LDLR-EGF66 that would presumably help maintain PCSK9 binding to

the LDLR, even in the lower calcium-concentration environment of fibroblast endosomes, could partially restore wild-type PCSK9 activity, but not PCSK9-D374Y activity. Therefore, the maintenance of PCSK9 binding to the LDLR would not be sufficient enough to direct the receptor to lysosomes for degradation in fibroblast cells. Zhang et al. (2008) supported a model in which the LDLR/PCSK9 complex might interact with another protein that signals lysosomal delivery of the complex. In this study, they indicated that although other regions such as at least three ligand-binding repeats and the β-propeller domain of LDLR as well as the C-terminal domain of PCSK9 were not required for PCSK9 binding or receptor internalization, they were required for PCSK9-mediated LDLR degradation (104). Thus, it is possible that loss of calcium from the EGF-A domain due to changed calcium titration along with considerably lower calcium concentrations in early endosomes of fibroblast cells could disrupt the binding interface between the LDLR/PCSK9 complex and the protein required for lysosomal degradation. Therefore, even when PCSK9-D374Y or the mutant LDLR-EGF66 still retained the binding, they failed to promote LDLR degradation in fibroblast cells. In fact, several studies have demonstrated that the calcium-binding site serves a critical role in maintaining the conformation and functions for diverse proteins containing EGF-like domain. Alterations in calcium-affinity of the EGF-A module that result in the local flexibility of this domain can significantly affect the global conformation of the receptor (127). Additional experiments will be needed not only to further characterize the LDLR-EGF66 mutation but also to address this possibility.

### 4.6 Future directions

The current studies not only determined the cell-type specificity of PCSK9 activity but also suggested the potential importance of endosomal calcium concentrations in PCSK9-

mediated LDLR degradation. However, there are still critical aspects related to dissimilar responses of hepatic cells and other cell-types to PCSK9 that have not been well understood, highlighting the need for future experiments to further characterize the cell-type dependent manner of PCSK9 as well as the role of endosomal calcium concentrations in LDLR degradation mediated by PCSK9.

As stated in the discussion, PCSK9 promoted LDLR degradation in mouse brains during development and following ischemic stroke whereas it had no effects on LDLR levels of adult mouse brains (120), suggesting PCSK9 might affect LDLRs differently under various conditions. Therefore, studies in which PCSK9-responsiveness of more cell lines from a wide range of conditions are assessed will be needed to address this question.

Our working model for dissimilar responses to PCSK9-mediated LDLR degradation in different cell types is the endosomal calcium concentration. This hypothesis will be further verified by examining the effects of altered calcium levels of endosomes on PCSK9-mediated LDLR degradation in nonresponsive and responsive cells. For example, we anticipate that using calcium chelators such as BAPTA (1,2-bis(o-aminophenoxy)ethane-N,N,N',N'-tetraacetic acid) to specifically decrease free calcium concentrations of endosomes would make hepatic cells become nonresponsive to PCSK9. In contrast, when endosomal calcium levels were increased by using bafilomycin, a specific inhibitor of the vacuolar-type proton ATPase, to block loss of calcium from endosomes (89) or expressing transient receptor potential mucolipins (TRPMLs), which are calcium-permeable ion channels within the endolysosomal system, fibroblast cells could turn into PCSK9-responsive cells.

In addition, we also want to further characterize the effects of LDLR-EGF66 as well as LDLR-E296Q mutations on LDLR degradation mediated by PCSK9. Indicated in the

discussion, E296Q mutation would presumably decrease calcium-affinity of the EGF-A domain more extensively according to the corresponding residue in coagulation factor IX (112). We expected that hepatic cells expressing this mutation would become PCSK9-nonresponsive due to the dramatic loss of calcium from the EGF-A module in endosomal environments that subsequently results to PCSK9 dissociation from the LDLR, even when these cells have higher levels of calcium in endosomes. However, the characterization of LDLR-E296Q variation is not a small order because this mutation fails to bind as well as uptake exogenous PCSK9, highlighting the need for binding studies in order to identify appropriate conditions by which PCSK9 can be internalized into cells expressing LDLR-E296Q.

### 4.7 Conclusion

Following its first discovery in 2003, PCSK9 has become the subject of growing interest and intense research in cholesterol regulation. Although our understanding of this proprotein convertase has advanced significantly over the past years, many critical mechanistic as well as clinical questions still need to be answered. Particularly, the mechanisms by which PCSK9 promotes LDLR degradation in lysosomes have not been fully determined. In the first stage, this thesis research aimed to define the cell-type specificity of PCSK9 activity, and more specifically, to investigate potential factors that result in dissimilar effects of PCSK9 on LDLRs in different cell-types. Consistent with numerous studies, we confirmed that PCSK9 caused robust degradation of LDLRs in hepatic cells whereas its activity was completely ineffective in fibroblast cells. Using these cells as representative models, we were able to further characterize the fate of PCSK9 after being internalized in responsive and non-responsive cells. In hepatic cells or responsive cells, our results supported the model in which PCSK9 is internalized in an LDLR-dependent manner. After

the LDLR/PCSK9 complex reaches early endosomes, both of wild-type PCK9 and PCSK9-D374Y maintain the binding to the LDLR and route the receptor to lysosomes where the whole complex is degraded, resulting in a significant reduction of LDLR levels in hepatic cells. Nevertheless, wild-type PCSK9 trafficking is not the same as the mutant in fibroblast cells. It was shown that wild-type PCSK9 dissociates from the LDLR in early endosomes, followed by the lysosomal delivery of wild-type PCSK9 while the receptor recycles to the cell surface. In contrast, higher percentage of the mutant PCSK9-D374Y, which has greater binding affinity toward the LDLR, was capable of retaining the binding to the receptor in early endosomes. Subsequently, the LDLR/PCSK9 complex then either goes to lysosomes for degradation or recycles to the cell surface. Combined together, we conclude that two factors may diminish PCSK9 activity in fibroblast cells: i) an increased dissociation from the LDLR in early endosomal compartments as we see in the situation of wild-type PCSK9, and ii) a decreased ability of bound PCSK9 to direct the LDLR to lysosomes for degradation for the mutant PCSK9-D374Y. These further insights provide us important cues for future studies to explore underlying mechanisms by which PCSK9 routes the LDLR to lysosomes for degradation in hepatic cells, but not in fibroblast cells. For example, the LDLR variation (EGF66) that binds PCSK9 in a calcium-independent manner could partially restore wild-type PCSK9 activity, but not PCSK9-D374Y activity, in fibroblast cells, suggesting a potential role of endosomal calcium concentrations in PCSK9-mediated LDLR degradation. In fact, by changing the calcium coordination geometry, the binding of PCSK9 could affect calcium titration of the LDLR EGF-A domain in early endosomes, and different endosomal calcium concentrations could account for dissimilar responses to PCSK9-mediated LDLR degradation in hepatic and fibroblast cells. This hypothesis will be addressed in future studies.

## 5. References


1. Chilton, R. J. (2004). Pathophysiology of coronary heart disease: A brief review. *J. Am. Osteopath. Assoc.* **104**: S7-S8.

2. Nabel, E. G. and Braunwald E. (2012). A tale of coronary artery disease and myocardial infraction. *N. Engl. J. Med.* **366**: 54-63.

3. Golomb B. A. and Evans M. A. (2008). Statin adverse effects: A review of the literature and evidence for a mitochondrial mechanism. *Am. J. Cardiovasc. Drugs.* **8**: 373-418.

4. Maxwell, K. N. and Breslow, J. L. (2004). Adenoviral-mediated expression of PCSK9 in mice results in a low-density lipoprotein receptor knockout phenotype. *Proc. Natl. Acad. Sci. USA.* **101**: 7100-7105.

5. Benjannet, S., Rhainds, D., Essalmani, R., Mayne, J., Wickham, L., Jin, W., Asselin, M., Hamelin, J., Varret, M., Allard, D., Trillard, M., Abifadel, M., Tebon, A., Attie, A. D., Rader, D. J., Boileau, C., Brissette, L., Chretien, M., Prat, A., and Seidah, N. G. (2004). NARC-1/PCSK9 and its natural mutants: Zymogen cleavage and effects on the low density lipoprotein (LDL) receptor and LDL cholesterol. *J. Biol. Chem.* **279**: 48865-48875.

6. Park, S. W., Moon, Y., Horton, J. D. (2004). Post-transcriptional regulation of low density lipoprotein receptor protein by proprotein convertase subtilisin/kexin type 9a in mouse liver. *J. Biol. Chem.* **279**: 50630-50638.

7. Lagace, T. A., Curtis, D. E., Garuti, R., McNutt, M. C., Park, S. W., Prather, H. B., Anderson, N. N., Ho, Y. K., Hammer, R. E., and Horton, J. D. (2006). Secreted PCSK9 decreases the number of LDL receptors in hepatocytes and in livers of parabiotic mice. *J. Clin. Invest.* **116**: 2995 – 3005.

8. Cohen, J. C., Boerwinkle, E., Mosley, T. H., and Hobbs, H. H (2006). Sequence variations in PCSK9, low LDL, and protection against coronary heart disease. *N. Engl. J. Med.* **354**: 1265 – 1272.

9. Roth, E. M., McKenney J. M., Hanotin, C., Asset, G., and Stein, E. A. (2012). Atorvastatin with or without an antibody to PCSK9 in primary hypercholesterolemia. *N. Engl. J. Med.* **367**: 1891-1900.

10. Koren, M. J., Scott, R., Kim, J. B., Knusel, B., Liu, T., Lei, L., Bolognese, M., and Wasserman, S. M. (2012). Efficacy, safety, and tolerability of a monoclonal antibody to proprotein convertase subtilisin/kexin type 9 as monotherapy in patients with hypercholesterolemia (MENDEL): A randomized, double-blind, placebo-controlled, phase 2 study. *Lancet* **380**:1995-2006.

11. Vance, D. E. and Van den Bosch H. (2000). Cholesterol in the year 2000. *Biochim. Biophys. Acta* **1529**: 1-8.
12. Dietschy, J. M. and Turley, S. D. (2001). Cholesterol metabolism in the brain. *Curr. Opin. Lipidol.* **12**: 105-112.

13. Goedeke, L. and Fernandez-Hernando, C. (2012). Regulation of cholesterol homeostasis. *Cell. Mol. Life Sci.* **69**: 915-930.

14. Horton, J. D., Goldstein, J. L., and Brown, M. S. (2002) SREBPs: activators of the complete program of cholesterol and fatty acid synthesis in the liver. *J. Clin. Invest.* **109**: 1125-1131.

15. Jasinska, M., Owczarek, J., Orszulak-Michalak, D. (2007). Statins: a new insight into their mechanisms of action and consequent pleiotropic effects. *Pharmacol. Rep.* **59**: 483-499.

16. Tansey, T. R. and Shechter, I. (2000). Structure and regulation of mammalian squalene synthase. *Biochim. Biophys. Acta* **1529**: 49-62.

17. Waterham, H. R. and Wanders, R. J. (2000). Biochemical and genetic aspects of 7-dehydrocholesterol reductase and Smith-Lemli-Optiz syndrome. *Biochim. Biophys. Acta* **1529**: 340-356.

18. Kandutsch, A. A. and Russell A. E. (1960) Preputial gland tumor sterols. III. A metabolic pathway from lanosterol to cholesterol. *J. Biol. Chem.* **235**: 2256-2261.

19. Ponticorvo, L., Rittenberg, D., and Bloch, K. (1949). The utilization of acetate for the synthesis of fatty acids, cholesterol, and protoporphyrin. J. Biol. Chem. 179: 839-842.

20. Goldstein, J. L. and Brown, M. S. (1982). The LDL receptor defect in familial hypercholesterolemia. Implications for pathogenesis and therapy. *Med. Clin. North. Am.* **66**: 335-362.

21. Grundy, S. M. (1983) Absorption and metabolism of dietary cholesterol. *Annu. Rev. Nutr.* **3**: 71-96.

22. Brown, M. S. and Goldstein, J. L. (1976). Receptor-mediated control of cholesterol metabolism. *Science* **191**: 150-154.

23. Marsh, D. (2009). Cholesterol-induced fluid membrane domains: a compendium of lipid-raft ternary phase diagrams. *Biochim. Biophys. Acta* **1788**: 2114-2123.

24. Fernandez, C., Lobo, Md. Mdel. V, Gomez-Coronado, D., and Lasuncion, M. A. (2004) Cholesterol is essential for mitosis progression and its deficiency induces polyploidy cell formation. *Exp. Cell. Res.* **300**:109-120.

25. Fernandez, C., Martin, M., Gomez-Coronado, D., and Lasuncion, M. A. (2005) Effects of distal cholesterol biosynthesis inhibitors on cell proliferation and cell cycle progression. *J. Lipid Res.* **46**: 920-929.

26. Ikonen, E. (2006). Mechnanisms for cellular cholesterol transport: defects and human disease. *Physiol. Rev.* **86**: 1237-1261.

27. Brown, M. S. and Goldstein, J. L. (2009). Cholesterol feedback: from Schoenheimer's bottle to Scap's MELADL. *J. Lipid Res.* **Appril Supplement**: S15-S27.

28. Brown, M. S. and Goldstein, J. L. (1997). The SREBP pathway: regulation of cholesterol metabolism by proteolysis of a membrane-bound transcriptional factor. *Cell* **89**: 331-340.

29. Eberle, D., Hegarty, B., Bossard, P., Ferre, P., and Foufelle, F. (2004). SREBP transcriptional factors: master regulators of lipid homeostasis. Biochimie 86: 839-848.

30. Horton, J. D., Goldstein, J. L., and Brown, M. S. (2002). SREBPs: activators of the complete program of cholesterol and fatty acid synthesis in the liver. *J. Clin. Invest.* **109**: 1125-1131.

31. Horton J. D. and Shimomura, I. (1999). Sterol regulatory element-binding proteins: activators of cholesterol and fatty acid biosynthesis. Curr. Opin. Lipidol. 10: 143-150.

32. Hua, X., Yokoyama, C., Wu, J., Briggs, M. R., Brown, M. S., Goldstein, J. L., and Wang X. (1993). SREBP-2, a second basic-helix-loop-helix-leucine zipper protein that stimulates transcription by binding to a sterol regulatory element. *Proc. Natl. Acad. Sci. USA* **90**: 11603-11607.

33. Ducan, E. A., Brown, M. S., Goldstein, J. L., and Sakai, J. (1997). Cleavage site for sterol-regulated protease localized to a leu-Ser bond in the lumenal loop of sterol regulatory element-binding protein-2. *J. Biol. Chem.* **272**: 12778-12785.

34. Brown, A. J., Sun, L. P., Feramisco, J. D., Brown, M. S., and Goldstein J. L. (2002). Cholesterol addition to ER membranes alters conformation of SCAP, the SREBP escort protein that regulates cholesterol metabolism. *Mol. Cell* **10**: 237-245.

35. Sun, L. P., Li, L., Goldstein, J. L., and Brown, M. S. (2005). Insig required for sterol-mediated inhibition of Scap/SREBP binding to COPII proteins in vitro. *J. Biol. Chem.* **280**: 26483-26490.

36. Sun, L. P., Seemann, J., Goldstein, J. L., and Brown, M. S. (2007). Sterol-regulated transport of SREBPs from endoplasmic reticulum to Golgi: Insig renders sorting signal in Scap inaccessible to COPII proteins. *Proc. Natl. Acad. Sci. USA* **104**: 6519-6526.

37. Yang, T., Espenshade, P. J., Wright, M. E., Yabe, D., Gong, Y., Aebersold, R., Goldstein, J. L., and Brown, M. S. (2002). Crucial step in cholesterol homeostasis:

sterols promote binding of SCAP to INSIG-1, a membrane protein that facilitates retention of SREBPs in ER. *Cell* **110**: 489-500.

38. Hirano, Y., Yoshida, M., Shimizu, M., and Sato, R. (2001). Direct demonstration of rapid degradation of nuclear sterol regulatory element-binding proteins by the ubiquitin-proteasome pathway. *J. Biol. Chem.* **276**: 36431-36437.

39. Hirano, Y., Murata, S., Tanaka, K., Shimizu, M., and Sato, R. (2003). Sterol regulatory element-binding proteins are negatively regulated through SUMO-1 modification independent of the ubiquitin/26S proteasome pathway. *J. Biol. Chem.* **278**: 16809-16819.

40. Walker, A. K., Yang, F., Jiang, K., Ji, J. Y., Watts, J. L., Purushotham, A., Boss, O., Hirsch, M. L., Ribich, S., Smith, J. J., Israelian, K., Westphal, C. H., Rodgers, J. T., Shioda, T., Elson, S. L., Mulligan, P., Najafi-Shoushtari, H., Black, J. C., Thakur, J. K., Kadyk, L. C., Whetstine, J. R., Mostoslavsky, R., Puigserver, P., Li, X., Dyson, N. J., Hart, A. C., and Naar, A. M. (2010). Conserved role of SIRT1 orthologs in fasting-dependent inhibition of the lipid/cholesterol regulator SREBP. *Genes Dev.* **24**: 1403-1417.

41. Yamamoto, T., Davis, C. G., Brown, M. S., Schneider, W. J., Casey, M. L., Goldstein, J. L., and Russell, D. W. (1984). The human LDL receptor: a cysteine-rich protein with multiple Alu sequences in its mRNA. *Cell* **39**: 27-38.

42. Goldstein, J. L. and Brown, M. S. (2009). The LDL receptor. *Arterioscler. Thromb. Vasc. Biol.* **29**, 431 – 438.

43. Brown, M. S., Kovanen, P. T., and Goldstein, J. L. (1981) Regulation of plasma cholesterol by lipoprotein receptors. *Science* **212**: 628-635.

44. Esser, V., Limbird, L. E., Brown, M. S., Goldstein, J. L., and Russell, D. W. (1988). Mutational analysis of the ligand binding domain of the low density lipoprotein receptor. *J. Biol. Chem.* **263**: 13282-13290.

45. Russell, D. W., Brown, M. S., and Goldstein, J. L. (1989). Different combinations of cysteine-rich repeats mediate binding of low density lipoprotein receptor to two different proteins. *J. Biol. Chem.* **264**: 21682-21688.

46. Davis, C. G., Goldstein, J. L., Sudhof, T. C, Anderson, R. G. W., Russell, D. W., and Brown, M. S. (1987). Acid-dependent ligand dissociation and recycling of LDL receptor mediated by growth factor homology region. *Nature* **326**: 760-765.

47. Westhuyzen, D. R., Stein, M. L, Henderson, H. E., Marais, A. D., Fourie, A. M., and Coetzee, G. A. (1991). Deletion of two growth-factor repeats from the low-density lipoprotein receptor accelerates its degradation. *Biochem. J.* **278**: 677-682.

48. Boswell, E. J., Jeon, H., Blacklow, S. C., and Downing, A. K. (2004). Global defects in the expression and function of the low density lipoprotein receptor (LDLR) associated with two familial hypercholesterolemia mutations resulting in misfolding of the LDLR epidermal growth factor-AB pair. *J. Biol. Chem.* **279**: 30611-30621.

49. Beglova, N., Jeon, H., Fisher C., and Blacklow S. C. (2004). Cooperation between fixed and low pH-inducible interfaces controls lipoprotein release by the LDL receptor. *Mol. Cell* **16**: 281 – 292.

50. Lehrman, M. A., Goldstein, J. L., Brown, M. S., Russell, D. W., and Schneider, W. J. (1985). Internalization-defective LDL receptors produced by genes with nonsense and frameshift mutations that truncate the cytoplasmic domain. *Cell* **41**: 735-743.

51. Davis, C. G., Driel, I. R, Russell, D. W., Brown, M. S., and Goldstein, J. L. (1987). The low density lipoprotein receptor. Identification of amino acids in cytoplasmic domain required for rapid endocytosis. *J. Biol. Chem.* **262**: 4075-4082.

52. Gent, J. and Braakman, I. (2004). Low-density lipoprotein receptor structure and folding. *Cell. Mol. Life Sci.* **61**: 2461-2470.

53. Bu, G. (2001). The roles of receptor-associated protein (RAP) as a molecular chaperone for members of the LDL receptor family. *Int. Rev. Cytol.* **209**: 79-116.

54. Culi, J., Springer, T. A., and Mann, R. S. (2004). Boca-dependent maturation of β-propeller/EGF modules in low-density lipoprotein receptor proteins. *EMBO J.* **23**: 1372-1380.

55. Fass, D., Balcklow, S. C, Kim, P.S., and Berger J. M. (1997). Molecular basis of familial hypercholesterolemia from structure of LDL receptor module. *Nature* **388**: 691-693.

56. Rudenko, G., Henry, L., Henderson, K., Ichtchenko, K., Brown, M. S., Goldstein, J. L., and Deisenhofer, J. (2002). Structure of the LDL receptor extracellular domain at endosomal pH. *Science* **298**: 2353-2358.

57. Blacklow, S. C. and Kim, P. S. (1996). Protein folding and calcium binding defects arising from familial hypercholesterolemia mutations of the LDL receptor. *Nat. Struct. Biol.* **3**: 758-762.

58. Beglova, N. and Blacklow, S. C. (2005). The LDL receptor: how acid pulls the trigger. *Trends Biochem. Sci.* **30**, 309 – 317.

59. Windler, E. E., Kovanen, P. T., Chao, Y. S., Brown, M. S., Havel, R. J., and Goldstein, J. L. (1980). The estradiol-stimulated lipoprotein receptor of rat liver. A binding site that membrane mediates the uptake of rat lipoproteins containing apoproteins B and E. *J. Biol. Chem.* **255**: 10464-10471.

60. Segrest, J. P., Jones, M. K., De Loof, H., and Dashti, N. (2001). Structure of apolipoprotein B-100 in low density lipoproteins. *J. Lipid Res.* **42**: 1346-1367.

61. Brown, M. S., Deuel, T. F., Basu, S. K., and Goldstein, J. L. (1978). Inhibition of the binding of low-density lipoproteins to its cell surface receptor in human fibroblasts by positively charged proteins. *J. Supramol. Struct.* **8**: 223-234.

62. Jeon, H. and Shipley, G. G. (2000). Vesicle-reconstituted low density lipoprotein receptor. Visualization by cryoelectron microscopy. *J. Biol. Chem.* **275**: 30458-30464.

63. Anderson, R. G., Brown, M. S., and Goldstein, J. L. (1977). Role of the coated endocytic vesicle in the uptake of receptor-bound low density lipoprotein in human fibroblasts. *Cell* **10**: 351-364.

64. He, G., Gupta, S., Yi, M., Michaely, P., Hobbs, H. H., and Cohen, J. C. (2002). ARH is a modular adaptor protein that interacts with the LDL receptor, clathrin, and AP-2. *J. Biol. Chem.* **277**: 44044-44049.

65. Zhao, Z. and Michaely, P. (2009). The role of calcium in lipoprotein release by the low – density lipoprotein receptor. *Biochemistry* **48**: 7313 – 7324.

66. Brown, M. S., Anderson, R. G. W., and Goldstein, J. L. (1983). Recycling receptors: The round-trip itinerary of migrant membrane proteins. *Cell* **32**: 663-667.

67. Seidah, N. G., Benjannet, S., Wickham, L., Marcinkiewicz, J., Jasmin, S. B., Stifani, S., Basak, A., Prat, A., and Chretien, M. (2003). The secretory proprotein convertase neural apoptosis-regulated convertase 1 (NARC-1): Liver regeneration and neuronal differentiation. *Proc. Natl. Acad. Sci. USA* **100**: 928-933.

68. Abifadel, M., Varret, M., Rabes, J. P., Allard, D., Ouguerrram, K., Devillers, M., Cruaud, C., Benjannnet, S., Wickham, L., Erlich, D., Derre, A., Villeger, L., Farnier, M., Beucler, I., Bruckert, E., Chambaz, J., Chanu, B., Lecerf, J., Luc, G., Moulin, P., Weissenbach, J., Prat, A., Krempf, M., Junien, C., Seidah, N. G., and Boileau, C. (2003). Mutations in PCSK9 cause autosomal dominant hypercholesterolemia. *Nature Genet.* **34**: 154-156.

69. Maxwell, K. N., Soccio, R. E., Duncan, E. M., Sehayek, E., and Breslow, J. L. (2003). Novel putative SREBP and LXR target genes identified by microarray analysis in liver of cholesterol-fed mice. *J. Lipid Res.* **44**: 2109-2119.

70. Horton, J. D., Shah, N. A., Warrington, J. A., Anderson, N. N., Park, S. W., Brown, M. S., and Goldstein, J. L. (2003). Combined analysis of oligonucleotide microarray data from transgenic and knockout mice identifies direct SREBP target genes. *Proc. Natl. Acad. Sci. USA* **100**:12027-12032.

71. Zaid, A., Roubtsova, A., Essalmani, R., Marcinkiewicz, J., Chamberland, A., Hamelin, J., Tremblay, M., Jacques, H., Jin, W., Davignon, J., Seidah, N. G., Prat, A. (2008). Proprotein convertase subtilisin/kexin type 9 (PCSK9): hepatocyte-specific low-density lipoprotein receptor degradation and critical role in mouse liver regeneration. *Hepatology* **48**: 646-654.

72. Horton, J. D., Cohen J. C., and Hobbs H. H. (2009). PCSK9: a convertase that coordinates LDL catabolism. *J. Lipid Res.* **April Supplement**: S172 – S177.

73. Grozdanov, P. N., Petkov, P. M., Karagyozov, L. K., Dabeva, M. D. (2006). Expression and localization of PCSK9 in rat hepatic cells. *Biochem. Cell. Biol.* **84**: 80-92.

74. Cunningham, D., Danley D. E., Geoghehan, K. F., Griffor, M. C., Hawkins, J. L., Subashi, T. A., Varghese, A. H., Ammirati, M. J., Culp, J. S., Hoth, L. R., Mansour, M. N., McGrath, K. M., Seddon, A. P., Shenolikar, S., Stutzman-Engwall, K. J., Warren, L. C., Xia, D., and Qiu, X. (2007). Structural and biophysical studies of PCSK9 and its mutants linked to familial hypercholesterolemia. *Nat. Struct. Mol. Biol.* **14**: 413-419.

75. Duff, C. J. and Hooper, N. M (2011). PCSK9: an emerging target for treatment of hypercholesterolemia. *Expert Opin. Ther. Targets* **15**: 157-168.

76. Lambert, G., Charlton, F., Rye, K., and Piper, D. E. (2009). Molecular basis of PCSK9 function. *Atherosclerosis* **203**: 1-7.

77. Seidah, N. G. and Prat, A. (2007). The proprotein convertases are potential targets in the treatment of dyslipidemia. *J. Mol. Med.* **85**: 685-696.

78. Hampton, E. N., Knuth, M. W., Li, J., Harris, J. L., Lesley, S. A., and Spraggon, G. (2007). The self-inhibited structure of full-length PCSK9 at 1.9 Å reveals structural homology with resistin within the C-terminal domain. *Proc. Natl. Acad. Sci. USA* **105**: 1820-1825.

79. Piper, D. E., Jackson, S., Liu, Q., Romanow, W. G., Shetterly, S., Thibault, S. T., Shan, B., and Walker, N. P. C. (2007). The crystal structure of PCSK9: A regulator of plasma LDL-cholesterol. *Structure* **15**: 545-552.

80. Cohen, J., Pertsemlidis, A., Kotowski, I. K., Graham, R., Garcia, C. K., and Hobbs, H. H. (2005). Low LDL cholesterol in individuals of African descent resulting from frequent nonsense mutations in PCSK9. *Nat. Genet.* **37**: 161-165.

81. Dubuc, G., Chamberland, A., Wasserf, H., Davignon, J., Seidah, N. G., Bernier, L., and Prat, A. (2004). Statins upregulate PCSK9, the gene encoding the proprotein convertase neural apoptosis-regulated convertase-1 implicated in familial hypercholesterolemia. *Arterioscler. Thromb. Vasc. Biol.* **24**: 1454-1459.

82. Costet, P., Cariou, B., Lambert, G., Lalanne, F., Lardeux, B., Jarnoux, A. L., Grefhorst, A., Staels, B., and Krempf, M. (2006). Hepatic PCSK9 expression is regulated by nutritional status via insulin and sterol regulatory element-binding protein 1c. *J. Biol. Chem.* **281**: 6211-6218.

83. Jeong, H., J., Lee, H., S., Kim., K. S., Kim, Y. K., Yoon, D., and Park, S. W. (2008). Sterol-dependent regulation of proprotein convertase subtilisin/kexin type 9 expression by sterol-regulatory element binding protein-2. *J. Lipid Res.* **49**: 399-409.

84. Mayne, J., Dewpura, T., Raymond, A., Cousins, M., Chaplin, A., Lahey, K. A., Lahaye, S. A., Mbikay, M., Ooi, T. C., and Chretien, M. (2008). Plasma PCSK9 levels are significantly modified by statins and fibrates in humans. *Lipids Health Dis.* **7**: 22.

85. Careskey, H. E., Davis, R. A., Alborn, W. E., Troutt, J. S., Cao, G., and Konrad, R. J. (2008). Atorvastatin increases human serum levels of proprotein convertase subtilisin/kexin type 9. *J. Lipid. Res.* **49**: 394-398.

86. Lakoski, S. G., Lagace, T. A., Cohen J. C., Horton, J. D., and Hobbs, H. H. (2009). Genetic and metabolic determinants of plasma PCSK9 levels. *J. Clin. Endocrinol. Metab.* **94**: 2537-2543.

87. Rashid, S., Curtis, D. E., Garuti, R., Anderson, N. N., Bashmakov, Y., Ho, Y. K., Hammer, R. E., Moon, Y., and Horton, J. D. (2005). Decreased plasma cholesterol and hypersensitivity to statins in mice laking Pcsk9. *Proc. Natl. Acad. Sci. USA* **102**: 5374-5379.

88. Lalanne, F., Lambert, G., Amar, M. J. A., Chetiveaux, M., Zair, Y., Jarnoux, A., Ouguerram, K., Friburg, J., Seidah, N. G., Brewer, H. B., Krempf, M., and Costet, P. (2005). Wild-type PCSK9 inhibits LDL clearance but does not affect apoB-containing lipoprotein production in mouse and cultured cells. *J. Lipid Res.* **46**: 1312-1319.

89. Benjannet, S., Rhainds, D., Hamelin, J., Nassoury, N., and Seidah, N. G. (2006). The proprotein convertase (PC) PCSK9 is inactivated by furin and/or PC5/6A: functional consequences of natural mutations and post-trasnlational modifications. *J. Biol. Chem.* **281**: 30561-30572.

90. Cameron, J., Holla, O. L., Ranheim, T., Kulseth, M. A., Berge, K. E., and Leren, T. P. (2006). Effects of mutations in the PCSK9 gene on the cell surface LDL receptors. *Hum. Mol. Genet.* **15**: 1551-1558.

91. Zhang D., Lagace, T. A., Garuti, R., Zhao, Z., McDonald, M., Horton, J. D., Cohen, J. C., and Hobbs, H. H. (2007). Bindings of proprotein convertases subtilisin/kexin type 9 to epidermal growth factor-like repeat A of low-density lipoprotein receptor decreases receptor recycling and increases degradation. *J. Biol. Chem.* **282**: 18602-18612.

92. Fisher, T. S., Surdo, P. L., Pandit, S., Mattu, M., Santoro, J. C., Wisniewski, D., Cummings, R. T., Calzetta, A., Cubbon, R. M., Fischer, P. A., Tarachandani, A., De

Francesco, R., Wright, S. D., Sparrow, C. P., Carfi, A., and Sitlani, A. (2007). Effects of pH and low density lipoprotein (LDL) on PCSK9-dependent LDL receptor regulation. *J. Biol. Chem.* **282**: 20502-20512.

93. Bottomley, M. J., Cirillo, A., Orsatti, L., Ruggeri, L., Fisher, T. S., Santoro, J. C., Cummings, R. T., Cubbon, R. M., Surdo, P. L., Calzetta, A., Noto, A., Baysarowich, J., Mattu, M., Talamo, F., De Francesco, R., Sparrow, C. P., Sitlani, A., and Carfi, A. (2009). Structural and biochemical characterization of the wild type PCSK9-EGF(AB) complex and natural familial hypercholesterolemia mutants. *J. Biol. Chem.* **284**: 1313-1323.

94. Surdo, P. L., Bottomley, M. J., Calzetta, A., Settembre, E. C., Cirillo, A., Pandit, S., Ni, Y. G., Hubbard, B., Sitlani, A., and Carfri, A. Mechanistic implications for LDL receptor degradation from the PCSK9/ LDLR structure at neutral pH. *EMBO Rep.* **12**: 1300-1305.

95. McNutt, M. C., Kwon, H. J., Chen, C., Chen, J. R., Horton, J. D., and Lagace, T. A. (2009). Antagonism of secreted PCSK9 increases low density lipoprotein receptor expression in HepG2 cells. *J. Biol. Chem.* **284**: 10561 – 10570.

96. Kwon, H. J., Lagace, T. A., McNutt, M. C., Horton, J. D., and Deisenhofer, J. (2008). Molecular basis for LDL receptor recognition by PCSK9. *Proc. Nalt. Acad. Sci. USA* **105**: 1820 – 1825.

97. Yamamoto, T., Lu, C., and Ryan, R. O. (2011). A two-step binding model of PCSK9 interaction with the low density lipoprotein receptor. *J. Biol. Chem.* **286**: 5464-5470.

98. Tveten, K., Holla, O. L., Cameron, J., Strom, T. B., Berge, K. E., Laerdahl, J. K., and Leren, T. P. (2012). Interaction between the ligand-binding domain of the LDL receptor and the C-terminal domain of PCSK9 is required for PCSK9 to remain bound to the LDL receptor during endosomal acidification. *Hum. Mol. Genet.* **21**: 1402-1409.

99. Qian, Y., Schmidt, R. J., Zhang, Y., Chu, S., Lin, A., Wang, H., Wang, X., Beyer, T. P., Bensch, W. R., Li, W., Ehsani, M. E., Lu, D., Konrad, R. J., Eacho, P. I., Moller, D. E., Karathanasis, S. K., and Cao, G. (2007). Secreted PCSK9 downregulates low density lipoprotein receptor through receptor-mediated endocytosis. *J. Lipid Res.* **48**: 1488-1498.

100. Pearse, B. M. F., and Robinson, M. S. (1990). Clathrin, adaptors, and sorting. *Annu. Rev. Cell Biol.* **6**: 151-171.

101. Nassoury, N., Blasiole, D. A., Oler, A. T., Benjannet, S., Hamelin, J., Poupon, V., McPherson, P. S., Attie, A. D., Prat, A., and Seidah, N. G. (2007). The cellular trafficking of the secretory proprotein convertase PCSK9 and its dependence on the LDLR. *Traffic* **8**: 718-732.

102. Wang, Y., Huang, Y., Hobbs, H. H., and Cohen, J. C. (2012). Molecular characterization of proprotein convertase subtilisin/kexin type 9 (PCSK9)-mediated degradation of the LDLR. *J. Lipid Res.* **53**: 1932-1943.

103. McNutt, M. C., Lagace, T. A., and Horton, J. D. (2007). Catalytic activity is not required for secreted PCSK9 to reduce low density lipoprotein receptors in HepG2 cells. *J. Biol. Chem.* **282**: 20799-20803.

104. Zhang, D, Garuti, R., Tang, W., Cohen, J. C., and Hobbs, H. H. (2008). Structural requirements for PCSK9-mediated degradation of the low-density lipoprotein receptor. *Proc. Natl. Acad. Sci. USA* **105**: 13045 - 13050.

105. Mayer, G., Poirier, S., and Seidah, N. G. (2008). Annexin A2 is a C-terminal PCSK9-binding protein that regulates endogenous low density lipoprotein receptor levels. *J. Biol. Chem.* **283**: 31791-31801.

106. Grefhorst, A., McNutt M. C., Lagace, T. A., Horton, J. D. (2008). Plasma PCSK9 preferentially reduces liver LDL receptors in mice. J. Lipid Res. 49, 1303 – 1311.

107. Maxwell, K. N., Fisher, E. A., and Breslow, J. L. (2005). Overexpression of PCSK9 accelerates the degradation of the LDLR in a post-endoplasmic reticulum compartment. *Proc. Natl. Acad. Sci. USA* **102**: 2069-2074.

108. Poirier, S., Mayer, G., Poupon, V., McPherson, P. S., Desjardins, R., Ly, K., Asselin, M., Day, R., Duclos, F. J., Witmer, M., Parker, R., Prat, A., and Seidah, N. G. (2009). Dissection of the endogenous cellular pathways of PCSK9-induced low density lipoprotein receptor degradation: Evidence for an intracellular route. *J. Biol. Chem.* **284**: 28856-28864.

109. Liu, H. and Naismith, J. H. (2008). An efficient one-step site-directed deletion, insertion, single and multiple-site plasmid mutagenesis protocol. *BMC Biotechnol*. **8**: 91.

110. Poirier, S., Mayer, G., Benjannet, S., Bergeron, E., Marcinkiewicz, J., Naasoury, N., Mayer, H., Nimpf, J., Prat, A., and Seidah, N. G. (2008). The proprotein convertase PCSK9 induces the degradation of low density lipoprotein receptor (LDLR) and its closest family members VLDLR and ApoER2. *J. Biol. Chem.* **283**: 2363-2372.

111. Hoof, D. V., Rodenburg, K. W., and Van der Horst, D. J. (2005). Intracellular fate of LDL receptor family members depends on the cooperation between their ligand-binding and EGF domains. *J. Cell. Sci.* **118**: 1309-1320.

112. Handford, P. A., Mayhew, M., Baron, M., Winship, P. R., Campbell, I. D., and Brownlee, G. G. (1991). Key residues involved in calcium-binding motifs in EGF-like domains. *Nature* **351**: 164 – 167.

113. Jackle, S., Runquist, E. A., Miranda-Brady, S., and Havel, R. J. (1991). Trafficking of the epidermal growth factor receptor and transferrin in three hepatocytic endosomal fractions. *J. Biol. Chem.* **266**: 1396-1402.

114. Stein, B. S., Bensch, K. G., and Sussman, H. H. (1984). Complete inhibition of transferrin recycling by monensin in K562 cells. *J. Biol. Chem.* **259**: 14762-14772.

115. Zhang, Y., Zhou, L., Beltran, M. K., Li, W., Moran, P., Wang, J., Quan, C., Tom, J., Kolumam, G., Elliott, J. M., Skelton, N., Peterson, A., and Kirchhofer, D. (2012) Calcium-independent inhibition of PCSK9 by affinity-improved variants of the LDL receptor EGF(A) domain. *J. Mol. Biol.* **422**: 685 – 696.

116. Schmidt, R. J., Beyer, T. P., Bensch, W. R., Qian, Y., Lin, A., Kowala, M., Alborn, W. E., Konrad, R. J., and Cao, G. (2008). Secreted proprotein convertase subtilisin/kexin type 9 reduces both hepatic and extrahepatic low-density lipoprotein receptors in vivo. *Biochem. Biophys. Res. Commun.* **370**: 634-640.

117. Liu, M., Wu, G., Baysarowich, J., Kavana, M., Addona, G. H., Bierilo, K. K., Mudgett, J. S., Pavlovic, G., Sitlani, A., Renger, J. J., Hubbard, B. K., Fisher, T. S., and Zerbinatti, C. V. (2010). PCSK9 is not involved in the degradation of LDL receptors and BACE1 in the adult mouse brain. *J. Lipid Res.* **51**: 2611-2618.

118. Luo, Y., Warren, L., Xia, D., Jensen, H. Sand, T., Petras, S., Qin, W., Miller, K. S., and Hawkins, J. (2009). Function and distribution of circulating human PCSK9 expressed extrahepatically in transgenic mice. *J. Lipid Res.* **50**: 1581-1588.

119. Spady, D. K. and Dietschy, J. M. (1985). Rates of cholesterol synthesis and low-density lipoprotein uptake in the adrenal glands of the rat, hamster and rabbit in vivo. *Biochim. Biophys. Acta* **836**: 167-175.

120. Rousselet, E., Marcinkiewicz, J., Kriz, J., Zhou, A., Hatten, M. E. Prat, A., and Seidah, N. G. (2011). PCSK9 reduces the protein levels of the LDL receptor in mouse brain during development and after ischemic stroke. *J. Lipid Res* **52**: 1383-1391.

121. DeVay, R. M., Shelton, D. L., and Liang, H. (2013). Characterization of proprotein convertase subtilisin/kexin type 9 (PCSK9) trafficking reveals a novel lysosomal targeting mechanism via amyloid precursor-like protein 2 (APLP2). *J. Biol. Chem.* **288**: 10805-10818.

122. Gregory, L. A., Thielens, N. M., Arlaud, G. J., Fontecilla-Camps, J. C., and Gaboriaud, C. (2003). X-ray structure of the $Ca^{2+}$-binding interaction domain of C1s. *J. Biol. Chem.* **278**: 32157-32164.

123. Stenflo, J., Stenberg, Y., and Muranyi, A. (2000). Calcium-binding EGF-like modules in coagulation proteinases: function of the calcium ion in module interaction. *Biochim. Biophys. Acta* **1477**: 51-63.

124. Winship, P. R., and Dragon, A. C. (1991). Identification of haemophilia B patients with mutations in the two calcium binding domains of factor IX: importance of a β-OH Asp64 → Asn change. *Br. J. Haematol.* **77**: 102 – 109.

125. Gerasimenko, J. V., Tepikin, A. V., Petersen, O. H., and Gerasimenko, O. V. (1998). Calcium uptake via endocytosis with rapid release from acidifying endosomes. *Curr. Biol.* **8**: 1335 – 1338.

126. Malby, S., Pickering, R., Saha, S., Smallridge, R., Linse, S., and Downing, A. K. (2001). The first epidermal growth factor-like domain of low-density lipoprotein receptor contains a noncanonical calcium binding site. *Biochemistry* **40**: 2555-2563.

127. Rao, Z., Handford, P., Mayhew, M., Knott, V., Brownlee, G. G., and Stuart, D. (1995). The structure of a $Ca^{2+}$- binding epidermal growth factor – like domain: its role in protein – protein interactions. *Cell* **82**: 131-141.

## Curriculum Vitae

### Summary

I have been considered as a promising student who possessed valuable abilities and characteristics to become an outstanding researcher such as energetic, hard working, intelligent and determined. During my studies, I have set myself up as one of top students who obtained excellent academic achievements, and granted honorable scholarships. At work, I have distinguished myself by a high sense of responsibility, creativity, honesty and strong analytical skills.

### Education

- Master's in Biochemistry (2011-present)
  University of Ottawa – Department of Biochemistry, Microbiology and Immunology
  "Characterization of PCSK9-mediated LDLR degradation in hepatic and non-hepatic cells"
- Bachelor of Science (Honors) in Biotechnology (2005-2009)
  University of Science – Vietnam National University in Ho Chi Minh City
  Department of Biotechnology

### Distinctions

- Graduation with Honorable Mention, Magna Cum Laude
  University of Science – Vietnam National University in Ho Chi Minh City
  (B.Sc. 2005-2009)

### Scholarships and Awards

- FGPS Travel Award – Faculty of Graduate and Postdoctoral Studies, University of Ottawa (2012)
- BCH Travel Award – Biochemistry Graduate Program, University of Ottawa (2012)
- Ajinomoto's Scholarship – Ajinomoto Vietnam, Inc. (2008 – 2009)

- 3rd prize in "Mendel's nursery garden" – the annual biology contest at University of Science, Vietnam National University in Ho Chi Minh City (2008)
- Encouraging Scholarship – HSBC Bank, Vietnam (2006)
- Excellence Scholarship – University of Science, Vietnam National University in Ho Chi Minh City (2005 – 2009)
- 2nd prize in Ho Chi Minh City biological contest (2005)
- Encouraging Scholarship – United Airlines (2005)

**Conferences and Presentations**

- University of Ottawa Heart Institute Research Day (May 2013)
  Ottawa, Ontario, Canada
  Poster presentation
- The Ottawa Heart Research Conference: Emerging Pathways in Cardiovascular Disease (May 2013)
  Ottawa, Ontario, Canada
  Attendant
- University of Ottawa – Department of Biochemistry, Microbiology and Immunology Seminar Day (March 2013)
  Ottawa, Ontario, Canada
  Oral presentation
- "Frontiers in Lipid Biology" – Canadian Lipoprotein Conference (September 2012)
  Banff, Alberta, Canada
  Poster presentation
- University of Ottawa – Department of Biochemistry, Microbiology and Immunology Poster Day (May 2012)
  Ottawa, Ontario, Canada
  Poster presentation